UNIVERSITY OF ALBERTA

OSMOTIC TRANSPORT IN CRYOBIOLOGY

by

HEIDI YAKOUT ELMOAZZEN ©

A thesis submitted to the Faculty of Graduate Studies and Research in partial

fulfillment of the requirements for the degree of Doctor of Philosophy

in

Medical Sciences - Laboratory Medicine and Pathology

Edmonton, Alberta

Spring 2006

Library and
Archives Canada

Bibliothèque et
Archives Canada

Published Heritage
Branch

Direction du
Patrimoine de l'édition

395 Wellington Street
Ottawa ON K1A 0N4
Canada

395, rue Wellington
Ottawa ON K1A 0N4
Canada

NOTICE:
The author has granted a non-exclusive license allowing Library and Archives Canada to reproduce, publish, archive, preserve, conserve, communicate to the public by telecommunication or on the Internet, loan, distribute and sell theses worldwide, for commercial or non-commercial purposes, in microform, paper, electronic and/or any other formats.

The author retains copyright ownership and moral rights in this thesis. Neither the thesis nor substantial extracts from it may be printed or otherwise reproduced without the author's permission.

AVIS:
L'auteur a accordé une licence non exclusive permettant à la Bibliothèque et Archives Canada de reproduire, publier, archiver, sauvegarder, conserver, transmettre au public par télécommunication ou par l'Internet, prêter, distribuer et vendre des thèses partout dans le monde, à des fins commerciales ou autres, sur support microforme, papier, électronique et/ou autres formats.

L'auteur conserve la propriété du droit d'auteur et des droits moraux qui protège cette thèse. Ni la thèse ni des extraits substantiels de celle-ci ne doivent être imprimés ou autrement reproduits sans son autorisation.

In compliance with the Canadian Privacy Act some supporting forms may have been removed from this thesis.

While these forms may be included in the document page count, their removal does not represent any loss of content from the thesis.

Conformément à la loi canadienne sur la protection de la vie privée, quelques formulaires secondaires ont été enlevés de cette thèse.

Bien que ces formulaires aient inclus dans la pagination, il n'y aura aucun contenu manquant.

Canada

This thesis is dedicated to my parents,

Afaf and Yakout and my sister Randa.

Thank you for all of your love and support

during this endeavor and throughout my life.

I will be forever grateful.

ABSTRACT

Osmotic Transport in Cryobiology

In order to optimize the viability of cryopreserved cells and tissues, a better understanding of osmotic transport is required. The main objectives of this thesis are to gain insight into osmotic transport, understand the parameters that affect osmotic transport and the limitations of the current transport formalisms used in the literature, and develop a new set of transport equations.

Firstly, the effect of cell size distribution on the osmotic response of cells was examined. Cell size distributions did not stay constant over time when the cells were responding to a hypertonic environment. It was clearly shown using a novel tool developed in this thesis that the mean or median cell volume should be used.

Secondly, cryoprotectant equilibration in tissues was investigated. Thermodynamics predicts that the equilibrium concentration of cryoprotectant inside a tissue depends on the ability of the tissue system to maintain an equilibrium pressure difference. Tissues that are free to expand reach the same equilibrium cryoprotectant concentration as the surrounding solution while tissues that are not free to expand and can maintain a pressure difference do not.

Next, the current status of osmotic transport in the literature was provided. The assumptions, limitations and common misconceptions made when using the two-parameter formalism and the Kedem-Katchalsky formalism were examined.

A detailed derivation of non-dilute chemical potential equations for the solvent and the solute were presented. From these derivations, a thermodynamic basis for a new mixing rule for the osmotic virial equation was developed.

Lastly, an analysis of various equations for solute transport was provided. Statistical Rate Theory was used to determine the concentration dependence of the various solute permeability coefficients. Also, a new set of transport equations were developed eliminating a third fitting parameter and assumptions of dilute solution and near–equilibrium. It was demonstrated that there is less unexpected concentration dependence of permeability coefficients with the new transport equations compared with the previous model. Hence a significant amount of the unexpected concentration dependence of the permeability coefficient has been explained as being due to the use of inappropriate transport equations.

Acknowledgments

I wish to express my sincere appreciation and gratitude to the following people without whom this thesis would not have been possible.

To Dr. Locksley E. McGann, my co-supervisor. Your kindness has been deeply appreciated and your dedication and enthusiasm for science has been inspirational. I am proud to have been able to work with you.

To Dr. Janet A. W. Elliott, my co-supervisor. Your enthusiasm for this project has been contagious and your encouragement has been greatly appreciated. I am fortunate to have had such a wonderful co-supervisor.

To Dr. Jason Acker and Dr. Gregory Korbutt for serving as committee members. Thank you for your review of this thesis.

To Dr. John Bischof for serving as my external examiner. Thank you for your time and insightful comments which have improved the quality of this work.

To Dr. Hasan Uludag for serving as an examiner for my defense. I have always appreciated and enjoyed our conversations.

To Dr. Gregory Tyrrell for serving as my examination committee chairman.

To Juan Irizar, thank you for your much appreciated help with Mathematica.

To the members of the Acker Cryolab. Thank you for your friendship and moral support.

To all the past and current members of McGann / Elliott Cryolab that I have been fortunate to work with. Thank you for your endless support, enlightening conversations and the many needed coffee breaks. Special thanks to Lisa Ross-Rodriguez, Richelle Bannerman and Garson Law– your encouragement and friendship has meant a lot to me during these times.

Thank you to all of my friends who have been positive sources of encouragement throughout the years.

Finally, special thanks to family - my parents Afaf and Yakout and my sister Randa, for their continued love, patience and support throughout all of my endeavors. I feel very blessed and fortunate. I love you all.

TABLE OF CONTENTS

LIST OF TABLES

LIST OF FIGURES

SYMBOL LIST

A	cell surface area
$\tilde{A}$	conversion factor between units of molarity and mole fraction
B	the second osmotic virial coefficient (when units of mole fraction are used); an expression for the interchange energy (when units of mole fraction are used)
B^*	the second osmotic virial coefficient (when units of molarity are used); an expression for the interchange energy (when units of molarity are used)
B^+	the second osmotic virial coefficient (when units of molality are used); an expression for the interchange energy (when units of molality are used)
c	concentration
c^*	concentration of a pure substance
$\tilde{c}_s$	a value for the concentration defined by (Eq. 4-31) and (Eq. 4-32)
C	molarity
C_o	the initial concentration of internal non-permeating solute in (Eq. 4-7)
C_{eq}	equilibrium concentration
C_s^{ave}	average solute concentration across the membrane
C^+	the third osmotic virial coefficient (when units of molality are used)
D_s	diffusion coefficient
f_i	frequency of the ith class interval in (Eq. 2-1); frequency of the interval containing the median in (Eq. 2-2)

FP	freezing point depression
G	Gibbs free energy
G_{excess}	Excess Gibbs energy
G_{ideal}	Gibbs free energy of an ideal solution
iVto	isotonic cell volume
j_i	the number of observations away from reaching the median value after the lower limit of the interval containing the median has been reached in (Eq. 2-2)
J	flux
J_D	differential volume flux
J_V	total volume flux
k_1	water permeability constant
k_2	solute permeability constant
K_s^e	equilibrium exchange rate of the solute
l	the thickness of the membrane or distance
L	phenomenological coefficient
$\tilde{L}$	water permeability coefficient
L_i	lower limit of the interval containing the median in (Eq. 2-2); lower class boundary of the class containing the mode in (Eq. 2-3)
L_p	membrane hydraulic conductivity
m	molality
m_i	midpoint of the ith class interval in (Eq. 2-1)
M	molal concentration

$MW_{solution}$	molecular weight of the solution
$MW_{solvent}$	molecular weight of the solvent
N	mole number
$\dot{N}$	rate of change in the mole number
P	pressure
P^{Ref}	reference pressure
$\tilde{P}$	solute permeability coefficient
P_s	solute permeability coefficient
P_s^{*}	an expression for permeability defined by (Eq. 6-15)
R	universal gas constant
S	entropy
$\tilde{S}$	the amount of internal permeating solute
t	time
T	temperature
U	internal energy
U_i	upper limit of the interval containing the median in (Eq. 2-2); upper class boundary of the class containing the mode in (Eq. 2-3)
v	partial molar volume
$v_{solution}$	specific volume of a solution
v_b	osmotically inactive fraction of the isotonic cell volume
V	volume
V_b	osmotically inactive volume

V_C	total cell volume
V_s	solute volume
V_S	solute volume (permeating and non-permeating solutes)
V_w	water volume
V_{w+s}	volume of water plus solute
V_o	cell volume at the isotonic osmolality; the initial volume of solvent within the cell in (Eq. 4-7)
x	mole fraction
$x_{solvent}$	mole fraction of the solvent
$\bar{x}$	mean value in (Eq. 2-1)
X	a thermodynamic force
σ	reflection coefficient in the Kedem-Katchalsky equations
$\tilde{\sigma}$	reflection coefficient as used by Staverman
μ	chemical potential
λ	thickness of the membrane
π	osmolality or osmolarity
π_i	intracellular osmolality or osmolarity
π_o	isotonic osmolality or osmolarity
Π	osmotic pressure
ω	energy of interaction
$\tilde{\omega}$	solute mobility
ψ	unspecified function of temperature and pressure

φ unspecified function of temperature and pressure

Δ_1 excess of modal frequency over the frequency of the next lower class in (Eq. 2-3)

Δ_2 excess of modal frequency over the frequency of the next higher class in (Eq. 2-3)

Subscripts

i	denotes a solute in (Eq. 4-1), (Eq. 4-2)
j	denotes a solute in (Eq. 4-2)
n	non-permeating solutes
s	permeating solute
sys	isolated system
w	water
1	denotes solvent
2	denotes solute
3	denotes the "biological component" in chapter 3; denotes the non-permeating intracellular solute in chapter 5 and 6
4	denotes the non-permeating extracellular solute in chapter 3, 5 and 6

Superscripts

e	extracellular solution
i	intracellular solution or inside the cell
o	outside the cell
m	membrane
R	reservoir
*	denotes pure component

Chapter 1: Introduction

1.1   Introduction to Cryobiology

Cryobiology is the study of the effects of low temperature on biological systems. The science of cryobiology began in the 1940s [16] particularly with the emergence of the first book devoted to cryobiology which was written by Luyet in 1940 [42]. When cells or tissues are exposed to low temperature conditions major physical and chemical changes take place that directly or indirectly affect the cells and tissues. Water plays an essential role in the structure and function of living systems and a major role in cryobiology as well as biology. Hence as living systems freeze, the amount of water in the liquid portion of the system changes. When water solidifies and freezes, it is hardly surprising that it is usually lethal to living cells and tissues. However, paradoxically, temperatures below freezing can also be used to preserve cells and tissues for long-term storage. In cryobiology, when we refer to low temperatures, we are usually referring to temperatures below that at which water freezes.

Cryobiology is a highly multidisciplinary field and the freezing of cells and tissues has a wide array of practical applications in biotechnology, medicine, agriculture, forestry, aquaculture and biodiversity conservation [17]. The ability to "stop time" in cryogenic storage for indefinite periods of time, offers huge practical benefits. Cryobiology has been used for various applications in agriculture and forestry specifically in understanding how plants and seeds behave when frozen, which has led to improvements in seed preservation techniques as well as dramatically

1

increased the applicability to a wide range of plant material [17]. Cryopreservation is the technique used to store and preserve cells at low temperatures. In some areas, such as the assisted reproduction of animals and humans, cryopreservation of reproductive cells and tissues plays a pivotal role. The cryopreservation of bull sperm [60] and embryos [40,74] has revolutionized the cattle breeding industry. Every year over 25 million cows are artificially inseminated with frozen-thawed bull semen [12] and hundreds of thousands of calves have been born as the result of the implantation of cryopreserved embryos into cows [18]. On the human side of things, literally hundreds of thousands of children have been born as the result of artificial insemination with cryopreserved sperm [19] and thousands of others have been born by the implantation of cryopreserved human embryos [56].

One of the most practical applications of freezing has been in the medical application of cryobiology in the areas of cryopreservation of cells and tissues for transplantation. Often cryopreservation takes place at dry ice temperatures (-80°C) or in liquid nitrogen (-196°C). At temperatures this low, cells can often be stored for many years in a biologically stable state since chemical reactions are limited. At such low temperatures of storage, bacterial growth is prevented. The only limitation to the length of storage in liquid nitrogen is the accumulation of damage caused by background ionizing radiation [6,44]. Transplantation of cryopreserved cells and tissues has been used to replace cells and tissues that are no longer functional due to disease or injury.

2

With the advances that have taken place in cryobiology over the last 60 years, improved cryopreservation techniques for the preservation of cellular and tissue systems have been developed. There are many advantages to being able to bank cryopreserved cells and tissues for long periods of time. Cryopreservation allows time for donor screening and testing. This has recently become more important because of increased transmission of infectious diseases, thus requiring a full social, behavioral and medical history of the donor prior to transplantation. Long-term storage allows for more effective donor-recipient matching, tissue typing, infectious disease testing and national sharing of cells and tissues. The cryopreservation of cells and tissues also makes it easier to coordinate donor availability and recipient need.

The cryopreservation of mammalian cell lines has played a fundamental role in scientific research. Since mammalian cell lines are generally amenable to cryopreservation, it allows for storage of homogeneous aliquots [20]. The cryopreservation of most cells in suspension is now a routine procedure. Frozen red blood cells, lymphocytes, monocytes and hematopoietic progenitor cells from bone marrow and peripheral blood are currently being used for many clinical and diagnostic purposes [21]. Autologous bone marrow cells are routinely stored for transplantation after ablative therapy in the treatment of leukemia and other malignancies [58]. Sperm cells and embryo tissues for many different species including plants, insects, mammals and other animals have been stored for

3

several reasons including the preservation of biological diversity in rare and endangered species.

1.2 Cellular Cryobiology

As a biological sample is cooled to temperatures below its equilibrium freezing point, ice forms in the extracellular liquid either spontaneously or by induced freezing. For cells in suspension, when freezing is initiated, ice forms outside of the cells, concentrating the solutes in the remaining liquid of the extracellular solution. Ice does not immediately form intracellularly because the cell membrane acts as a barrier for the growth of ice crystals into the cell through the membrane [46] and the cytoplasm contains few effective nucleators [14,43,63]. The cells become exposed to an increasingly hypertonic solution due to the progressive increase in the external solute concentration that occurs as more extracellular ice forms and the cell contents remain unfrozen or supercooled. The water in the unfrozen cell then has, by definition, a higher chemical potential than that of water in the partially frozen solution. In response to this difference in chemical potential, an osmotic pressure gradient is created. This gradient provides the driving force for the efflux of water out of the cell which results in cell shrinkage.

The survival of cryopreserved cells is strongly dependent on the rate at which cells are cooled and warmed. In cryopreservation protocols, the sample is cooled at a finite rate that is optimized for each cell type. In 1963, Mazur [45]

suggested a quantitative approach to describing a cell's response during freezing. He proposed that the rate of efflux of water from a cell during exposure to low temperature could be predicted if the water permeability of the cell, the initial osmolality of the cells and the surface area to volume ratio were known. The expressions he developed allow one to calculate the extent of supercooling in cells as a function of the cooling rate and to estimate the probability of intracellular ice formation as a function of cooling rate. As a result, in theory, cryopreservation protocols could be designed that avoided cellular injury.

Cellular injury is largely related to the nature and kinetics of the cellular response to temperature-induced conditions. The damaging effects of freezing on cells in suspension are dependent on two variables: the permeability of the cell membrane and the cooling rate [44]. If cells are cooled at rates higher or lower than the optimal cooling rate, damage will occur to the cells. Mazur et al., [48] proposed a 'two-factor hypothesis' of freezing damage, according to which there are two independent mechanisms of damage during freezing, one active at low cooling rates and the other at high cooling rates.

1.2a Slow cool injury

If cooling rates are too low, the cell continues to shrink as the temperature decreases and no ice forms inside the cells [45]. The cell is able to lose water rapidly enough by exosmosis to concentrate the intracellular solutes sufficiently to eliminate supercooling and maintain the chemical potential of intracellular

5

water in equilibrium with that of extracellular water. Cell injury is thought to be due to the effects of exposure to highly concentrated intracellular and extracellular solutions [48] or to mechanical interactions between the cells and extracellular ice [47]. These 'solution effects' included dehydration, concentration of solutes, changes in pH and the precipitation of solutes.

1.2b Rapid cool injury

When cooling rates are too high, the formation of ice in the extracellular solution is much faster than the efflux of water from the cells. Because water efflux from the cell is too slow to maintain osmotic equilibrium, the cytoplasm becomes increasingly supercooled until it eventually freezes. Cells that are cooled too quickly don't shrink appreciably and equilibrate by forming intracellular ice [44], which is often lethal for cells in suspension [48]. There has been significant evidence for the correlation between cell injury and intracellular ice formation during rapid cooling [44].

1.2c Warming rates

The recovery of cells after freezing and thawing is not only dependent on the cooling rate but also on the rate of warming [3,55,59]. It has been found experimentally that cells that are cooled more slowly than the optimal rate survive better when the warming rate is low than when it is high. Because cells that are cooled slowly do not form intracellular ice but are severely dehydrated, if warmed rapidly, these cells may become osmotically stressed as the result of the rapid

6

water influx. As a result, slowly cooled cells give higher recovery when warmed slowly. Conversely, cells that are cooled more rapidly than the optimum rate of cooling survive better when the warming rate is high because the small intracellular ice crystals formed during rapid cooling grow into larger damaging crystals during warming by the process of recrystallization [13]. To minimize the effects of recrystallization, rapid warming rates should be used for rapidly cooled cells.

1.3   Traditional Cryopreservation of Cells

Damage to cells during freezing is caused by both the exposure to high concentrations of solutes during slow cooling and to intracellular freezing during rapid cooling. Successful cryopreservation protocols have been dependent on the development of novel techniques to minimize both types of damage. Many types of cells do not survive freezing and thawing unless a cryoprotectant is present. Cryoprotectants are chemical compounds that are added to cells and tissues to mitigate the negative effects of freezing. In 1949, Polge et al., [61] were the first to use chemical compounds to enhance the survival of frozen biological material, when they discovered the cryoprotective action of glycerol. They found an increased viability in fowl sperm after freezing when the samples were suspended in a medium containing glycerol [61]. There are two main groups of cryoprotective agents: the permeating cryoprotectants - those which can diffuse through the plasma membrane and equilibrate in the cytoplasm; and the non-permeating cryoprotectants - those which cannot cross the cell

7

membrane and don't enter the cytoplasm unaided [22]. Innovative cryopreservation protocols for the addition and dilution of permeating and non-permeating cryoprotectants that decrease the time of exposure and the concentration of the cryoprotectants continue to be developed in efforts to avoid their toxic effects when used in high concentrations.

1.3a Permeating cryoprotectants

The permeating cryoprotectants are generally small, non-ionic molecules that have high solubility in water at low temperatures and low cellular toxicity [22]. Examples of permeating cryoprotectants include glycerol, propylene glycol (PG) and dimethyl sulfoxide (DMSO). The permeating cryoprotectants are thought to act mainly colligatively by depressing the freezing point. As a result, the amount of ice formed at a given temperature is reduced; as well the electrolyte concentration inside and outside the cell is reduced at any given temperature (since less ice is formed both intracellularly and extracellularly and less osmotic shrinkage occurs) [41]. In general, as the concentration of cryoprotectant increases, cell survival improves. However, the cryoprotective chemicals themselves can be damaging and high concentrations of cryoprotectants have detrimental toxic and osmotic effects on cells, the latter of which are a consequence of the cell membrane being more permeable to the water than to the cryoprotectant.

8

1.3b Non-permeating cryoprotectants

The non-permeating cryoprotectants are those that cannot cross the cell membrane and are generally larger molecules such as sugars or macromolecules including long-chain polymers that are soluble in water. They generally increase the osmolality well above their molar concentrations [22]. Examples of non-permeating cryoprotectants include trehalose, hydroxyethyl starch, dextran and sucrose. These cryoprotectants are thought to act by dehydrating the cell before freezing. Therefore, the amount of water the cell needs to lose to remain close to equilibrium during freezing is reduced. The non-permeating cryoprotectants are then responsible for an additional osmotic stress on the cell that results in an increased loss of water at these high subzero temperatures. Protection against further cooling is obtained by osmotic shrinkage due to the increased concentration of the non-permeating cryoprotectant in the extracellular region [50]. The cytoplasm becomes less supercooled when non-permeating cryoprotectants are used, thus reducing the likelihood of intracellular ice forming.

1.4 Cellular Osmotics

As discussed earlier, water plays an essential role in cryobiology. Not only is the state of water in cells and the extracellular solution important, but also how water moves across cell membranes and the factors which affect this movement in and out of cells are of concern. Cells have a semi-permeable membrane so water and permeating solutes, such as permeating cryoprotectants are able to cross

9

the cell membrane. A semi-permeable membrane allows certain molecules to pass through it by diffusion. The rate of passage depends on the concentration, pressure and temperature of the solutes on either side of the membrane, as well as the permeability of the membrane to each solute. Because of the semi-permeable nature of cell membranes, water will move in and out of the cell in response to changes in the extracellular environment. These changes may be brought about by a number of factors including: 1-) the addition and removal of cryoprotectants – the cell will shrink or swell depending on the conditions of exposure; and 2-) the conversion of water to ice that takes place during freezing. As the extracellular solution becomes more concentrated as ice forms, water leaves the cell until osmotic equilibrium is reached. In general, the cells respond osmotically to the changes in the extracellular solution.

1.4a   Basic thermodynamic equations

Solution thermodynamics can be used to describe a variety of processes that occur in cryobiology. The change in Gibbs free energy (dG) of any simple system may be written as follows [9]:

(Eq.1- 1)

$$dG = -SdT + VdP + \sum_i \mu_i dN_i$$

where S is the entropy of the system, T is temperature, V is volume, P is pressure, μ is the chemical potential and N_i is the number of moles of species i. The chemical potential of species i is defined as follows [10]:

10

(Eq.1- 2)

$$\mu_i = \left(\frac{\partial G}{\partial N_i} \right)_{T,P,N_{j \neq i}}$$

where the chemical potential is the thermodynamic property of a solution that drives mass transport across a cell membrane. Osmosis will adjust the concentration of the solutes and the water inside the cell so that the chemical potential of each of the different species inside the cell is equal to that of the extracellular components, assuming that the cell is permeable to that component.

At equilibrium, the chemical potential of the water inside the cell, μ_1^i, will equal the chemical potential of the water outside the cell μ_1^o:

(Eq.1- 3)

$$\mu_1^i = \mu_1^o$$

For an ideal, dilute solution, the chemical potential of the water in terms of the mole fraction of the solute, x_2, may be written as follows:

(Eq.1- 4)

$$\mu_1(T,P,x_2) = \mu_1^*(T,P^{Ref}) + v_1^*(P - P^{Ref}) - RTx_2$$

where μ_1^* is the chemical potential of the pure water, v_1^* is the partial molar volume of water, P^{Ref} is some reference pressure, and R is the universal gas constant. For situations where the effects of hydrostatic pressure, P, may be neglected, the chemical potential for an ideal, dilute solution of one solute simply reduces to the following [10]:

11

(Eq.1- 5)

$$\mu_1(T,P) = \mu_1^*(T,P) - RTx_2$$

The chemical potential of the solvent may also be written in terms of the osmolality, π, the molecular weight of the solvent, $MW_{solvent}$ and the mole fraction of the solvent, $x_{solvent}$. The osmotic pressure, Π is equal to $\dfrac{RT(MW_{solvent})x_{solvent}\pi}{v_1^*}$.

(Eq.1- 6)

$$\mu_1 = \mu_1^* - RT(MW_{solvent})x_{solvent}\pi$$
$$\mu_1 = \mu_1^* - v_1^*\Pi$$

Similarly, for a cell placed in a solution of a permeating solute, the solutes will move until equilibrium is reached and the chemical potential of the solute inside the cell will equal the chemical potential of the solute outside the cell.

(Eq. 1- 7)

$$\mu_2^i = \mu_2^o$$

For an ideal, dilute solution, the chemical potential of the solute may be written as follows:

(Eq.1- 8)

$$\mu_2(T,P,x_2) = \psi(T,P^{\mathrm{Re}f}) + v_2^*(P - P^{\mathrm{Re}f}) + RT\ln(x_2)$$

where ψ is an unspecified function of temperature and pressure related to the standard state of the permeating solute usually taken to be infinite dilution. For situations where the effects of hydrostatic pressure, P may be neglected, the chemical potential for an ideal, dilute solution of one solute simply reduces to the following [10]:

12

(Eq.1- 9)

$$\mu_2(T, P, x_2) = \psi(T, P) + RT\ln(x_2)$$

1.4b Water transport across cell membranes

The rate of water movement across a cell membrane is proportional to the difference in chemical potentials of the water inside and outside the cell and hence is proportional to the difference in extracellular and intracellular osmolalities, osmolarities, or osmotic pressures. The equation for water transport across a cell membrane is given as follows:

(Eq.1- 10)

$$\frac{dV_w}{dt} = -L_p ART\left(\pi^e - \pi^i\right)$$

where $\frac{dV_w}{dt}$ is the change in cell water volume (V_w) as a function of time (t). L_p is the membrane hydraulic conductivity, which is a measure of the rate of water movement across a cell membrane. A is the cell surface area, π^e is the total extracellular solution osmolarity and π^i is the total intracellular solution osmolarity. The higher the value of L_p, the faster the rate of water movement will be across the cell membrane. Similarly, the higher the temperature of the system or the larger the concentration gradient across the cell membrane, the faster the rate of water movement will be. In general, the rate of water movement across a cell membrane is limited by the permeability properties of the membrane [23].

13

In order to investigate the water movement across a cell membrane, we can look at work that was done by McGann in 1984 [49]. The osmotic response of bovine chondrocytes was modeled when exposed to the addition and dilution of the non-permeating cryoprotectant, sucrose as shown in Figure 1-1. The osmotic response was investigated for various concentrations of sucrose at different temperatures. During addition of the non-permeating cryoprotectant, the cells start off at an isotonic volume. Since the sucrose cannot cross the cell membrane, the extracellular solution becomes more concentrated and the cells become exposed to an increased concentration of the non-permeating solute. In order to maintain osmotic equilibration, water leaves the cell and the cell shrinks. During the dilution stage, water rushes back into the cell in order to maintain osmotic equilibrium and the cell returns to the isotonic volume. In Figure 1-1, the rate of water movement across the cell membrane was shown to be temperature dependent as at the higher temperature the rate of water movement was faster. Similarly, at the higher concentrations, the gradient across the cell membrane was larger, thus the water movement across the cell membrane was faster.

1.4c   Solute transport across cell membranes

The chemical potential of the permeating solute is the driving force for solute transport across cell membranes. For a dilute solution, the solute chemical potential difference is proportional to the difference in solute concentration across the cell membrane. The equation for solute transport across a cell membrane is given as follows:

14

(Eq.1- 11)

$$\frac{dN_s}{dt} = P_s A \left(C_s^e - C_s^i \right)$$

where $\frac{dN_s}{dt}$ is the change in the intracellular number of permeating solute molecules as a function of time, P_s is the solute permeability, C_s^e is the extracellular solute molarity and C_s^i is the intracellular solute molarity. To convert from a solute flux to a volume flux, we can multiply by the partial molar volume of the solute, v_s, as follows:

(Eq.1- 12)

$$\frac{dV_s}{dt} = v_s \frac{dN_s}{dt} = v_s P_s A \left(C_s^e - C_s^i \right)$$

The higher the value of P_s, the faster the rate of solute movement will be across the cell membrane. Similarly, the higher the temperature of the system or the larger the solute concentration gradient across the cell membrane, the faster the rate of solute movement will be. In general, like the rate of water movement, the rate of solute movement across a cell membrane is limited by the permeability properties of the membrane.

The total cell volume and the overall movement of water and solutes is determined by using both (Eq.1- 10) and (Eq.1- 12). In order to investigate the water and solute movement across a cell membrane, we can look at work that was done by McGann [49] on the modeled osmotic response of bovine chondrocytes on the addition and dilution of various concentrations of the

15

permeating cryoprotectant, DMSO, at different temperatures, as shown in Figure 1-2. The cell initially starts off at its isotonic volume. Since water moves faster than DMSO, the cell initially shrinks and water rushes out of the cell. Water and DMSO will then both enter the cell in order to approach osmotic equilibrium and the cell returns back to the isotonic volume. During dilution, the cell initially swells since water will move faster than DMSO and then will shrink as both water and DMSO leave the cell to approach osmotic equilibrium. As shown in Figure 1-2, at the higher temperature, the rates of water and solute movement across the cell membrane were faster. Similarly, at the higher concentrations, the gradient across the cell membrane was larger, thus the water and solute movement across the cell membrane were faster.

1.4d   Modern day transport formalisms

In general, the cell will respond osmotically to both the addition and removal of cryoprotectants as well as to changes occurring during freezing. Since the 1930's, formalisms have been developed to describe the efflux of water and solutes across cell membranes [33,34]. The two-parameter (2-P) formalism, built on the work of Jacobs and Stewart [33,34], uses two parameters, L_p and P_s, to characterize membrane permeability when water, a permeating solute and a non-permeating solute are present. The formalism essentially involves the equations (Eq.1- 10), (Eq.1- 11), and (Eq.1- 12).

16

Another commonly used transport formalisms in cryobiology was developed by Kedem and Katchalsky in 1958 [37]. This formalism was developed specifically to handle situations for which water and solute transport across a cell membrane were physically coupled but was also used to describe situations where the solute and solvent fluxes did not interact. The Kedem-Katchalsky (K-K) formalism used three fitting parameters to describe osmotic transport, L_p, P_s, and the reflection coefficient, σ:

(Eq.1- 13)

$$\frac{dV_{w+s}}{dt} = -L_p ART \left\{ \left(C_n^e - C_n^i \right) + \sigma \left(C_s^e - C_s^i \right) \right\}$$

where C is the molarity with the superscripts denoting the internal cell solution (i) and the solution external to the cell (e) and the subscripts denoting the non-permeating solutes (n) and the permeating solutes (s).

In 1998, Kleinhans wrote a review paper comparing the 2-P formalism with the K-K formalism [38]. Kleinhans argues that although the K-K formalism is the most general and commonly used formalism in cryobiology, it is not without drawbacks. As a result of this, Kleinhans proposed that the K-K formalism and σ were often unnecessary and demonstrated that the 2-P formalism worked just as well as the K-K formalism and essentially gave the same results for a number of different transport situations in which a common channel for solute and solvent was not present.

17

It is important to recognize that when either the 2-P or the K-K equations are used to determine the permeability parameters, a dilute solution assumption is being made. The conditions of ideal and dilute solutions are not in general met in cryobiology, where conditions during freezing and when using high concentrations of cryoprotectants are not often dilute.

1.4e Methods for measuring osmotic parameters

In order to determine the osmotic properties of a cell, measurements of the equilibrium and non-equilibrium volume changes of the cell as a function of the osmolality of the extracellular solution are required. In order to measure cell membrane permeability parameters L_p and P_s, experimental data is fit to the various transport formalisms. Cell volume changes that take place upon exposure to hypertonic and hypotonic solutions may be measured using various techniques. Video or photomicrography involves measuring the cross sectional area changes of cells with time to measure the rate of volume change of a cell [24]. Other techniques used include stopped-flow spectrophotometers [7,70], a technique in which the cell volume change is monitored by using the linear relationship between the volume of the cell and the intensity of light that is scattered by the cell suspension. Diffusion and perfusion chambers are also used [53,71,75], whereby volume changes are observed using a light microscope while the extracellular media is changing. One of the most common means to determine permeability parameters has been to use electronic particle counters. Electronic particle counters are commonly used to study equilibrium size

18

distributions of cells [2,4,5,28-31,39,52], as well as to measure changes in mean or mode cell volume that occur over time during exposure to hypertonic and hypotonic solutions [1,5,8,26,27,51]. Cells passing through the aperture in an electronic counter displace a volume of the conducting fluid resulting in a voltage pulse proportional to the volume of the cells.

1.5   Tissue Cryobiology

1.5a   Challenges with tissue preservation

While the freezing of cells in suspension is fairly routine practice, the cryopreservation of tissues has proven to be a much more challenging task. The clinical demand for human tissue for transplantation continues to grow. The lack of native tissue available for transplantation has advanced tissue engineering as an emerging source of tissue for transplantation. With the development of engineered tissues for transplantation, there is an increasing demand to be able to preserve and store viable biomaterials [36]. Cryopreservation is often the only method for preserving the physiological structure, viability and function of tissues for long periods of time, thus making successful cryopreservation of native and engineered tissue even more important.

Cellular cryopreservation provides a starting point for cells within a tissue matrix. However, extrapolation to tissue preservation is not trivial for many reasons. Tissue cryopreservation has the added complexity of tissues containing more than one cell type, each with its own optimal cooling conditions. Also, tissues

19

have a fixed geometry, so heat and mass transfer issues often come into play. Cells in the tissue are attached both to other cells and to the matrix [57]. These interactions are crucial in the functioning of the tissue. Tissues also depend on both the presence of living cells and a physically intact extracellular matrix. Damage to the matrix during freezing may be the result of the formation of ice [78] or by an indirect effect of changes in the solution composition [57].

The transplantation of human tissue is becoming more a routine practice and tissue banks around the world are being developed. However tissue banking is fairly limited to tissues that do not require live cells for optimal function or to those tissues that are relatively simple in structure where basic freezing techniques may be applied – usually from techniques applied to cells in suspension [25]. Some tissues such as bone and tendon, do not require the presence of living cells in order to be utilized. Other tissues such as skin, vascular grafts, islets of Langerhans, blood, heart valves, corneas and articular cartilage, do require the presence of living cells in order to be functional. Cryopreservation of some tissues such as skin [77] and heart valves has been fairly successful whereas cryopreservation has been more challenging for other tissues such as articular cartilage [35] and corneas [69], where low temperature (hypothermic) storage is used over cryopreservation.

Despite the common use of many cryopreserved tissues such as skin, current traditional cryopreservation techniques are often damaging to cells resulting in a

20

reduction of tissue function [64]. As a result of the insufficient supply of fresh tissue, cryopreserved skin is still used, despite its limitations [32]. Therefore, improved cryopreservation methods for both native and engineered skin are needed.

1.5b   Vitrification as a non-traditional approach to tissue preservation

As a result of many of the problems resulting from ice formation inside tissues during freezing, current approaches towards tissue preservation attempt to eliminate ice formation by vitrification [11]. Vitrification involves the solidification of a supercooled liquid by adjusting the composition and cooling rate such that the crystal phase is avoided and a glassy state is formed (amorphous solidification). This is usually achieved by using high concentrations of cryoprotectants and high cooling rates [11]. Because the concentrations of cryoprotectants needed to achieve vitrification are so high, one of the primary challenges in vitrifying tissues is cryoprotectant toxicity. Vitrification has been used to successfully cryopreserve some cells and tissues, such as embryos [62], autologous vascular grafts [65,66], and attempts have been made with human skin [15,76].

1.6   Objectives and Scope of this Thesis

In order to optimize the viability of cryopreserved cells and tissues, a better understanding of osmotic transport is required. Passive transport plays a critical role in low temperature biology, especially since low temperatures tend to

21

diminish the relative importance of active transport processes. Cryobiologists are generally concerned with the concentration and movement of water and solutes inside and outside the cell before, during and after the freezing process [54]. The transport behavior observed at near physiological conditions may bare little resemblance to transport characteristics that take place during the cryopreservation process. The addition and removal of cryoprotectants as well as the conversion of water to ice that takes place during freezing, leaves the cells exposed to highly concentrated solutions and non-dilute conditions. The conditions under which solutions becomes dilute depends on the nature of the solute involved. A dilute solution is one in which the osmolality of the solution is equal to the molality of the solution (i.e. - where solute-solute interactions do not play a role in the solution). Thus, by definition, a solution is ideal and dilute if (Eq.1- 5) holds. Outside the regions where solutions are dilute, solute-solute interactions will always be important. Dilute solution assumptions may hold true for low concentrations of cryoprotectants such as dimethyl sulfoxide. However for high concentrations of dimethyl sulfoxide, the osmolality of the solution will not equal the molality. For example, a 1 molal dimethyl sulfoxide solution has an osmolal concentration of 1.08, while a 6 molal dimethyl sulfoxide solution has an osmolal concentration of over 9. For a solute such as hemoglobin, which is highly non-ideal, even at low concentrations, the osmolality of the solution will not equal the molality. For example, a 0.05 molal hemoglobin solution has an osmolal concentration of 3.4. As a result, accurate descriptions of osmotic transport are required in order to design effective cryopreservation protocols.

22

More accurate osmotic parameters can then be used in simulations to design cryopreservation protocols that may better predict and match experimental outcomes. More accurate simulations may cut down on experimental costs and allow for more complicated protocols to be tested. This will be particularly important when trying to preserve tissues particularly using vitrification where high concentrations of cryoprotectants are needed. With tissue preservation, there are a number of important factors to consider (multiple cell types, preserving the matrix, heat and mass transfer), and osmotic transport is just one of them. However, doing a good job of accurately describing osmotic transport will eventually assist in the successful preservation of tissues.

The main objective of this thesis is to gain insight into the role of non-dilute solution thermodynamics on passive osmotic transport in cryobiology and understand the parameters that affect osmotic transport, as well as the limitations of the current osmotic transport formalisms used in literature.

In the second chapter of this thesis, the effect of cell size distribution on the osmotic response of cells is examined. An understanding of the kinetics of the osmotic response of cells is important in understanding permeability properties of cell membranes and predicting cell responses during exposure to anisotonic conditions. Traditionally, a mathematical model of cell osmotic response is obtained by applying mass transport and Boyle-van't Hoff equations using numerical methods. In the usual application of these equations, it is assumed

23

that all cells are the same size equal to the mean or mode of the population. However, biological cells, (even if they had identical membranes and hence identical permeability characteristics - which they do not) have a distribution in cell size and will therefore shrink or swell at different rates when exposed to anisotonic conditions. A population of cells may therefore exhibit a different average osmotic response than that of a single cell. In this chapter, a mathematical model using mass transport and Boyle-van't Hoff equations was applied to measured size distributions of cells. Cell shrinkage data for Chinese hamster fibroblast cells (V-79W) and Madin-Darby canine kidney cells (MDCK) that were exposed to hypertonic solutions were analyzed. Consistent with the theoretical predictions, the size distributions of these cells were found to change over time, therefore the selection of the measure of central tendency (mean, median, and mode) for the population may affect the calculated osmotic parameters. The best measure of central tendency to describe osmotic volume changes in cell suspensions will be determined.

In the third chapter of this thesis, the role of cryoprotectant equilibration in tissues is investigated. The first step in the cryopreservation of cells or tissues is often the movement of a permeating cryoprotectant into the cells or tissues from the solution into which they have been placed. The cryoprotectant enters the cells or tissues by thermodynamic equilibration with the surroundings. In the reverse case, thermodynamic equilibration also drives the removal of permeating cryoprotectants by a dilution solution at the end of the preservation process when

24

the cells or tissues are being readied for use. There have been reports of tissues having equilibrium cryoprotectant concentrations lower than that of the surrounding carrier solution. For various tissues, the equilibrium concentration of cryoprotectant inside the tissue is either equal to, or lower than the cryoprotectant concentration of the surrounding solution. A simple thermodynamic treatment of the solution-tissue equilibrium will be applied to offer a possible explanation for the difference in cryoprotectant concentration.

In the fourth chapter of this thesis, a detailed look into the current status of osmotic transport in the literature will be provided. The traditional theoretical descriptions of osmotic transport across cell membranes are based on the work of Jacobs and Stewart [33,34]. The 2-P formalism along with the assumptions of the transport equations will be investigated. In the early 1950's, Staverman approached the problem of osmotic transport across cell membranes utilizing osmotic pressures by employing the linear theory of irreversible thermodynamics [67,68] and introduced the idea of a reflection coefficient. Kedem and Katchalsky built on this idea of a reflection coefficient and developed a formalism to describe osmotic transport across a cell membrane when water and solute transport across a membrane are physically coupled, usually through co-transport in a common channel. The derivation and assumptions made in the K-K formalism will be examined. In 1998, Kleinhans wrote a review paper comparing the 2-P formalism with the K-K formalism [38]. In this chapter a detailed examination of the paper will be discussed as well as discussion on the reflection coefficient and

a comparison between the 2-P and the K-K formalism. The main objective of this chapter is to outline the main assumptions, limitations and common mistakes and misconceptions made in the transport formalisms and their applications used in the literature today.

Because of the many limiting assumptions of the traditional transport formalism, a new set of transport equations that do not make dilute solution assumptions, will be developed. Mass transport across a cell membrane is driven by the chemical potential of the solvent and the solute. In the fifth chapter of this thesis, a detailed derivation of non-dilute chemical potential equations for the solvent and the solute will be presented. In the literature there are a number of mathematical relationships used to describe osmolarity or osmolality as a function of concentration and the osmotic virial equation is one of them. The osmotic virial equation treats osmolality (or osmolarity or osmotic pressure) as a polynomial expansion in concentration with the first term being linear in concentration. As well in this chapter, a thermodynamic basis for a new mixing rule for the osmotic virial equation will be provided.

In the sixth chapter of this thesis an analysis of various equations for solute transport will be presented. In order to better understand osmotic transport, a closer look needs to be taken at the solute transport equations. The solute transport equations may be examined from a number of different perspectives including Fick's Law of Diffusion, the Onsager approach and Statistical Rate

Theory. Statistical Rate Theory is a relatively new theory of non-equilibrium thermodynamics proposed by C. A. Ward [72,73]. The theory provides an expression for the instantaneous net molecular transport rate across the interface of two similar or different phases. No equilibrium assumptions are made in the development of Statistical Rate Theory and it can be used to derive rate equations that may be written entirely in terms of experimental and thermodynamic variables that may be tabulated, measured or controlled. As a result, Statistical Rate Theory can be used to indicate whether various solute permeability coefficients such as the diffusion coefficient in Fick's Law of Diffusion and the solute permeability coefficient, P_s, have a concentration dependence or not. As well, in this chapter a new set of transport equations were developed that make no near equilibrium or dilute solution assumptions. The new transport equations were fit to experimental data for human corneal epithelial cells exposed to various concentrations of DMSO.

Overall this thesis will provide insight into osmotic transport in cryobiology for both cellular and tissue systems.

27

1.6 References

[1] Acker, J.P., Pasch, J., Heschel, I., Rau, G., McGann, L.E., Comparison of optical measurement and electrical measurement techniques for the study of osmotic responses of cell suspensions, Cryoletters 20 (1999) 315-324.

[2] Adams, R.B., Voelker, W.H., Gregg, E.C., Electrical Counting and Sizing of Mammalian Cells in Suspension - an Experimental Evaluation, Physics in Medicine and Biology 12 (1967) 79-92.

[3] Akhtar, T., Pegg, D.E., Foreman, J., Effect of Cooling and Warming Rates on the Survival of Cryopreserved L-Cells, Cryobiology 16 (1979) 424-429.

[4] Anderson, E.C., Petersen, D.F., Cell Growth and Division .2. Experimental Studies of Cell Volume Distributions in Mammalian Suspension Cultures, Biophysical Journal 7 (1967) 353-364.

[5] Armitage, W.J., Juss, B.K., Osmotic response of mammalian cells: Effects of permeating cryoprotectants on nonsolvent volume, Journal of Cellular Physiology 168 (1996) 532-538.

[6] Ashwoodsmith, M.J., Friedmann, G.B., Lethal and Chromosomal Effects of Freezing, Thawing, Storage Time, and X-Irradiation on Mammalian-Cells Preserved at -196-Degrees in Dimethyl-Sulfoxide, Cryobiology 16 (1979) 132-140.

[7] Boroske, E., Elwenspoek, M., Helfrich, W., Osmotic Shrinkage of Giant Egg-Lecithin Vesicles, Biophysical Journal 34 (1981) 95-109.

[8] Buckhold, B., Adams, R.B., Cregg, E.C., Osmotic Adaptation of Mouse Lymphoblasts, Biochimica Et Biophysica Acta 102 (1965) 600-608.

[9] Callen, H.B., Thermodynamics and an Introduction to Thermostatistics (John Wiley & Sons, New York, 1985) p. 148.

[10] Callen, H.B., Thermodynamics and an Introduction to Thermostatistics (John Wiley & Sons, New York, 1985) p. 303.

[11] Fahy, G.M., Macfarlane, D.R., Angell, C.A., Meryman, H.T., Vitrification as an Approach to Cryopreservation, Cryobiology 21 (1984) 407-426.

[12] Foote, R.H., The artificial insemination industry, in: B.G. Brackett, G.E. Seidel, S.M. Seidel (Eds.), New Technologies in animal breeding (Academic Press, New York, 1981) 12-39.

[13] Forsyth, M., Macfarlane, D.R., Recrystallization Revisited, Cryo-Letters 7 (1986) 367-378.

[14] Franks, F., Mathias, S.F., Galfre, P., Webster, S.D., Brown, D., Ice Nucleation and Freezing in Undercooled Cells, Cryobiology 20 (1983) 298-309.

[15] Fujita, T., Takami, Y., Ezoe, K., Saito, T., Sato, K., Takeda, N., Yamamoto, Y., Homma, K., Jimbow, K., Sato, N., Successful preservation of human skin by vitrification, Journal of Burn Care & Rehabilitation 21 (2000) 304-309.

[16] Fuller, B.J., Lane, N., Benson, E.E. (Eds.), Life in the Frozen State, CRC Press, Boca Raton, 2004, Forward.

[17] Fuller, B.J., Lane, N., Benson, E.E. (Eds.), Life in the Frozen State, CRC Press, Boca Raton, 2004, Introduction.

[18] Fuller, B.J., Lane, N., Benson, E.E. (Eds.), Life in the Frozen State, CRC Press, Boca Raton, 2004, p. 349.

[19] Fuller, B.J., Lane, N., Benson, E.E. (Eds.), Life in the Frozen State, CRC Press, Boca Raton, 2004, p. 359.

[20] Fuller, B.J., Lane, N., Benson, E.E. (Eds.), Life in the Frozen State, CRC Press, Boca Raton, 2004, p. 438.

[21] Fuller, B.J., Lane, N., Benson, E.E. (Eds.), Life in the Frozen State, CRC Press, Boca Raton, 2004, p. 483.

[22] Fuller, B.J., Lane, N., Benson, E.E. (Eds.), Life in the Frozen State, CRC Press, Boca Raton, 2004, p. 77.

[23] Fuller, B.J., Lane, N., Benson, E.E. (Eds.), Life in the Frozen State, CRC Press, Boca Raton, 2004, p. 70.

[24] Fuller, B.J., Lane, N., Benson, E.E. (Eds.), Life in the Frozen State, CRC Press, Boca Raton, 2004, p. 17.

[25] Fuller, B.J., Lane, N., Benson, E.E. (Eds.), Life in the Frozen State, CRC Press, Boca Raton, 2004, p. 541.

[26] Gilmore, J.A., McGann, L.E., Ashworth, E., Acker, J.P., Raath, J.P., Bush, M., Critser, J.K., Fundamental cryobiology of selected African mammalian spermatozoa and its role in biodiversity preservation through the development of genome resource banking, Animal Reproduction Science 53 (1998) 277-297.

[27] Gilmore, J.A., Mcgann, L.E., Liu, J., Gao, D.Y., Peter, A.T., Kleinhans, F.W., Critser, J.K., Effect of Cryoprotectant Solutes on Water Permeability of Human Spermatozoa, Biology of Reproduction 53 (1995) 985-995.

[28] Gregg, E.C., Steidley, K.D., Electrical Counting and Sizing of Mammalian Cells in Suspension, Biophysical Journal 5 (1965) 393-405.

[29] Grover, N.B., Bensasso.S, Doljansk.F, Naaman, J., Electrical Sizing of Particles in Suspensions .3. Rigid Spheroids and Red Blood-Cells, Biophysical Journal 12 (1972) 1099-1117.

[30] Grover, N.B., Naaman, J., Bensasso.S, Doljansk.F, Electrical Sizing of Particles in Suspensions .I. Theory, Biophysical Journal 9 (1969) 1398-1414.

[31] Grover, N.B., Naaman, J., Bensasso.S, Doljansk.F, Nadav, E., Electrical Sizing of Particles in Suspensions .2. Experiments with Rigid Spheres, Biophysical Journal 9 (1969) 1415-1425.

[32] Harriger, M.D., Supp, A.P., Swope, V.B., Boyce, S.T., Reduced engraftment and wound closure of cryopreserved cultured skin substitutes grafted to athymic mice, Cryobiology 35 (1997) 132-142.

[33] Jacobs, M.H., The simultaneous measurement of cell permeability to water and to dissolved substances, Journal of Cellular and Comparative Physiology 2 (1933) 427-444.

[34] Jacobs, M.H., Stewart, D.R., A simple method for the quantitative measurement of cell permeability, Journal of Cellular and Comparative Physiology 1 (1932) 71-82.

[35] Jomha, N.M., Lavoie, G., Muldrew, K., Schachar, N.S., McGann, L.E., Cryopreservation of intact human articular cartilage, Journal of Orthopaedic Research 20 (2002) 1253-1255.

[36] Karlsson, J.O.M., Toner, M., Long-term storage of tissues by cryopreservation: Critical issues, Biomaterials 17 (1996) 243-256.

[37] Kedem, O., Katchalsky, A., Thermodynamic Analysis of the Permeability of Biological Membranes to Non-Electrolytes, Biochimica Et Biophysica Acta 27 (1958) 229-246.

[38] Kleinhans, F.W., Membrane permeability modeling: Kedem-Katchalsky vs a two-parameter formalism, Cryobiology 37 (1998) 271-289.

[39] Kubitschek, H.E., Electronic Counting and Sizing of Bacteria, Nature 182 (1958) 234-235.

[40] Leibo, S.P., Field Trials of One-Step Diluted Frozen-Thawed Bovine Embryos, Cryobiology 20 (1983) 742-742.

[41] Lovelock, J.E., The Mechanism of the Protective Action of Glycerol against Haemolysis by Freezing and Thawing, Biochimica Et Biophysica Acta 11 (1953) 28-36.

[42] Luyet, B.J., Gehenio, P.M., Life and death at low temperatures (Biodynamica, Normandy, MO, 1940).

[43] Mazur, P., Cryobiology: the freezing of biological systems, Science 168 (1970) 939-949.

[44] Mazur, P., Freezing of living cells - mechanisms and implications, American Journal of Physiology 247 (1984) C125-C142.

[45] Mazur, P., Kinetics of Water Loss from Cells at Subzero Temperatures and the Likelihood of Intracellular Freezing, The Journal of General Physiology 47 (1963) 347-369.

[46] Mazur, P., The role of cell membranes in the freezing of yeast and other cells, Annals of the New York Academy of Science 125 (1965) 658-676.

[47] Mazur, P., Role of Intracellular Freezing in Death of Cells Cooled at Supraoptimal Rates, Cryobiology 14 (1977) 251-272.

[48] Mazur, P., Leibo, S.P., Chu, E.H., A two-factor hypothesis of freezing injury. Evidence from Chinese hamster tissue-culture cells, Experimental Cell Research 71 (1972) 345-355.

[49] McGann, L.E., in: (1984) Unpublished data.

[50] Mcgann, L.E., Differing Actions of Penetrating and Nonpenetrating Cryoprotective Agents, Cryobiology 15 (1978) 382-390.

[51] Mcgann, L.E., Turc, J.M., Determination of Water and Solute Permeability Coefficients, Cryobiology 17 (1980) 612-613.

[52] Mcgann, L.E., Turner, A.R., Turc, J.M., Microcomputer Interface for Rapid Measurements of Average Volume Using an Electronic Particle Counter, Medical & Biological Engineering & Computing 20 (1982) 117-120.

[53] Mcgrath, J.J., A Microscope Diffusion Chamber for the Determination of the Equilibrium and Non-Equilibrium Osmotic Response of Individual Cells, Journal of Microscopy-Oxford 139 (1985) 249-263.

[54] McGrath, J.J., Diller, K.R. (Eds.), Low Temperature Biotechnology: Emerging Applications and Engineering Contributions, ASME Press, New York, 1988, 273-330.

[55]   Miller, R.H., Mazur, P., Survival of Frozen-Thawed Human Red-Cells as a Function of Cooling and Warming Velocities, Cryobiology 13 (1976) 404-414.

[56]   Nygren, K.G., Andersen, A.N., Assisted reproductive technology in Europe, 1999. Results generated from European registers by ESHRE, Human Reproduction 17 (2002) 3260-3274.

[57]   Pegg, D.E., The current status of tissue cryopreservation, Cryoletters 22 (2001) 105-114.

[58]   Pegg, D.E., Freezing of Bone Marrow for Clinical Use, Cryobiology 1 (1964) 64-71.

[59]   Pegg, D.E., Diaper, M.P., Skaer, H.L., Hunt, C.J., The Effect of Cooling Rate and Warming Rate on the Packing Effect in Human-Erythrocytes Frozen and Thawed in the Presence of 2-M Glycerol, Cryobiology 21 (1984) 491-502.

[60]   Polge, C., Rowson, L.E.A., Fertilizing Capacity of Bull Spermatozoa after Freezing at-79-Degrees-C, Nature 169 (1952) 626-627.

[61]   Polge, C., Smith, A.U., Parkes, A.S., Revival of Spermatozoa after Vitrification and Dehydration at Low Temperatures, Nature 164 (1949) 666-666.

[62]   Rall, W.F., Factors Affecting the Survival of Mouse Embryos Cryopreserved by Vitrification, Cryobiology 24 (1987) 387-402.

[63]   Rasmussen, D.H., Macaulay, M.N., Mackenzie, A.P., Supercooling and Nucleation of Ice in Single Cells, Cryobiology 12 (1975) 328-339.

[64]   Robb, E.C., Bechmann, N., Plessinger, R.T., Boyce, S.T., Warden, G.D., Kagan, R.J., Storage media and temperature maintain normal anatomy of cadaveric human skin for transplantation to full-thickness skin wounds, Journal of Burn Care & Rehabilitation 22 (2001) 393-396.

[65]   Song, Y.C., Hagen, P.O., Lightfoot, F.G., Taylor, M.J., Smith, A.C., Brockbank, K.G.M., In vivo evaluation of the effects of a new ice-free cryopreservation process on autologous vascular grafts, Journal of Investigative Surgery 13 (2000) 279-288.

[66]   Song, Y.C., Khirabadi, B.S., Lightfoot, F., Brockbank, K.G.M., Taylor, M.J., Vitreous cryopreservation maintains the function of vascular grafts, Nature Biotechnology 18 (2000) 296-299.

[67] Staverman, A.J., Apparent Osmotic Pressure of Solutions of Heterodisperse Polymers, Recueil Des Travaux Chimiques Des Pays-Bas-Journal of the Royal Netherlands Chemical Society 71 (1952) 623-633.

[68] Staverman, A.J., The Theory of Measurement of Osmotic Pressure, Recueil Des Travaux Chimiques Des Pays-Bas-Journal of the Royal Netherlands Chemical Society 70 (1951) 344-352.

[69] Taylor, M.J., Clinical Cryobiology of Tissues - Preservation of Corneas, Cryobiology 23 (1986) 323-353.

[70] Terwilliger, T.C., Solomon, A.K., Osmotic Water Permeability of Human Red-Cells, Journal of General Physiology 77 (1981) 549-570.

[71] Walcerz, D.B., Diller, K.R., Quantitative Light-Microscopy of Combined Perfusion and Freezing Processes, Journal of Microscopy-Oxford 161 (1991) 297-311.

[72] Ward, C.A., Rate of Gas Absorption at a Liquid Interface, Journal of Chemical Physics 67 (1977) 229-235.

[73] Ward, C.A., Findlay, R.D., Rizk, M., Statistical Rate Theory of Interfacial Transport .1. Theoretical Development, Journal of Chemical Physics 76 (1982) 5599-5605.

[74] Wilmut, I., Rowson, L.E.A., Experiments on Low-Temperature Preservation of Cow Embryos, Veterinary Record 92 (1973) 686-690.

[75] Woods, E.J., Zieger, M.A.J., Lakey, J.R.T., Liu, J., Critser, J.K., Osmotic characteristics of isolated human and canine pancreatic islets, Cryobiology 35 (1997) 106-113.

[76] Zhu, Z.M., Jia, X.M., Chai, J.K., Gao, W.Y., Kong, Q.H., Clinical Use of Homograft Stored by Vitrification, Chinese Medical Journal 107 (1994) 574-576.

[77] Zieger, M.A.J., Tredget, E.E., McGann, L.E., Mechanisms of cryoinjury and cryoprotection in split-thickness skin, Cryobiology 33 (1996) 376-389.

[78] Zieger, M.A.J., Tredget, E.E., Sykes, B.D., McGann, L.E., Injury and protection in split-thickness skin after very rapid cooling and warming, Cryobiology 35 (1997) 53-69.

Figure 1-1 Osmotic response during the addition and dilution of cryoprotectants: non-permeating solutes
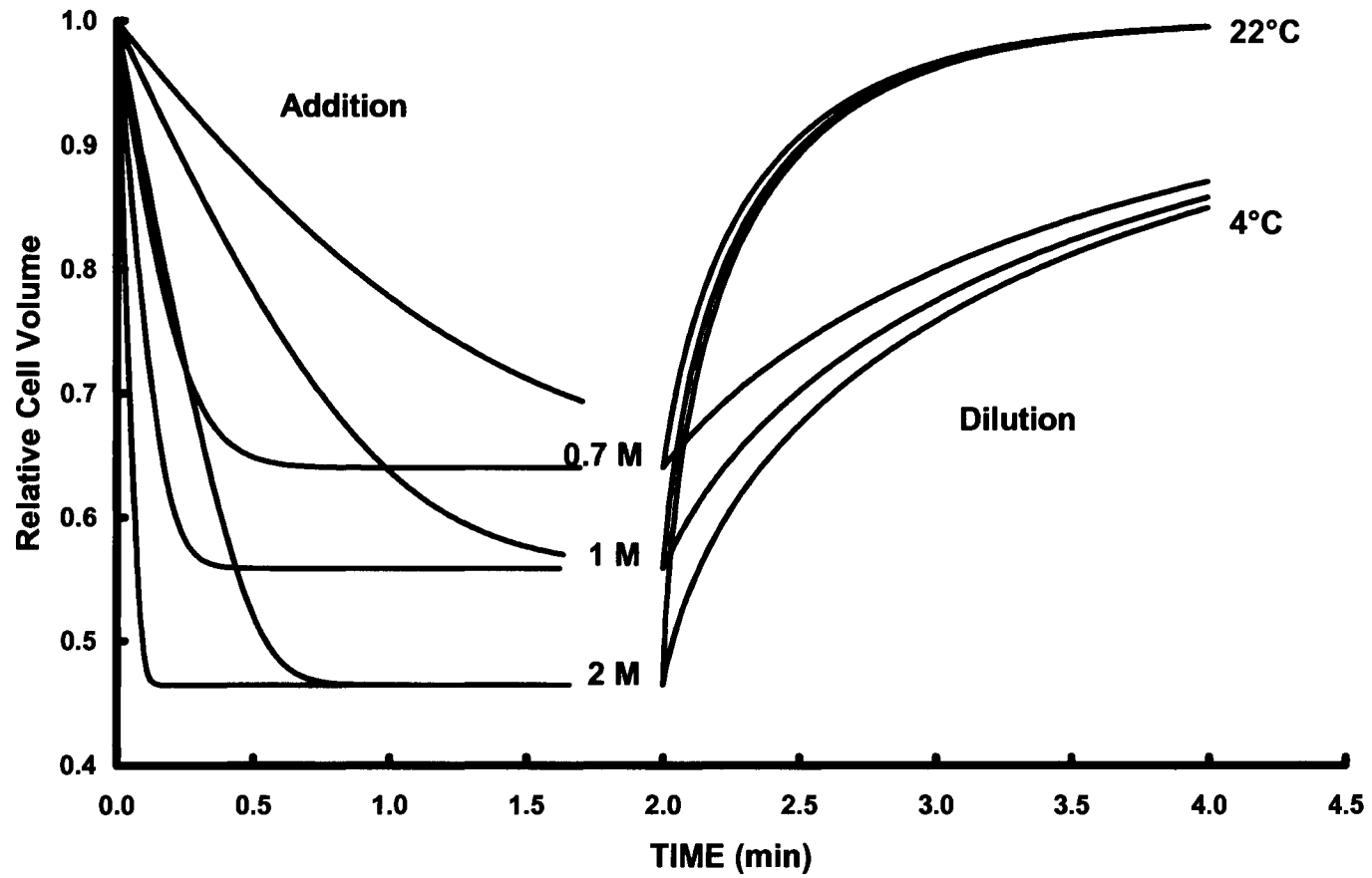
Figure 1-2 Osmotic response during the addition and dilution
of cryoprotectants: permeating solutes
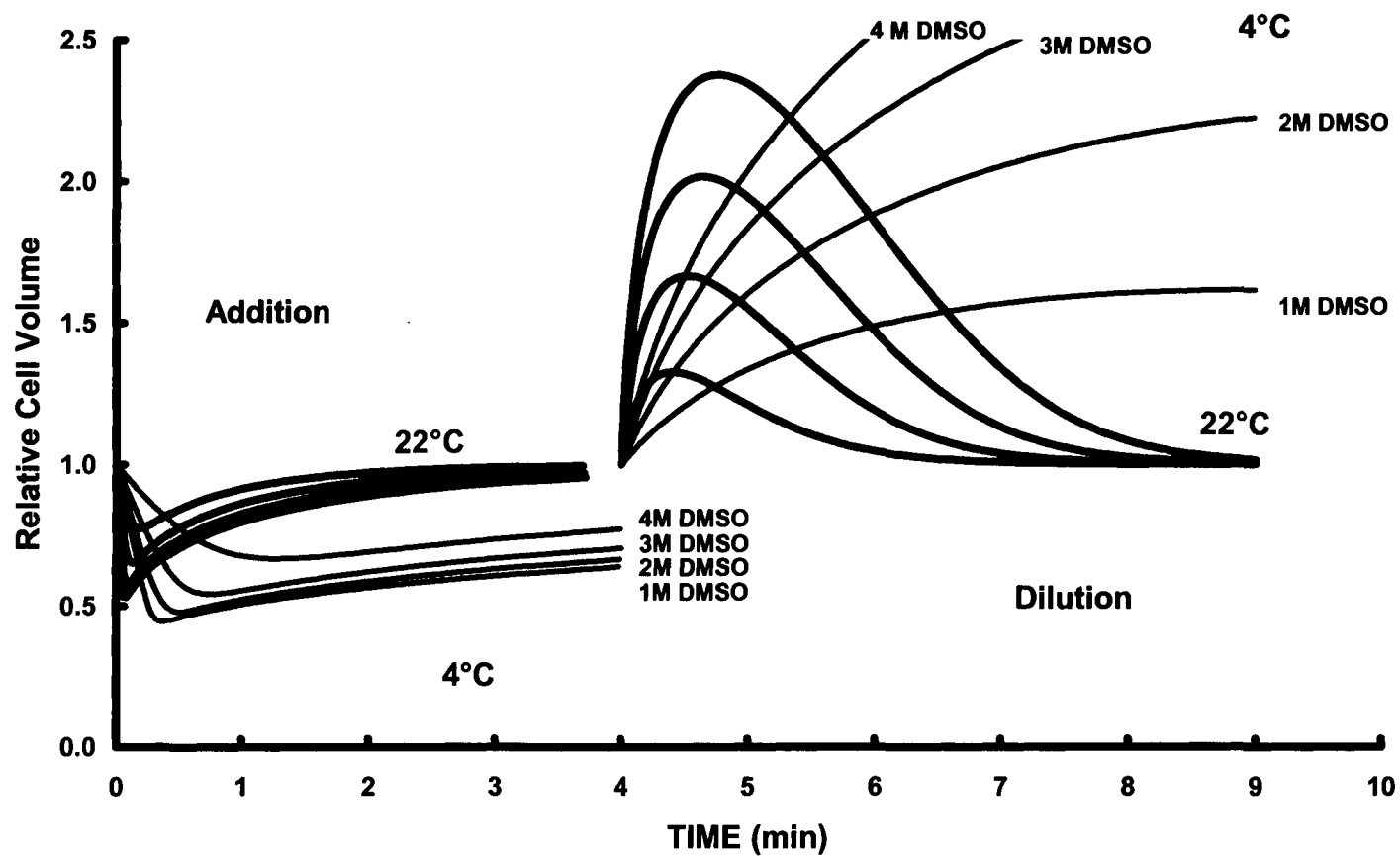
Chapter 2: The Effect of Cell Size Distribution on the Predicted Osmotic Response of Cells*

2.1 Introduction

Understanding the kinetics of cell osmotic response is a critical step in estimating water and solute fluxes across cell membranes, and in determining cellular osmotic permeability characteristics. Calculation of the osmotic properties requires measurements of the equilibrium cell volume and the non-equilibrium cell volume as a function of time. Estimates of the membrane hydraulic conductivity of the plasma membrane to water and various solutes are obtained by fitting these experimental data to theoretical predictions.

Since the 1950's, there have been a number of mathematical models developed to predict the osmotic parameters of cells [8,17,20]. Changes in cell volume caused by differences in concentration across the cell membrane have been used extensively to determine the permeability characteristics of cell membranes to both water and permeating solutes [16,17]. Currently, a mathematical model of the osmotic response of cells is obtained by applying the membrane mass transport equation [16] and the Boyle-van't Hoff equation [19] using numerical methods. In applying these equations, it is normally assumed that all the cells are the same size, (equal to the mean or mode of the population) and have the

36

same permeability characteristics. In cell populations with a distribution of cell sizes, cells will shrink or swell at different rates when exposed to anisotonic environments. The size distribution of a population of cells will affect the average osmotic response, as larger spherical cells take longer to reach their final volume than smaller cells. When there is a broad, non-Gaussian distribution of cell volumes, determining an 'average' volume that accurately represents the cell population is not trivial. Identifying the measure of central tendency for the cell population will affect the calculated osmotic parameters [4,13-15]. Armitage and Juss [4] showed that cell size distributions for keratocytes were positively skewed, which is typical for mammalian cells. They concluded that the mean was not an appropriate measure of central tendency, and suggested that the mode may be more applicable. The importance of cell water content in cryobiology and the effect of cell size distribution on a population of cells was recognized in a study by Cosman [6], that examined the distributions in properties needed to analyze water transport for a cell population such as area, permeability, initial water content and activation energy. The analysis was performed assuming a normal distribution of cell properties.

Electronic particle counters are commonly used to study equilibrium size distributions of cells [2-4,12-15,18,22] as well as to measure changes in mean or mode cell volume that occur over time during exposure to hypertonic and hypotonic solutions [1,4,5,10,11,21]. In kinetic studies, electronic particle counters are used to obtain rapid measurements of cell volumes that are then

37

used to determine the cell permeability characteristics using theoretical models. This technique has been applied to many cell types such as mouse lymphoblasts [5], human lymphocytes [21], sperm cells from various species [10], and human keratinocytes [1]. One of the benefits of using the electronic particle counter over optical methods is that it can rapidly and reproducibly collect data for the equilibrium and non-equilibrium volumes of the cell population [1]. Electronic particle counters have been used in the past to study both the time evolution of a cell population as a whole [5] and equilibrium size distributions [4]. Previous results have documented the time course of osmotic adaptation of a population distribution of cells [5]; but have not examined the time dependence of the distributions during osmotic volume change.

In the present study, the equipment and methods used allowed recording of both the volume of each cell, and the time at which it passed through the aperture of an electronic particle counter. This process allowed the time evolution of the cell size distribution to be monitored over short time intervals (1 sec) for moderately rapid-responding cells. Several parameters influence osmotic responses of cells, such as permeability parameters, surface area and volume. The common use of sampling cell suspensions during osmotic volume excursions to estimate volume changes introduces the question of the most appropriate measure of central tendency. This is the first detailed study on the use of cell size distributions to predict cellular osmotic parameters using theoretical simulations correlated with experimental measurements. Experiments

38

were conducted specifically for the purpose of analyzing the time-dependence of cell size distributions during osmotic changes in cell volume.

Calculated distributions based on hypothetical hydraulic conductivities and osmotically inactive fractions and actual initial cell size distributions were used to compare three different methods of obtaining the 'average' cell volume - the mean, median and mode - to determine which measure of central tendency best described the osmotic behavior of cell populations.

Mean

The mean is the most common measure of central tendency. When data is presented in a frequency distribution, the arithmetic mean computed from grouped data is given by the following formula:

(Eq. 2- 1)

$$\bar{x} = \frac{\sum_{i=1}^{k} m_i f_i}{\sum_{i=1}^{k} f_i}$$

where k is the number of class intervals, m_i is the midpoint of the ith class interval and f_i is the frequency of the ith class interval [7].

Median

The median of a set of numbers arranged in order of magnitude is either the middle value or the arithmetic mean of the middle two values. To compute the

39

median from grouped data, the first step is to define the class interval in which the median is located. This is done by finding the n/2 value, where n is the number of values in the sample. The median can then be computed using the following formula:

(Eq. 2- 2)

$$median = L_i + \frac{j_i}{f_i}(U_i - L_i)$$

where L_i is the lower limit of the interval containing the median, U_i is the upper limit of the interval containing the median, j_i is the number of observations away from reaching the median value after the lower limit of the interval containing the median has been reached, and f_i is the frequency of the interval containing the median [7].

Mode

The mode of a set of numbers is the value that occurs with the greatest frequency. To compute the mode from grouped data the first step is to locate the class interval in which the mode is located. This is done by finding the class interval with the highest number of samples. In the case of grouped data, from a frequency distribution, the mode can be obtained from the following formula:

(Eq. 2- 3)

$$mode = L_i + \left(\frac{\Delta_1}{\Delta_1 + \Delta_2}\right)(U_i - L_i)$$

40

where L_i is the lower class boundary of the class containing the mode, U_i is the upper class boundary of the class containing the mode, Δ_1 is excess of modal frequency over the frequency of the next lower class, and Δ_2 is excess of modal frequency over the frequency of the next higher class [24].

2.2 Osmotic Response of Cells of a Single Size

When a single cell is placed in an environment where the effective osmolality due to impermeant solutes outside the cell is greater than the osmolality of the solution inside the cell, water will move out of the cell. The membrane mass transport model [16] describes the rate of volume change:

(Eq. 2- 4)

$$\frac{dV}{dt} = L_p ART(\pi_i - \pi_e)$$

where L_p is the membrane hydraulic conductivity, A is the cell surface area, R is the universal gas constant, T is the absolute temperature, π_i is the intracellular osmolality and π_e is the extracellular osmolality.

The Boyle van't Hoff equation [19] is used to relate the cell volume, V, to the intracellular osmolality, π_i and the isotonic osmolality, π_o,

(Eq. 2- 5)

$$\frac{V}{V_o} = \frac{\pi_o}{\pi_i}(1 - v_b) + v_b$$

41

where V_o is the cell volume at the isotonic osmolality π_o, and v_b is the osmotically inactive fraction of the isotonic cell volume.

2.3   Osmotic Response of Cells with Size Distributions

In order to compare a theoretical evolution of the size distribution of a population of cells with experimental measurements, the measured initial size distribution of the cells used for the experiment was chosen as the basis for the calculations. Volumes at different times for each cell in the distribution were calculated from simulations using in-house software.   This distribution program creates a population of 10^5 cells, all with the specified permeability parameters, and with isotonic volumes distributed to fit a selected volume distribution.   The program then calculates the osmotic response of each individual cell by applying (Eq. 2-4) and (Eq. 2- 5).   This allows theoretical size distributions to be generated at the time intervals during osmotic shrinkage of the population.

2.4   Materials and Methods

2.4a   Cell culture

Two cell lines with different cell size distributions were used to investigate the effects of cell size distribution on the osmotic response of the cells.   The V-79W line of Chinese hamster fibroblasts has a narrow, non-Gaussian size distribution. The fibroblasts were incubated at $37°C$ in an atmosphere of 95% (v/v) air + 5% (v/v) carbon dioxide in a supplemented medium consisting of minimum essential medium (MEM) with Hanks' salts, 16 mM sodium bicarbonate, 2 mM L-

42

glutamine, 10% (v/v) fetal bovine serum and antibiotics (penicillin G (50 μg/mL), streptomycin (50 μg/mL)) (all components from GIBCO Laboratories, Grand Island, NY). Cells were maintained in tissue culture flasks (25 cm²; Corning Glass Works, Corning, NY) and harvested by exposure to a 0.25% trypsin solution (GIBCO) for 10 min at 37°C. Single fibroblast cells were re-suspended in the supplemented MEM before being used experimentally.

The second cell line was the Madin-Darby Canine Kidney (MDCK; CCL 34, American Type Culture Collection) cell line, with a broad cell size distribution. These cells were cultured at 37°C in an atmosphere of 95% (v/v) air + 5% (v/v) carbon dioxide in an antibiotic–free minimum essential medium (MEM) containing 10% (v/v) fetal bovine serum (all components from Gibco Laboratories). Cells were maintained in tissue culture flasks (25 cm², Corning Glass Works) before being dissociated into single cells by exposure to a 0.25% trypsin-EDTA solution (GIBCO) for 10 min at 37°C. The MDCK cells were re-suspended into the cell-specific tissue culture medium before being used experimentally. For both cell lines, samples were examined microscopically to ensure a single-cell suspension, with few aggregates.

2.4b Experimental volume distributions

Electronic particle counters have been used previously to determine the membrane permeability characteristics of cells [1,5,10,21]. Cells passing through the aperture in an electronic counter displace a volume of the conducting fluid

43

resulting in a voltage pulse proportional to the volume of the cells. In this study, a Coulter counter (model ZB1, Coulter Inc, Hialeah, FL) was connected to a personal computer via a pulse-height analyzer (The Great Canadian Computer Company, Spruce Grove, AB, Canada). This device, with the accompanying Cell Size Analyzer software, recorded the time of passage and size of each cell passing through the Coulter aperture [22]. A calibration factor, determined using latex beads of known sizes (Coulter Calibration Standards: 10.0 μm diameter), was used to determine cell volumes. Histograms were generated over 1 second intervals during the course of osmotic shrinkage. Measurements were accumulated for ±0.5 seconds of the stated interval. For the experimental measurements, bin sizes were set at 194 μm^3 (22 bins) and 74.4 μm^3 (25 bins) for MDCK and V-79W cells, respectively, in order to have a sufficient number of cells in each bin to generate the histograms. The total cell count for the MDCK and V-79W cells were 23,913 and 55,155, respectively, in order to maintain the probability of multiple cells simultaneously passing through the Coulter aperture to <<1%.

2.4c Theoretical volume distributions created to compare to experimental volume distributions

Theoretical volume distributions were created from the measured experimental isotonic volume distributions, using the same resolution as the Cell Size Analyzer data acquisition software, i.e. 256 volume levels. No further binning was performed during the simulations. The effective surface area for osmotic transport was assumed to vary as the surface of a sphere. As in common

44

practice, mean volumes were used to calculate L_p from the experimental data. These same values of the hydraulic conductivity, osmotically inactive fraction, temperature and solution concentrations were used to calculate theoretical volume distributions as a function of time to compare with the experimental distributions for V-79W and MDCK cells.

2.4d Hypothetical distributions created to compare various measures of central tendency

Four initial, hypothetical cell size distributions (Table 2-1) were created using built-in functions in Microsoft Excel (NORMDIST and LOGNORMDIST), and were then used as the initial distributions in the simulation program to calculate distributions as a function of time during osmotic shrinkage. From these hypothetical size distributions the three measures of central tendency were calculated as a function of time. The three calculated 'averages' as a function of time were independently fit to the transport equations in order to derive permeability parameters from the resulting distributions. This is equivalent to the use of experimental measurements of cell volumes in the determination of osmotic permeability parameters. The resulting parameters were then compared to the actual parameters used in the simulation. Figure 2-1 outlines this process and shows the hypothetical parameters used in the simulation.

45

Table 2-1: Hypothetical cell size distributions

Description	Distribution	Mean	Standard Deviation
Normal Narrow	Normal Distribution	Mean = 1280	128
Normal Wide	Normal Distribution	Mean = 1280	384
Lognormal Narrow	Lognormal Distribution	(ln) mean = 6.3	(ln) standard deviation = 0.3
Lognormal Wide	Lognormal Distribution	(ln) mean = 6.3	(ln) standard deviation =1.0

2.4e Osmotic experiments

Experimental solutions were prepared by diluting a 10X isotonic phosphate buffered saline solution (Gibco). V-79W fibroblast or MDCK cells in an isotonic solution (300 mOsmol/kg) were abruptly transferred into a well-mixed hypertonic solution of 1790 mOsmol/kg or 1530 mOsmol/kg respectively at 22°C, and the cell volumes captured as a function of time. In these experimental solutions, cells shrink down to their equilibrium size and remain shrunken over the duration of the experiment. The osmolalities of the experimental solutions were measured with a freezing point depression osmometer (model 5004, Precision Systems, Inc.).

2.5 Results

2.5a Experimental cell size distribution as a function of time

Experimental cell size distributions as functions of time for the MDCK and V-79W cells were used to calculate experimental osmotic parameters. Using the mean as the measure of central tendency as is normally done in published studies, and fitting the mean of the experimental volume distribution to the transport equations using a least square error method, gave the values listed in Table 2-2. The values of these parameters are similar to those previously reported for the MDCK cells [9] and for the V-79W cells [23].

Figure 2-2a shows a sample experimentally-measured cell size distribution as a function of time during the course of osmotic shrinkage for MDCK cells. The hydraulic conductivity and osmotically inactive fraction for this particular run were 0.19 $\mu m^3/\mu m^2$/atm/min and 0.40 respectively. Similar results for V-79W cells are shown in Figure 2-3a. The hydraulic conductivity and osmotically inactive fraction for this particular run were 1.19 $\mu m^3/\mu m^2$/atm/min and 0.36 respectively.

Table 2-2: Average experimental values calculated using the mean (n=5)

	MDCK Cells	V-79W Cells
Isotonic Volume	1715 μm^3	738 μm^3
L_p	0.19 ± 0.02 $\mu m^3/\mu m^2$/atm/min	1.09 ± 0.2 $\mu m^3/\mu m^2$/atm/min
v_b	0.39 ± 0.1	0.37 ± 0.1

2.5b Theoretical cell size distributions as functions of time

Starting with the measured isotonic volume distributions (i.e. the initial isotonic distributions shown in Figures 2-2a and 2-3a), theoretical size distributions were calculated as a function of time in the hypertonic solutions. Figure 2-2b shows the theoretical size distribution for the MDCK cells as a function of time in a 1530 mOsmol/kg solution using an L_p of 0.19 $\mu m^3/\mu m^2/atm/min$ and an osmotically inactive fraction of 0.40 at a temperature of 22°C. Similarly, Figure 2-3b shows the theoretical size distribution for the V-79W cells as a function of time using an L_p of 1.19 $\mu m^3/\mu m^2/atm/min$ and an osmotically inactive fraction of 0.36 in a 1790 mOsmol/kg solution at a temperature of 22°C.

2.5c Effects of various measures of central tendency

Figure 2-4 shows four different hypothetical theoretical cell size distributions (lognormal wide, lognormal narrow, normal wide, normal narrow), used to generate histograms of size distributions as functions of time during osmotic shrinkage. From these size distributions, the mean, median, and mode volumes as functions of time were calculated. Fitting these curves to the osmotic transport equations resulted in the values for the hydraulic conductivity shown in Table 2-3. These results were compared to the value of the hydraulic conductivity for individual cells (1.5 $\mu m^3/\mu m^2/atm/min$) used in the simulations, and the error (%) was determined.

48

Table 2-3: Hydraulic conductivity values calculated using different measures of central tendency for various theoretical cell size distributions

Distribution	Theoretical L_p ($\mu m^3/\mu m^2/atm/min$)	Calculated L_p ($\mu m^3/\mu m^2/atm/min$)		
		Mean	**Median**	**Mode**
Normal Narrow	1.5	1.51 (0.97 % error)	1.54 (2.88 % error)	1.53 (1.85 % error)
Normal Wide	1.5	1.49 (0.64 % error)	1.54 (2.87 % error)	1.59 (5.82 % error)
Lognormal Narrow	1.5	1.51 (0.75 % error)	1.57 (4.60 % error)	1.68 (11.70 % error)
Lognormal Wide	1.5	1.38 (7.85 % error)	1.61 (7.37 % error)	1.81 (20.80 % error)

2.6 Discussion

The size distribution for both the MDCK and the V-79W cells shown in Figures 2-2a, 2-2b, 2-3a, and 2-3b indicate that the shape of the size distribution changes during osmotic shrinkage. This is expected because cells with identical permeability characteristics have a distribution in cell size and therefore will shrink or swell at different rates when exposed to anisotonic conditions. Smaller cells, with a higher surface-area-to-volume ratio, will respond more rapidly than larger cells. This is supported by experimental observations and theoretical calculations. Therefore a population of cells will have different shrinkage kinetics than a single cell (or cells with a uniform size), and one may need to choose carefully the measure of central tendency to use with the single-cell membrane

49

mass transport equation to obtain the membrane hydraulic conductivity for a population of cells.

The experimental system is limited by the number of cells available. When sampling at time intervals during osmotic shrinkage, there are too few cells to create experimental distributions with sufficient accuracy for comparison of the mean, median, and mode of the experimental data. Theoretical distributions, created from the experimental, isotonic distributions allowed a large number of cells (10^5) to be used for each time increment, compared to (~200) for the experimental data. While the experimental distributions were created over 1 second time intervals and the theoretical distributions were taken at specific times, not cumulated over a time interval, Figures 2-2 and 2-3 show that the experimental and theoretical distributions are similar. These similarities in the shapes of the experimental and theoretical distributions indicate that the theoretical distributions can provide insight into the kinetics of osmotic responses in populations of cells.

Sampling a population is a statistical method to track changes in a population as a function of time. Unlike the theoretical distributions where each cell in the population is tracked throughout the course of the simulation, the experimental population is sampled continuously and individual cells cannot be tracked. Hypothetically, values of L_p could be obtained by fitting (Eq. 2- 4) and (Eq. 2- 5)

to the unmodified Coulter data but this requires fitting for the isotonic volume, which itself includes an assumption of a measure of central tendency.

Changes in cell volume, brought about by changes in the external solute concentration, have been used to determine cell membrane permeability characteristics to both water and to solutes. Fundamental to these experiments is the ability to determine values for the hydraulic conductivity. The values for the hydraulic conductivity may be different depending on the measure of central tendency used to analyze the osmotic response of cells. From the analysis of the various methods of central tendency, it was found that there was some degree of error with each measure of central tendency that was investigated. For normal distributions all measures of central tendency gave fairly low errors with the mode giving the largest error when the distribution was "wide". It should be noted that, although the distribution is normal initially and after equilibrium in the hypertonic solution, it diverges from a normal distribution during the course of osmotic shrinkage, as smaller cells in the population shrink more rapidly than larger cells because of their higher surface area to volume ratio. Since the order of a cell in the distribution cannot change if the bins over volume and time were infinitely thin (impossible experimentally), then the cell that is the median or mode would remain unchanged. However, in real experimental systems, there is a finite number of bins, with one bin representing a collection of cells. The cells that make up that collection will change as individual cells cross the bin boundaries. For both normal and skewed experimental distributions, the mean,

51

median and mode follow different kinetics during shrinkage, so will result in different values for the hydraulic conductivity. For lognormal (skewed distributions), which are more representative of actual cell size distributions, the mean and median gave comparable errors and the mode was found to be the worst measure of central tendency to use, with errors up to 20.80% for the wide lognormal distribution investigated. The results validate the current practice in published literature of using the mean cell volume to analyze cell osmotic kinetics [1,5,10,11,21], contrary to published suggestions that the mode should be used [4].

2.7 Conclusions

Analysis of the experimental data for both the MDCK and the V-79W cells, two cell types with different isotonic volumes and different cell size distributions, showed that the shapes of the cell size distributions change with time during osmotic volume changes. This implies that one must carefully choose the measure of central tendency to use when analyzing the osmotic response of cells with size distributions. A novel tool was developed to test which method of central tendency should be used when analyzing osmotic data. It was clearly shown that the mean or median cell volume rather than the mode should be used to analyze osmotic data. However, in many cases the errors associated with using various measures of central tendency were small and may be acceptable considering other experimental errors in measuring osmotic permeability parameters.

52

2.8 References

[1] Acker, J.P., Pasch, J., Heschel, I., Rau, G., McGann, L.E., Comparison of optical measurement and electrical measurement techniques for the study of osmotic responses of cell suspensions, Cryoletters 20 (1999) 315-324.

[2] Adams, R.B., Voelker, W.H., Gregg, E.C., Electrical Counting and Sizing of Mammalian Cells in Suspension - an Experimental Evaluation, Physics in Medicine and Biology 12 (1967) 79-92.

[3] Anderson, E.C., Petersen, D.F., Cell Growth and Division .2. Experimental Studies of Cell Volume Distributions in Mammalian Suspension Cultures, Biophysical Journal 7 (1967) 353-364.

[4] Armitage, W.J., Juss, B.K., Osmotic response of mammalian cells: Effects of permeating cryoprotectants on nonsolvent volume, Journal of Cellular Physiology 168 (1996) 532-538.

[5] Buckhold, B., Adams, R.B., Cregg, E.C., Osmotic Adaptation of Mouse Lymphoblasts, Biochimica Et Biophysica Acta 102 (1965) 600-608.

[6] Cosman, M.D., Effects of cooling rate and supercooling on the formation of ice in a cell population, PhD, MIT, 1983.

[7] Daniel, W.W., Biostatistics: A foundation for analysis in the health sciences (John Wiley & Sons Inc., 1995).

[8] Davson, W.W., Danielli, J.F., The permeability of natural membranes (Cambridge: The University Press, 1952).

[9] Farinas, J., Verkman, A.S., Cell volume and plasma membrane osmotic water permeability in epithelial cell layers measured by interferometry, Biophysical Journal 71 (1996) 3511-3522.

[10] Gilmore, J.A., McGann, L.E., Ashworth, E., Acker, J.P., Raath, J.P., Bush, M., Critser, J.K., Fundamental cryobiology of selected African mammalian spermatozoa and its role in biodiversity preservation through the development of genome resource banking, Animal Reproduction Science 53 (1998) 277-297.

[11] Gilmore, J.A., Mcgann, L.E., Liu, J., Gao, D.Y., Peter, A.T., Kleinhans, F.W., Critser, J.K., Effect of Cryoprotectant Solutes on Water Permeability of Human Spermatozoa, Biology of Reproduction 53 (1995) 985-995.

[12] Gregg, E.C., Steidley, K.D., Electrical Counting and Sizing of Mammalian Cells in Suspension, Biophysical Journal 5 (1965) 393-405.

53

[13]   Grover, N.B., Bensasso.S, Doljansk.F, Naaman, J., Electrical Sizing of Particles in Suspensions .3. Rigid Spheroids and Red Blood-Cells, Biophysical Journal 12 (1972) 1099-1117.

[14]   Grover, N.B., Naaman, J., Bensasso.S, Doljansk.F, Electrical Sizing of Particles in Suspensions .I. Theory, Biophysical Journal 9 (1969) 1398-1414.

[15]   Grover, N.B., Naaman, J., Bensasso.S, Doljansk.F, Nadav, E., Electrical Sizing of Particles in Suspensions .2. Experiments with Rigid Spheres, Biophysical Journal 9 (1969) 1415-1425.

[16]   Jacobs, M.H., Stewart, D.R., A simple method for the quantitative measurement of cell permeability, Journal of Cellular and Comparative Physiology 1 (1932) 71-82.

[17]   Kedem, O., Katchalsky, A., Thermodynamic Analysis of the Permeability of Biological Membranes to Non-Electrolytes, Biochimica Et Biophysica Acta 27 (1958) 229-246.

[18]   Kubitschek, H.E., Electronic Counting and Sizing of Bacteria, Nature 182 (1958) 234-235.

[19]   Lucke, B., McCutcheon, M., The Living Cell as an Osmotic System and its Permeability to Water, Physiological Reviews 12 (1932) 68-139.

[20]   Mazur, P., Kinetics of water loss from cells at subzero temperatures and the likelihood of intracellular freezing, The Journal of General Physiology 47 (1963) 347-369.

[21]   Mcgann, L.E., Turc, J.M., Determination of Water and Solute Permeability Coefficients, Cryobiology 17 (1980) 612-613.

[22]   Mcgann, L.E., Turner, A.R., Turc, J.M., Microcomputer Interface for Rapid Measurements of Average Volume Using an Electronic Particle Counter, Medical & Biological Engineering & Computing 20 (1982) 117-120.

[23]   Rule, G.S., Law, P., Kruuv, J., Lepock, J.R., Water Permeability of Mammalian-Cells as a Function of Temperature in the Presence of Dimethylsulfoxide - Correlation with the State of the Membrane-Lipids, Journal of Cellular Physiology 103 (1980) 407-416.

[24]   Spiegel, M.R., Schaum's outline of theory and problems of statistics, in: (McGraw-Hill Inc., 1991).
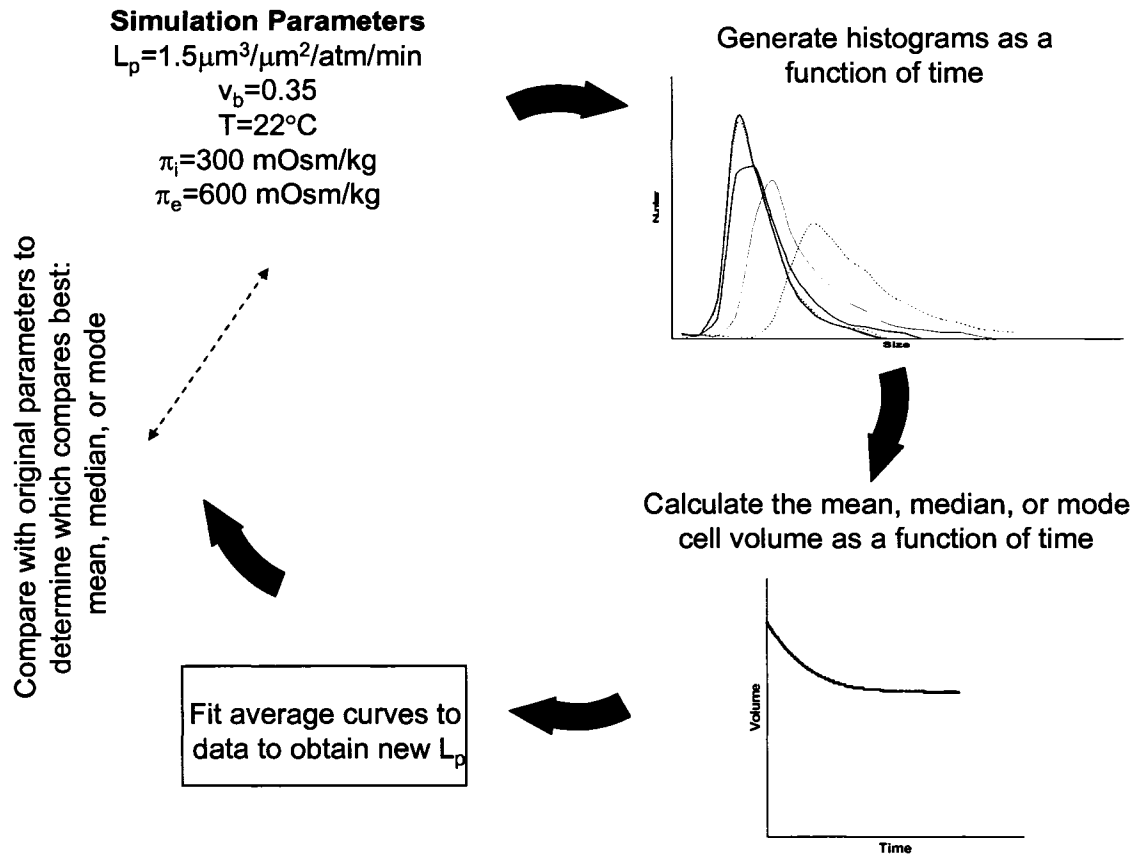
Figure 2-1: Outline of the process used to create theoretical distributions in order to compare the various measures of central tendency
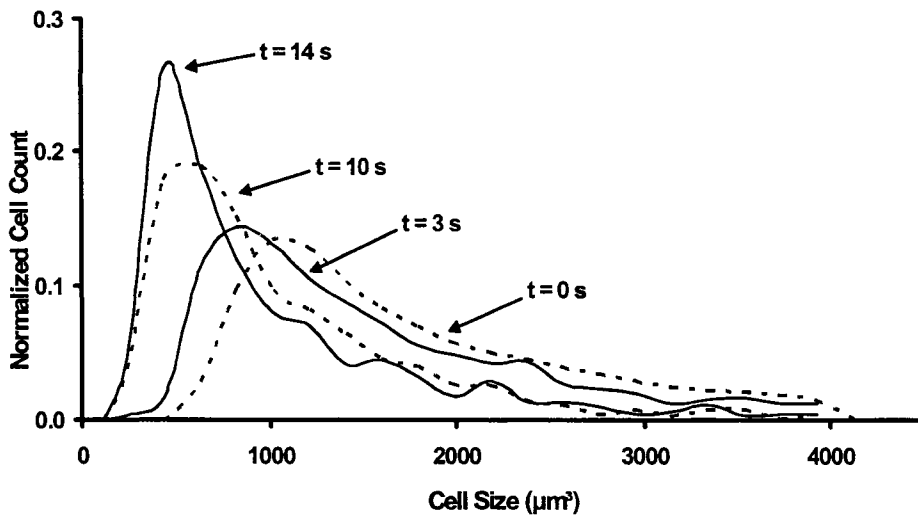
Figure 2-2a: Experimental MDCK cell size distribution as a function of time (L_p = 0.19 $\mu m^3/\mu m^2$/atm/min, v_b= 0.40, solution concentration = 1530 mOsmol/kg)
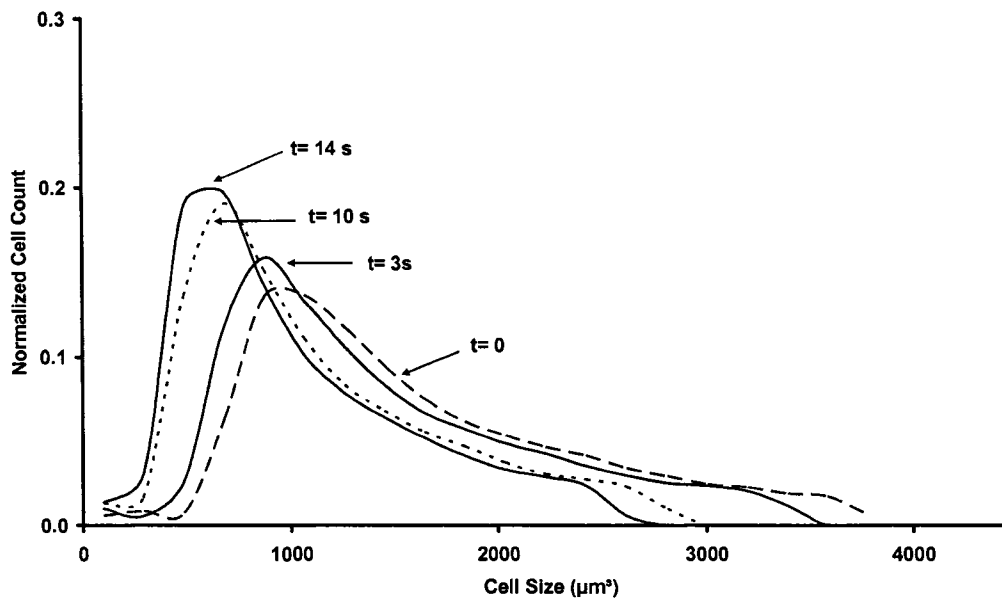
Figure 2-2b: Theoretical MDCK cell size distribution as a function of time using an L_p of 0.19 $\mu m^3/\mu m^2$/atm/min and a v_b of 0.40, (solution concentration = 1530 mOsmol/kg)

56
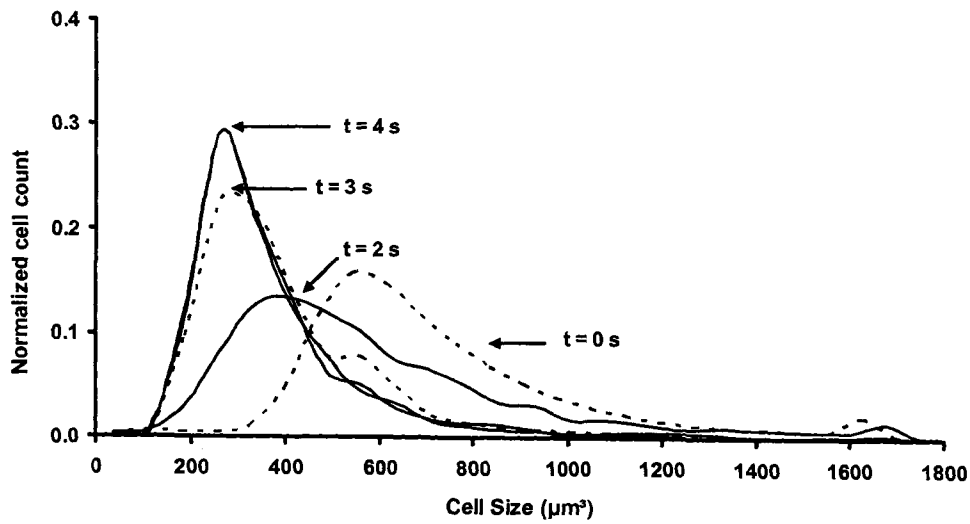
Figure 2-3a: Experimental V-79W cell size distribution as a function of time (L_p = 1.19 $\mu m^3/\mu m^2$/atm/min, v_b= 0.36, solution concentration = 1790 mOsmol/kg)
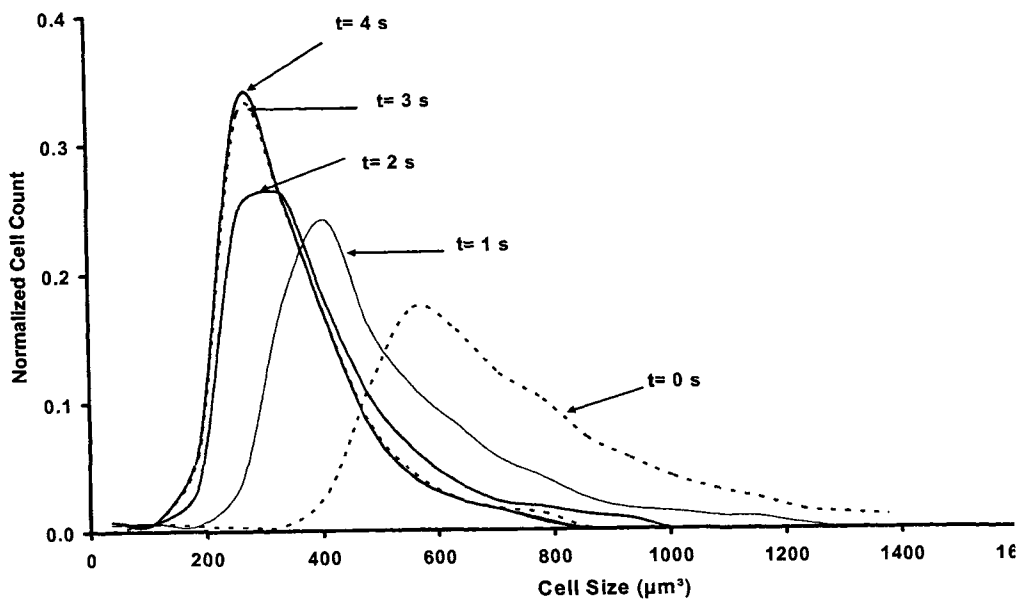
Figure 2-3b: Theoretical V-79W cell size distribution as a function of time using an L_p of 1.19 $\mu m^3/\mu m^2$/atm/min and a v_b of 0.36, (solution concentration = 1790 mOsmol/kg)

57
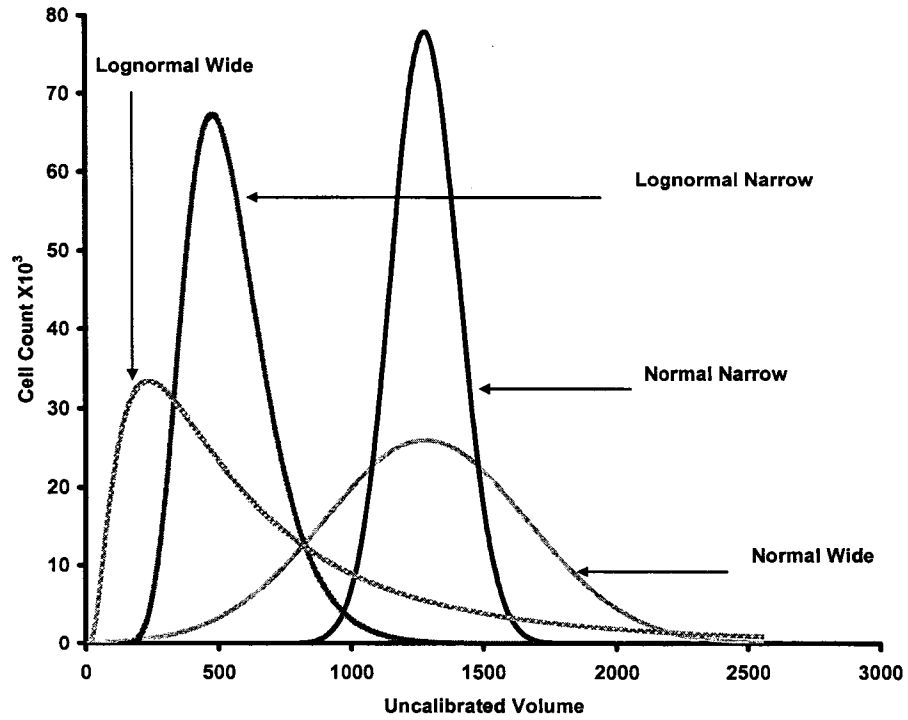
Figure 2-4: Theoretical cell size distributions: lognormal wide, lognormal narrow, normal wide, normal narrow

58

Chapter 3: Cryoprotectant Equilibration in Tissues[*]

3.1 Introduction

Cryopreservation protocols often require the use of cryoprotective compounds to improve the survival of cells and tissues upon freezing [1,2,17,20,23], and to moderate the normally lethal effects of extracellular salt concentration, intracellular ice and ice in the matrix of tissues. In traditional cryopreservation of cells in suspension, cryoprotectants are used to manipulate the intracellular and extracellular freezing-point dependence on concentration and thus the amount of ice formed at a given temperature. Many current approaches towards tissue preservation use high concentrations of cryoprotectants and high cooling rates with the aim of vitrifying the tissue, thereby avoiding problems resulting from ice formation inside tissues during traditional freezing protocols [10]. For both traditional cryopreservation and vitrification, the first step in the preservation of cells or tissues is often the movement of a permeating cryoprotectant into the cells or tissues. The success of a particular protocol normally depends on the concentration of cryoprotectant inside the cell or tissue. The cryoprotectant enters the cells or tissues by thermodynamic equilibration with the surroundings. In the reverse case, thermodynamic equilibration also drives the removal of permeating cryoprotectants by a dilution solution at the end of the preservation process when the cells or tissues are being readied for use. Thus, an

---

59

understanding of cryoprotectant equilibration is necessary in optimizing preservation protocols.

In order to develop successful cryopreservation protocols, it is necessary to determine the final equilibrium concentration of the selected cryoprotectants in the tissue. Three main experimental methods are used to measure cryoprotectant concentrations in tissues: proton nuclear magnetic resonance (H-NMR), magnetic resonance (MR) imaging and high performance liquid chromatography (HPLC). Proton NMR has been used successfully in the past as a rapid and effective method to measure the final equilibrium concentrations of cryoprotectants in various tissues including skin [29], corneas [26,27], articular cartilage [23], kidney tissue [15,16], liver tissue [11,12,15,16], arteries [1], and heart valves [20]. Nuclear magnetic resonance spectroscopy provides a quantitative measurement of absolute concentrations of species in aqueous solutions. The second method that can be used is MR imaging. Magnetic resonance imaging is a common non-destructive technique used to quantify the concentration of molecules inside a 3D structure [2]. Magnetic resonance imaging techniques have been developed to quantify the concentration of cryoprotectants in tissues such as embryos [14] and engineered dermal replacements [2], allowing examination of temporal and spatial distribution of water and cryoprotectant within a tissue. The third method used to determine the concentration of cryoprotectant in a tissue sample is HPLC, which has been used to determine the concentration of dimethyl sulfoxide in porcine myocardium [4].

Using the above techniques, there have been reports of tissues having equilibrium cryoprotectant concentrations lower than that of the surrounding carrier solution [2,11,23,26,29]. Table 3-1 illustrates that there have been many reports of tissues in equilibrium with differences in concentration between the inside and the outside, and the degree of these differences appear to vary with the type of tissue. The first three entries are for arteries [1,28], myocardium [4] and heart valves [20] where the equilibrium cryoprotectant concentration within the tissue approaches that of the external medium. The lower entries in Table 3-1 for skin [29], cartilage [23,24], corneas [26,27] and liver tissue [12] appear to reach equilibrium at a lower concentration than the external medium. The purpose of this paper is to point out the role of an equilibrium pressure differential in the equilibrium cryoprotectant concentration in the tissues.

61

Table 3-1:   Various experimental results from the literature

Tissue	Cryoprotectant	Relative Tissue Concentration
Rabbit arteries	DMSO	99-100% [1,2]
	Ethylene glycol	94%[†] [28]
Porcine myocardium	DMSO	100% [4]
Porcine heart valves	DMSO	~100% [20]
Freeze-dried cross-linked collagen	DMSO	~60% [2]
Skin	Glycerol	44-69% [29]
Porcine articular cartilage	DMSO	70% [23]
Ovine articular cartilage	DMSO	88% [24]
Corneas	DMSO	82-88% [26,27]
Liver tissue	DMSO	55-75% [11]
Rat hepatocytes (Sandwiched between two layers of collagen)	DMSO	65-68% [25]

[†] 94% equilibration was the result after one hour of exposure which was all the time investigated

There is confusion in the literature as to the role of pressure in tissue equilibration. Levin makes a model of transport in tissues assuming 4-component ideal dilute solutions [21]. Levin considers transport, while our paper addresses equilibrium. However, we note that while Levin included the possibility of a pressure differential in the water transport equation, the role of pressure in the solute transport was not included. Thus a simple yet careful look at the role of pressure on solute equilibrium is necessary. Eventually solute transport equations will need to be revisited as well. A thermodynamic analysis shows that the equilibrium concentration of cryoprotectant inside the tissue is either equal to, or lower than the cryoprotectant concentration of the surrounding solution, depending on whether the tissue can maintain an equilibrium pressure differential above the surrounding solution.

3.2   A Model Based on Ideal Dilute Solution Equations

Consider the equilibration between the extracellular solution and tissue shown schematically in Figure 3-1, where N is the number of moles of water (1), cryoprotectant (2), "biological component" (3) within the tissue, and extracellular solute in the carrier solution (4). It is assumed that water and cryoprotectant are free to cross the solution-tissue boundary and that the "biological component" (e.g. - the matrix) stays in the tissue and that any additional carrier solution solute stays outside of the tissue. The entire system is held at a constant temperature (T). At thermodynamic equilibrium, the chemical potential of the water inside the tissue (μ_1^i) will equal the chemical potential of the water outside the tissue (μ_1^o).

63

Similarly, at equilibrium, the chemical potential of the cryoprotectant inside the tissue (μ_2^i) will equal the chemical potential of the cryoprotectant outside the tissue (μ_2^o).

(Eq. 3- 1)

$$\mu_1^i = \mu_1^o$$

(Eq. 3- 2)

$$\mu_2^i = \mu_2^o$$

A common misconception is that (Eq. 3- 2) implies that at thermodynamic equilibrium the *concentration* of the cryoprotectant in the solution surrounding the tissue and the *concentration* of the cryoprotectant in the solution within the tissue will be equal. As the chemical potentials may, in general, depend on concentration and pressure, only for situations with no pressure difference between the inside of the tissue and the outside, will (Eq. 3- 2) imply cryoprotectant concentrations are equal.

For ideal, dilute solutions in the tissue and carrier solutions, the chemical potential equations are written as follows [3]:

(Eq. 3- 3)

$$\mu_1^i\left(T, P^i, x_2^i, x_3^i\right) = \mu_1^*\left(T, P^{Ref}\right) + v_1^*\left(P^i - P^{Ref}\right) - RTx_2^i - RTx_3^i$$

(Eq. 3- 4)

$$\mu_1^o\left(T, P^o, x_2^o, x_4^o\right) = \mu_1^*\left(T, P^{Ref}\right) + v_1^*\left(P^o - P^{Ref}\right) - RTx_2^o - RTx_4^o$$

64

(Eq. 3- 5)

$$\mu_2^i\left(T,P,x_2^i\right)=\psi_2\left(T,P^{Ref}\right)+v_2^*\left(P^i-P^{Ref}\right)+RT\ln\left(x_2^i\right)$$

(Eq. 3- 6)

$$\mu_2^o\left(T,P,x_2^o\right)=\psi_2\left(T,P^{Ref}\right)+v_2^*\left(P^o-P^{Ref}\right)+RT\ln\left(x_2^o\right)$$

where P is pressure, R is the universal gas constant and x is mole fraction. P^{Ref} is a reference pressure. The pressure on the inside of the tissue is assumed to be uniform. The subscripts 1, 2, 3 and 4 denote the water, cryoprotectant, "biological component" and extracellular solute, respectively. The superscripts i and o refer a quantity to the intracellular and extracellular solutions respectively. v_1^* and v_2^* are the partial molar volumes of components 1 and 2 respectively. μ_1^* and μ_2^* are chemical potentials of the pure components. The standard state for the solvent, water, is usually taken to be pure water. The function ψ_2 is related to the standard state for the cryoprotectant usually taken to be infinite dilution. In the above equations it has been assumed that the partial molar volumes are independent of pressure.

Substituting (Eq. 3- 3) and (Eq. 3- 4) into (Eq. 3- 1) gives:

(Eq. 3- 7)

$$\mu_1^*\left(T,P^{Ref}\right)+v_1^*\left(P^i-P^{Ref}\right)-RTx_2^i-RTx_3^i=\mu_1^*\left(T,P^{Ref}\right)+v_1^*\left(P^o-P^{Ref}\right)-RTx_2^o-RTx_4^o$$

Simplifying (Eq. 3- 7) results in:

(Eq. 3- 8)

$$v_1^*\left(P^o-P^i\right)=RT\left(x_2^o+x_4^o-x_2^i-x_3^i\right)$$

65

Substituting (Eq. 3- 5) and (Eq. 3- 6) into (Eq. 3- 2) gives:

(Eq. 3- 9)

$$v_2^* \left(P^o - P^i \right) = RT \ln\left(\frac{x_2^i}{x_2^o} \right)$$

Equating the pressure differences in (Eq. 3- 8) and (Eq. 3- 9) results in:

(Eq. 3- 10)

$$v_2^* \left(x_2^o + x_4^o - x_2^i - x_3^i \right) = v_1^* \ln\left(\frac{x_2^i}{x_2^o} \right)$$

3.3   Implications of the Model

For a freely expanding system (i.e. $P^0 = P^i$), (Eq. 3- 9) implies $x_2^i = x_2^o$ and (Eq. 3- 8) implies that $x_4^o - x_3^i = 0$. This means that for a tissue that is free to swell, the equilibrium cryoprotectant concentration inside the tissue will be equal to that of the surrounding solution and the tissue will be able to expand until the mole fraction of the "biological component" equals the mole fraction of the extracellular component ($x_3^i = x_4^o$).

For a tissue structure that can maintain a pressure difference (i.e. $P^o \neq P^i$) and is not free to swell infinitely, (Eq. 3- 9) implies $x_2^i \neq x_2^o$ and (Eq. 3- 8) implies that $x_3^i \neq x_4^o$. Therefore, if the tissue cannot swell to sufficiently dilute the biological component, at equilibrium there will be a pressure difference between the tissue and the surrounding solution, and the equilibrium cryoprotectant concentration

66

inside the tissue will be different from that of the surrounding solution, even for dilute solutions.

3.4 Other Models

To accurately model the equilibration of cryoprotectant in cells and tissues, one must use more accurate non-dilute chemical potential equations. While the non-dilute equations are much more complex, a similar derivation to that presented above leads to the same qualitative conclusions as the dilute equations. That is, if the pressure inside the tissue or cell is equal to that of the surroundings, then the equilibrium concentration of cryoprotectant inside the cell or tissue will be equal to that of the surrounding solution and the cell will swell until the contribution from the biological component equals that from the non-permeating components in the surrounding solution. On the other hand if the tissue is able to maintain a pressure difference from the surroundings, then the tissue can be kept from expanding to sufficiently dilute the biological component and the equilibrium concentration of cryoprotectant inside the tissue will be different from that of the surroundings. To make numerical predictions using this approach will require parameters in the non-dilute chemical potential equations for specific biological components that are not yet available.

There have been many published thermodynamic models used to describe the water and cryoprotectant transport in multicellular tissue. One of the more successful models has been the network thermodynamic model using bond

67

graphs, which works well with irreversible thermodynamic equations to describe passive membrane transport in biological systems [5,7-9,18,19] or the concentration polarization of solutes within cells during osmotic experiments [22]. This model has been used successfully to describe transport in a number of biological systems including islets of Langerhans [5] and kidneys [18,19]. However, in the use of this model, the pressure term in the chemical potential equations for the solute and solvent are often left out [5,6,9,18].

3.5 Discussion

In the past, researchers have tried to explain the discrepancy between the equilibrium cryoprotectant concentration measured in the tissue and that measured in the external solution. One explanation cited is the presence of impermeable compartments within the tissue [2,14]. However, in the simple system of freeze dried cross-linked collagen [2], there was no evidence that impermeable compartments existed within the freeze-dried tissue, yet the cryoprotectant concentration measured in the tissue did not equal that in the surrounding solution. Others have hypothesized that the measurement of the concentration of cryoprotectants by NMR is not accurate because some water is bound to the extracellular matrix components in the tissue [26,29]. Water molecules are associated with both proteins and proteoglycans, so these bound water molecules, if detected by NMR, will influence estimates of the concentration of cryoprotectant in the tissue [2,26,29]. Taylor and Busza [26] discussed the possibility that a portion of "NMR visible" tissue water may be

68

inaccessible to cryoprotectant, and might reflect mitochondrial compartments as suggested by Garlid [13]. For porcine articular cartilage, the equilibrium concentration of dimethyl sulfoxide (DMSO) within the tissue was only about half of the concentration of dimethyl sulfoxide in the bathing medium [23]. The researchers explained that the discrepancy was due to the high amount of water in the cartilage, and that this was enough to lower the DMSO concentration to about 70% of its initial value. Muldrew et al. [23] went on to explain that this reasoning did not fully account for the low equilibrium concentration observed and several reasons as to this observation were cited, including the methodology of the experiment. NMR depends on the reversibility of the uptake of DMSO and any irreversible binding of DMSO within the cartilage could have resulted in a lower measurement of the DMSO concentration. Investigators have mentioned that further studies were necessary to investigate the reasons for the inability to achieve "full" cryoprotectant permeation [11].

We have applied thermodynamics to examine the role of pressure in tissue equilibration as a possible explanation as to why some tissue systems come to the same equilibrium concentration as the surrounding solutions and other systems do not. Thermodynamics predicts that the equilibrium concentration of cryoprotectant inside the tissue will depend on the ability of the tissue system to maintain an equilibrium pressure difference. Tissues that are free to expand (i.e. $P^0 = P^i$) reach the same equilibrium cryoprotectant concentration as the surrounding solution. Tissues that are not free to expand and can maintain a

69

pressure difference (i.e. $P^o \neq P^i$), do not reach the same equilibrium cryoprotectant concentration within the tissue as in the surrounding solution. This work proposes a possible explanation of the discrepancies often observed, but can not yet be used to predict the equilibrium concentration that would be reached by a tissue system. In order to utilize the equations as a predictive tool, accurate non-dilute chemical potential equations would be needed. In order to test such a prediction, a method to accurately measure the pressure difference between a tissue and a surrounding immersion solution would also be needed.

3.6 Conclusions

If a biological system is placed in a solution of permeating cryoprotectant, thermodynamic equilibrium predicts that:

1- If the system may freely expand, then the equilibrium cryoprotectant concentration inside the cells or tissue should be equal to that of the surroundings.

2- If the system has a structure that can maintain a pressure difference, then the equilibrium cryoprotectant concentration inside the tissue will be less than that of the surroundings.

This study shows that a difference in cryoprotectant concentration between the inside and outside of the tissue is expected if there is also a pressure difference. Theoretical models that do not include pressure in the chemical potential equations cannot therefore be used to describe cryoprotectant transport in tissues.

3.7 References

[1] Bateson, E.A.J., Busza, A.L., Pegg, D.E., Taylor, M.J., Permeation of Rabbit Common Carotid Arteries with Dimethyl-Sulfoxide, Cryobiology 31 (1994) 393-397.

[2] Bidault, N.P., Hammer, B.E., Hubel, A., Rapid MR imaging of cryoprotectant permeation in an engineered dermal replacement, Cryobiology 40 (2000) 13-26.

[3] Callen, H.B., Thermodynamics and an introduction to thermostatistics (Wiley, New York, 1985) P-303.

[4] Carpenter, J.F., Dawson, P.E., Quantitation of Dimethyl-Sulfoxide in Solutions and Tissues by High-Performance Liquid-Chromatography, Cryobiology 28 (1991) 210-215.

[5] De Freitas, R.C., Diller, K.R., Lachenbruch, C.A., Merchant, F.A., Network thermodynamic model of coupled transport in a multicellular tissue the islet of Langerhans, Biotransport: Heat and Mass Transfer in Living Systems 858 (1998) 191-204.

[6] Diller, K.R., Lynch, M.E., An Irreversible Thermodynamic Analysis of Cell Freezing in the Presence of Membrane Permeable Additives .1. Numerical-Model and Transient Cell-Volume Data, Cryo-Letters 4 (1983) 295-308.

[7] Diller, K.R., Lynch, M.E., An Irreversible Thermodynamic Analysis of Cell Freezing in the Presence of Membrane-Permeable Additives .2. Transient Electrolyte and Additive Concentrations, Cryo-Letters 5 (1984) 117-130.

[8] Diller, K.R., Lynch, M.E., An Irreversible Thermodynamic Analysis of Cell Freezing in the Presence of Membrane-Permeable Additives .3. Transient Water and Additive Fluxes, Cryo-Letters 5 (1984) 131-144.

[9] Diller, K.R., Raymond, J.F., Water Transport through a Multicellular Tissue During Freezing - a Network Thermodynamic Modeling Analysis, Cryo-Letters 11 (1990) 151-162.

[10] Fahy, G.M., Macfarlane, D.R., Angell, C.A., Meryman, H.T., Vitrification as an Approach to Cryopreservation, Cryobiology 21 (1984) 407-426.

[11] Fuller, B.J., Busza, A.L., Proton Nmr-Studies on the Permeation of Tissue Fragments by Dimethyl-Sulfoxide - Liver as a Model for Compact Tissues, Cryo-Letters 15 (1994) 131-134.

[12] Fuller, B.J., Busza, A.L., Proctor, E., Studies on Cryoprotectant Equilibration in the Intact Rat-Liver Using Nuclear Magnetic-Resonance Spectroscopy - a Noninvasive Method to Assess Distribution of Dimethyl-Sulfoxide in Tissues, Cryobiology 26 (1989) 112-118.

[13] Garlid, K., Cell Associated Water (Academic Press, New York, 1979).

[14] Hagedorn, M., Hsu, E.W., Pilatus, U., Wildt, D.E., Rall, W.F., Blackband, S.J., Magnetic resonance microscopy and spectroscopy reveal kinetics of cryoprotectant permeation in a multicompartmental biological system, Proceedings of the National Academy of Sciences of the United States of America 93 (1996) 7454-7459.

[15] Isbell, S.A., Development of a protocol for the quantitative evaluation of contrast in NMR images of cryoprotective solvents in intact tissues, Cryobiology 34 (1997) 165-175.

[16] Isbell, S.A., Fyfe, C.A., Ammons, R.L.M., Pearson, B., Measurement of cryoprotective solvent penetration into intact organ tissues using high-field NMR microimaging, Cryobiology 35 (1997) 165-172.

[17] Karlsson, J.O.M., Toner, M., Long-term storage of tissues by cryopreservation: Critical issues, Biomaterials 17 (1996) 243-256.

[18] Lachenbruch, C.A., Diller, K.R., A network thermodynamic model of kidney perfusion with a cryoprotective agent, Journal of Biomechanical Engineering-Transactions of the Asme 121 (1999) 574-583.

[19] Lachenbruch, C.A., Diller, K.R., Pegg, D.E., Sensitivity of kidney perfusion protocol design to physical and physiological parameters, Biotransport: Heat and Mass Transfer in Living Systems 858 (1998) 298-309.

[20] Lakey, J.R.T., Helms, L.M.H., Moser, G., Lix, B., Slupsky, C.M., Rebeyka, I.M., Sykes, B.D., McGann, L.E., Dynamics of cryoprotectant permeation in porcine heart valve leaflets, Cell Transplantation 12 (2003) 123-128.

[21] Levin, R.L., Osmotic Effects of Introducing and Removing Cryoprotectants: Perfused Tissues and Organs, in: 1981 Advances in Bioengineering: Presented at the winter annual meeting of the American Society of Mechanical Engineers, Washington, D.C. November 15-20, 1981 (American Society of Mechanical Engineers, Washington, D.C, 1981).

[22] Levin, R.L., Cravalho, E.G., Huggins, C.E., Concentration Polarization Effect in a Multicomponent Electrolyte Solution - Human Erythrocyte, Journal of Theoretical Biology 71 (1978) 225-254.

72

[23]   Muldrew, K., Sykes, B., Schachar, N., McGann, L.E., Permeation kinetics of dimethyl sulfoxide in articular cartilage, Cryo-Letters 17 (1996) 331-340.

[24]   Pegg, D., Cryobiology of cells in situ: experiments with ovine articular cartilage, Cryobiology 37 (1998) 381-382.

[25]   Rinkes, I.H.M.B., Toner, M., Ezzell, R.M., Tompkins, R.G., Yarmush, M.L., Effects of Dimethyl-Sulfoxide on Cultured Rat Hepatocytes in Sandwich Configuration, Cryobiology 29 (1992) 443-453.

[26]   Taylor, M.J., Busza, A.L., A Convenient, Noninvasive Method for Measuring the Kinetics of Permeation of Dimethyl-Sulfoxide into Isolated Corneas Using Nmr-Spectroscopy, Cryo-Letters 13 (1992) 273-282.

[27]   Walcerz, D.B., Taylor, M.J., Busza, A.L., Determination of the Kinetics of Permeation of Dimethyl-Sulfoxide in Isolated Corneas, Cell Biophysics 26 (1995) 79-102.

[28]   Wusteman, M., Busza, A., Boylan, S., Hayes, A., Pegg, D., Ethylene-Glycol Permeation and Toxicity in the Rabbit Common Carotid-Artery, Cryobiology 32 (1995) 428-435.

[29]   Zieger, M.A.J., Tredget, E.E., Sykes, B.D., McGann, L.E., Injury and protection in split-thickness skin after very rapid cooling and warming, Cryobiology 35 (1997) 53-69.

Figure 3-1: Cryoprotectant equilibration between the extracellular solution and a tissue

Tissue Solution

N_1- Water

N_2- Cryoprotectant

N_3- Biological Component

Carrier Solution

N_1- Water

N_2- Cryoprotectant

N_4- Extra Solute

Constant Temperature (T)

74
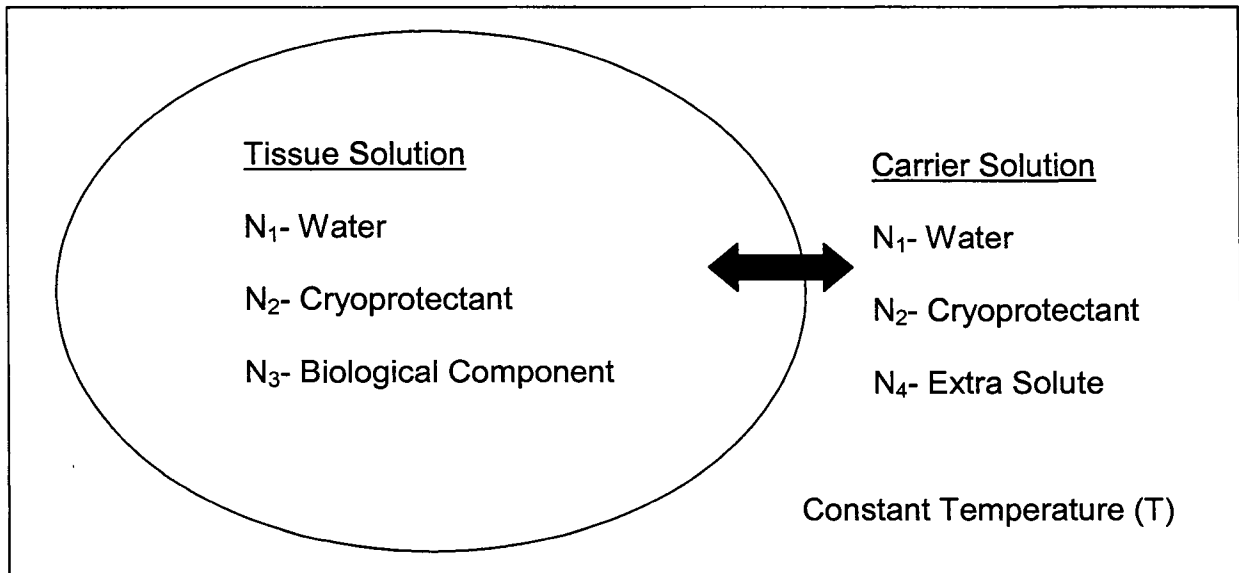
Chapter 4: Current Status of Osmotic Transport

4.1 Osmotic Transport Across Cell Membranes

All living cells are enclosed by at least one plasma membrane that separates the intracellular solution from its extracellular environment. Biological membranes are made up of proteins, phospholipids and small amounts of carbohydrates. The relative proportions of lipids and proteins differ depending on the membrane. In general, membranes of active organelles have a higher portion of proteins, such as the inner membrane of the mitochondria (75% protein) [44]. A biological membrane may be thought of as a matrix of phospholipid molecules into which proteins are inserted. Phospholipids have an electrically charged hydrophilic polar head that has a strong attraction for water, and two electrically neutral hydrophobic non-polar tails. The polar head groups are tightly packed together while the hydrophobic tails are very flexible. Molecules that possess both a polar and non-polar portion are known as amphiphilic. Some of the membrane proteins, extrinsic proteins, are loosely attached to the cell membrane and are entirely outside of the membrane while other proteins are more firmly bound and are embedded in the membrane and are known as intrinsic proteins. The carbohydrates in the membrane are either attached to the proteins or to some of the lipids [44]. A schematic diagram of the lipid bilayer membrane is shown in Figure 4-1.

Molecules must cross the phospholipid bilayer of cell membranes in order to enter or leave the cell. The lipid portion of the membrane is almost always fluid

75

at physiological temperatures. For a molecule to cross the cell membrane, it must enter the lipid region, which is hydrophobic, cross it, and leave the other side of the membrane [44]. Since the early 1930's, there have been numerous articles published on the mechanisms of water and solute movement across cell membranes [8,9,13,16,17,25,40,46]. Water moves passively across the cell membrane in response to osmotic gradients. Despite the fact that water crosses the cell membrane by diffusion through the lipid bilayer when a concentration gradient is present, some cells are known to exhibit a more rapid trans-membrane water transport through specialized protein water channels [26,39,46] known as aquaporins.

4.2 Rationale for Transport Formalisms in Cryobiology

The cell membrane is semi-permeable, i.e., water and permeating solutes (such as permeating cryoprotectants) can cross the cell membrane and move in and out of the cell, while other solutes are kept either inside or outside the cell. The composition of the extracellular solution can be changed by a number of factors including the addition and removal of cryoprotectants. The cell will shrink or swell based on the conditions the cell is exposed to. The cell will respond osmotically during the freezing process when a cell is cooled down and extracellular water gets converted to ice. With freezing, the extracellular solution becomes more concentrated and as a result, water leaves the cell until osmotic equilibrium is reached. In general, the cell will respond osmotically to both the addition and removal of cryoprotectants as well as to changes occurring during

76

freezing. As a result, an understanding of cell membrane permeability is very important in predicting successful outcomes from cryopreservation protocols. Specifically, cryobiologists are interested in the water (solvent) and cryoprotectant (solute) permeability of membranes [23]. These permeability parameters are used to develop cryopreservation protocols, model the addition and removal of cryoprotectants from cells and tissues as well as to predict the optimal cooling rate for cryopreservation [10,28]. The permeability parameters may also be used to determine whether solute and water movement occurs through channels or by solubility-diffusion through the lipid bilayer [8,12,35,39]. Since the 1930's, formalisms have been developed to describe the efflux of water and solutes across cell membranes [15,17].

4.3 Measures of Concentration

When dealing with osmotic transport and solutions, it becomes important to know or measure the concentration. The concentration refers to the amount of one substance relative to the amounts of the other substances in solution. There are several different ways to express the concentration including molarity (C), osmolarity (π(C)), molality (m) and osmolality (π(m)). The molarity is defined as the number of moles of solute per liter of solution. Since the molarity depends on solution volume, there is a temperature-dependence. The osmolarity is defined as the number of moles of solute per liter of solution, of an ideal, dilute solute that would be needed to produce the same osmotic activity as a particular concentration of a non-dilute solute. Like the molarity, the osmolarity is

77

temperature dependent. A measure of concentration that is as easy to use as the molarity is the molality. The molality is defined as the number of moles of solute per kilogram of solvent. As it is directly related to a weight-per-unit-weight expression of concentration, the molality value of a solution does not change with variations in temperature or pressure. Similarly to osmolarity, the osmolality is defined as the number of moles of an ideal, dilute solute, per kg of solvent, that would be needed to produce the same osmotic activity as a particular concentration of a non-dilute solute.

There are a number of mathematical relationships in the literature to describe osmolarity or osmolality as a function of concentration. The osmotic virial equation, first proposed by McMillan and Mayer in 1945 [32], treats osmolality (or osmolarity or osmotic pressure) as a polynomial expansion in concentration with the first term being linear in concentration. The osmotic virial equation for a solution containing a single solute, i, describes the osmolality, π, as a polynomial in molality of the solute, m_i.

(Eq. 4- 1)

$$\pi = m_i + B_i^+ m_i^2 + C_i^+ m_i^3 + ...$$

The B^+ and C^+ are known as osmotic virial coefficients. B_i^+ is called the second osmotic virial coefficient and C_i^+ the third osmotic virial coefficient, etc. The superscript (+) is to denote the virial coefficients are being used for a specific unit of concentration – in this case, molality. The osmotic virial coefficients B_i^+ for the

78

pure species (i.e. single solute) can be obtained from freezing point depression experiments or from a vapor pressure osmometer [2]. When determining the osmolality of a multi-solute solution, it is often assumed that the contribution of each solute to the overall osmolality of the solution is additive [27].

A study by Bannerman et al., [2], pointed out that when the osmolalities of binary solutions are summed to predict osmolalities of multi-solute solutions, the interactions between the different types of solutes are often not accounted for, leading to incorrect predictions of the solution osmolality. Accounting for the solute-solute interactions will always be important particularly outside the region where solutions are ideal and dilute. For a solution with two solutes i and j, they assumed that the osmotic virial equation took the form:

(Eq. 4- 2)

$$\pi = m_i + m_j + B_i^+ m_i^2 + B_j^+ m_j^2 + 2B_{ij}^+ m_i m_j$$

For many simple solutes, the osmotic virial equation can usually be truncated to include only second order terms as shown in (Eq. 4- 2), however, for macromolecules, the third order terms are needed [2].

The above equation describes the contribution of each solute to the overall osmolality. The B^+ in the equation is unique to each type of solute. The parameter B_i^+ accounts for the interactions between two identical solute molecules of type i, and B_j^+ accounts for the interactions between two identical

79

molecules of type j. The cross coefficient, B_{ij}^+, accounts for interactions between solutes i and j. In order to determine the cross coefficient, B_{ij}^+, Bannerman et al., [2] proposed a mixing rule of the form:

(Eq. 4- 3)

$$B_{ij}^+ = \frac{\left(B_i^+ + B_j^+\right)}{2}$$

Substituting (Eq. 4- 3) into (Eq. 4- 2) results in the following:

(Eq. 4- 4)

$$\pi = m_i + m_j + B_i^+ m_i^2 + B_j^+ m_j^2 + \left(B_i^+ + B_j^+\right)m_i m_j$$

For a dilute solution with two solutes, i and j, the osmolality is expressed as:

(Eq. 4- 5)

$$\pi = m_i + m_j$$

For a non-dilute solution of two solutes, the osmolality without the cross terms is expressed as:

(Eq. 4- 6)

$$\pi = m_i + m_j + B_i^+ m_i^2 + B_j^+ m_j^2$$

It is more correct and accurate to express the osmolality with the second order terms. The most correct way to express the osmolality would be to include the cross terms as shown in (Eq. 4- 4) [2].

80

4.4 Theories of Osmotic Transport

4.4a Jacobs and Stewart

In 1931 Jacobs and Stewart [17] conducted some simple quantitative measurements to measure cell membrane permeability. They were interested in obtaining quick and accurate measurements of volume changes in Arbacia eggs as well as other cells. A mathematical analysis to describe the swelling of a cell in a solution of a permeating cryoprotectant was developed by making 4 simple assumptions. They assumed that:

1- the extracellular solution concentration remained constant during the course of the experiment

2- diffusion across the cell membrane was slower than in the body of the solution or the interior of the cell so that the only gradient that needed consideration was that across the membrane

3- the concentration gradient across the cell membrane may be expressed as $\dfrac{C^o - C^i}{l}$ (where C^o is the concentration outside, C^i is the concentration inside the cell and l is the thickness of the membrane) instead of the true gradient $-\dfrac{\partial C}{\partial l}$

81

4- the thickness of the membrane remained constant during the course of the experiment.

They developed a set of transport equations that were based on their assumptions as well as Fick's Law of Diffusion which states that the rate of diffusion across a given surface is proportional to the concentration gradient at that surface. They also assumed that the osmotic pressure for a given substance may be taken as directly proportional to its concentration [15,17], in other words, a dilute solution assumption was made. Based on these conditions, they came up with the two differential equations to describe the simultaneous penetration of a cell by water and by a dissolved substance. The following equation was used to describe water transport across a cell membrane:

(Eq. 4- 7)

$$\frac{dV_w}{dt} = k_1 A \left(\frac{\widetilde{S} + C_o V_o}{V} - C_s - C_n \right)$$

where $\dfrac{dV_w}{dt}$ is the change in cell water volume (V_w) as a function of time (t), k_1 is the water permeability constant, A is the cell surface area, $\widetilde{S}$ is the amount of internal permeating solute, C_o is the initial concentration of internal non-permeating solutes, V_o is the initial volume of solvent within the cell, C_s is the concentration of the external permeating solute and C_n is the concentration of the external non-permeating solute. They also developed an equation to describe solute transport across the cell membrane:

82

(Eq. 4- 8)

$$\frac{d\widetilde{S}}{dt} = k_2 A \left(C_s - \frac{\widetilde{S}}{V} \right)$$

where $\dfrac{d\widetilde{S}}{dt}$ is the change in the amount of internal permeating solute $(\widetilde{S})$ as a

function of time and k_2 is the solute permeability constant. The numerical values

of k_1 and k_2 depend on the units of concentration, volume and area used. In

both of the equations, Jacobs and Stewart said that the concentrations are taken

to be osmolar [15,17].

Jacobs and Stewart did recognize that the expression for concentration should

be in units of osmolarity. However, it appears in their equations they were using

units of molarity. They also recognized in their 1932 paper [17] that they were

making an inaccurate assumption that the osmotic pressures of the solutions

they were using were related to the concentration in a linear fashion. Hence,

they were making a dilute solution assumption.

4.4b Modern two parameter formalism

The two parameter (2-P) formalism commonly used in cryobiology today was

developed from the work of Jacobs and Stewart [15,17]. The 2-P transport

formalism uses the hydraulic conductivity, L_p ($\mu m^3/\mu m^2/min/atm$) and the solute

permeability, P_s (cm/s) to characterize membrane permeability when water, a

permeating solute and a non-permeating solute are present. The hydraulic

83

conductivity is a measure of the rate of water movement across the cell membrane and the solute permeability is a measure of the rate of solute permeability across the cell membrane. To describe the change in cell water volume as a function of time, the 2-P formalism is commonly written as follows:

(Eq. 4- 9)

$$\frac{dV_w}{dt} = -L_p ART\left(\pi^e - \pi^i\right)$$

where R is the universal gas constant, T is absolute temperature, π^e is the total extracellular solution osmolarity $\left(\pi^e = \pi_n^e + \pi_s^e\right)$, and π^i is the total intracellular solution osmolarity $\left(\pi^i = \pi_n^i + \pi_s^i\right)$. The subscript 'n' denotes non-permeating solutes and the subscript 's' denotes permeating solutes. To describe the solute flux, the following equation is often used in the literature [14,36,50]:

(Eq. 4- 10)

$$\frac{dN_s}{dt} = P_s A\left(C_s^e - C_s^i\right)$$

where $\dfrac{dN_s}{dt}$ is the change in the intracellular number of permeating solute molecules as a function of time, C_s^e is the extracellular solute molarity and C_s^i is the intracellular solute molarity. To convert from a solute flux to a volume flux, we can multiply by the partial molar volume of the solute, v_s, as follows:

(Eq. 4- 11)

$$\frac{dV_s}{dt} = v_s \frac{dN_s}{dt} = v_s P_s A\left(C_s^e - C_s^i\right)$$

The total cell volume, V_C, is given as:

84

(Eq. 4- 12)

$$V_C = V_w + V_s + V_b$$

where, V_b is the osmotically inactive volume. The equations to describe water and solute transport assume no physical interaction between the water and the solute fluxes, however, it is important to note that the equations are coupled by the definition of the intracellular molarity for a dilute solution as follows: $\left(C^i = C^i_n + C^i_s \right)$ [23].

In attempting to generalize (Eq. 4- 8) from dilute solutions to more general solutions, there has been a common misconception as to the meaning of osmolarity. The osmolarity represents the water activity. As a result, (Eq. 4- 7) is correctly generalized to (Eq. 4- 9) for non-dilute solutions by using osmolarity rather than molarity as the concentration units. In contradiction to the body of literature existing [23,52], (Eq. 4- 8) and (Eq. 4- 10) cannot be generalized to a non-dilute form in an analogous manner (by replacing molarity with osmolarity) since it is the <u>solute</u> that is the driving force and osmolarity is related to the chemical potential of <u>water</u> in the presence of solute. (Eq. 4- 8) was developed based on Fick's Law which depends on the gradient in concentration. It is also important to note that while L_p and P_s have similar meanings (the rate of water movement and the rate of solute movement across the cell membrane, respectively), they have different units.

Often in the literature, the concentration expression in the bracket of (Eq. 4- 9) is incorrectly referred to as osmolarity interchangeably with osmolality. In order for the hydraulic conductivity in (Eq. 4- 9) to have units of ($\mu m^3/\mu m^2$/min/atm), the concentration must be in terms of osmolarity (or molarity). In order to convert between the two expressions of concentration, one must use the value for the density of water. For a dilute solution, the molarity is proportional to the molality with the proportionality being the water density. The density of water is equal to $1 g/cm^3$ at 4°C and 1 atmosphere of pressure. This may be why in biological literature, osmolality and osmolarity are often used interchangeably. However, it is important to note this is only true for a dilute solution at 4°C at 1 atmosphere, not at conditions that may apply in cryobiology with concentrated solutions over large temperature ranges. In their work, Jacobs and Stewart [15,17] did recognize that the expression for concentration should have units of osmolar. However, it appears that they were actually just using molar concentration not osmolar. In using molar concentration instead of osmolar, an implicit dilute solution assumption is being made. (Eq. 4- 9) developed by Jacobs and Stewart could be extended to include non-dilute solutions if the expression for concentration used is actually osmolarity. In the literature it is often assumed that if the 2-P model is being used, there are no dilute solution restrictions on the equations [23]. However, this is only true if osmolarity is used and only for (Eq. 4- 9), since (Eq. 4- 10) is in terms of water activity instead of solute activity as it should be. (Eq. 4- 10) is by definition incorrect for a non-dilute solution if molarity

is simply replaced by osmolarity. If molarity is used, then a dilute solution assumption is being made when using either of the 2-P equations.

4.4c   Staverman

Classical thermodynamics differentiates between processes which are reversible and those which are irreversible. In a reversible process, there is no production of entropy and the process takes place infinitely slowly [44]. Most natural processes, such as diffusion and permeation, are irreversible [44]. Much of our understanding of transport phenomena is based on linear irreversible thermodynamics, and cell volume change due to solute and solvent flow across cell membranes is an example of such a phenomenon. In the early 1950's, Staverman approached the problem of osmotic transport across cell membranes by employing the linear theory of irreversible thermodynamics [42,43] which was formalized most notably by Onsager in 1931 [37,38]. Staverman was interested in looking at permeability in "leaky" membranes. By "leaky", Staverman was referring to membranes that were permeable to solutes. His idea was that leakage of solute molecules affected the measurements through the gradual change of the solute concentrations in the cells [43]. The leakage of a membrane was described by a reflection coefficient, $\tilde{\sigma}$, ranging from 0 for a completely permeable membrane (unselective membrane) to 1 for a semi-permeable membrane (permeable to the solvent only and impermeable to the solute molecules). A value of $\tilde{\sigma}$ = 1 refers to the idea that 100% of the solutes get reflected back from the membrane. Staverman specified that these

conditions were for a dilute system with a single permeating solute and were inappropriate to use for concentrated or multicomponent systems, but could be generalized to cover systems for which linear flux equations were applicable [43,51]. Researchers have done work to try and generalize the reflection coefficient to be applicable to systems with non-ideal, non-isothermal and multicomponent systems [4]. The reflection coefficient is concentration dependent and describes the selectivity of the membrane to a specific solute [43] so the value of sigma is determined by both the properties of the membrane and the permeable solute.

4.4d Kedem and Katchalsky

In 1958, Kedem and Katchalsky modified and extended the work of previous authors again using Onsager's irreversible thermodynamics approach [21]. The theory is based on the premise that for a system sufficiently close to equilibrium, any flux, J, (such as a heat flux or a mass flux) is linearly proportional to a driving force, X, (or a gradient in an intensive property such as pressure or concentration). To identify the fluxes and forces in a system, the entropy production is written in a form whereby fluxes are multiplied by independent forces. For a system with a single flux as a result of a single thermodynamic force driving the system towards equilibrium, the entropy production has the following form:

(Eq. 4- 13)

$$\frac{dS}{dt} = JX$$

88

where S is the entropy. For sufficiently small driving forces, an equation for the flux is then assumed to be of the following form:

(Eq. 4- 14)

$$J = LX$$

where L is a phenomenological coefficient also known as an Onsager coefficient. The amount of flux produced is related to the amount of force by a phenomenological coefficient [44]. Many transport processes such as diffusion, heat conduction, and electrical conduction, are given in the above form. In Fick's Law of Diffusion, the flux, J, is that of a diffusing solute and the driving force, X, is the concentration gradient. The phenomenological coefficient in this case is the diffusion coefficient. In Fourier's Law of Heat Transfer, the flux is the heat flux and the driving force is the gradient in temperature. The phenomenological coefficient is the thermal conductivity. In Ohm's Law, the flux is current density and the driving force is a voltage gradient. The phenomenological coefficient is the electrical conductivity.

In the case of a system with two fluxes, J_1 and J_2, that are linearly dependent on two forces, X_1 and X_2, the entropy production has the following form:

(Eq. 4- 15)

$$\frac{dS}{dt} = J_1 X_1 + J_2 X_2$$

For sufficiently small driving forces, flux equations are then assumed to be of the following form:

89

(Eq. 4- 16)

$$J_1 = L_{11}X_1 + L_{12}X_2$$

(Eq. 4- 17)

$$J_2 = L_{21}X_1 + L_{22}X_2$$

where once again the L's are phenomenological coefficients.

A reciprocity relation known as Onsager's reciprocity relation is assumed to hold between the phenomenological cross coefficients, L_{12} and L_{21}:

(Eq. 4- 18)

$$L_{12} = L_{21}$$

Since the 1850's, much work has been published [22,24,34,41] discussing the reciprocity relation [37]. This reciprocity was theoretically proven for cases of osmotic transport across cell membranes by linearizing Statistical Rate Theory [6] and the conditions under which the equations could be linearized were outlined [6]. Statistical Rate Theory is a general and complete far-from-equilibrium theory of non-equilibrium thermodynamics that was developed in 1977 [48] and is discussed in detail in reference [7]. One advantage to finding Onsager coefficients by linearizing a general theory was that rather than being phenomenological, such coefficients were expressed in terms of physical experimental variables. Another advantage of linearizing a general theory was that explicit conditions under which the linearity assumption holds may be derived, whereas there is no way from within the Onsager approach to determine

90

whether a system is close enough to equilibrium for the Onsager equations to apply.

In the case of more than two thermodynamic forces and fluxes, there will be multiple reciprocal relations. For example, in a system with three forces, X_1, X_2 and X_3, the flux equations may be written as follows:

(Eq. 4- 19)

$$J_1 = L_{11}X_1 + L_{12}X_2 + L_{13}X_3$$

(Eq. 4- 20)

$$J_2 = L_{21}X_1 + L_{22}X_2 + L_{23}X_3$$

(Eq. 4- 21)

$$J_3 = L_{31}X_1 + L_{32}X_2 + L_{33}X_3$$

and the phenomenological coefficients are related by:

(Eq. 4- 22)

$$L_{12} = L_{21}, \; L_{23} = L_{32}, \; L_{31} = L_{13}$$

Kedem and Katchalsky developed a formalism to describe osmotic transport across a cell membrane when water and solute transport across a membrane are physically coupled, usually through co-transport in a common channel. As a result, the water and solute interact and the degree of interaction between the solvent and solute was characterized by a reflection coefficient, σ. However, the equations developed were general enough to be applied empirically to a number

91

of transport situations in the presence or absence of co-transport channels. In the Kedem-Katchalsky (K-K) equations, three parameters are used to characterize the membrane permeability: the water permeability (hydraulic conductivity, L_p), the solute mobility, $(\tilde{\omega})$, and the reflection coefficient (sigma, σ). The solute mobility may be expressed as a solute permeability, $P_s = \tilde{\omega}RT$, where again R is the universal gas constant and T is absolute temperature.

To investigate how Kedem and Katchalsky derived their solution thermodynamics motivated transport equations, we can consider mass transport across a cell membrane in the presence of both an osmotic and a pressure gradient. Consider a biological cell that in the context of the K-K model can be treated as a two-component composite system as illustrated in Figure 4-2. The cell is immersed in a hypertonic or hypotonic solution and undergoes osmotic shrinkage or swelling. We assume the cell contains a solution of water (w) and solute (s) and is immersed in a solution of water and the same solute and that the cell is permeable to both the water and the solute. To be most general, there may be a tension in the membrane that results in a pressure difference between the inside (i) and the outside (o) of the cell. We assume that the inside and outside of the cell are not at equilibrium with respect to water concentration, solute concentration or pressure but that the cell membrane is in mechanical equilibrium at all times so that the pressure difference is balanced by the membrane tension. We also assume that our entire system is surrounded by a thermal reservoir that keeps the cell and the surroundings at a constant temperature, T.

92

The first step in the Onsager approach is to write the entropy production for the entire process. For the system shown in Figure 4-2, the differential change in entropy for the isolated system, dS_{sys} may be written as:

(Eq. 4- 23)

$$dS_{sys} = dS^o + dS^i + dS^m + dS^R$$

where S^o, S^i, S^m and S^R are the entropies of the fluid outside the cell, the fluid inside the cell, the cell membrane and the reservoir, respectively. The differential entropies of each of the subsystems may be written in terms of the independent extensive variables of each of the subsystems by using the fundamental thermodynamic equation in the entropy form [3].

For the fluid outside the cell:

(Eq. 4- 24)

$$dS^o = \frac{1}{T}dU^o + \frac{P^o}{T}dV^o - \frac{\mu_w^o}{T}dN_w^o - \frac{\mu_s^o}{T}dN_s^o$$

where U^o, P^o and V^o are the internal energy, the pressure and the volume, respectively, of the fluid outside the cell; μ_w^o and N_w^o are the chemical potential of the water outside the cell and the number of molecules of water outside the cell, respectively and μ_s^o and N_s^o are the chemical potential of the solute outside the cell and the number of molecules of solute outside the cell, respectively.

Similarly, for the fluid inside the cell, the cell membrane and the reservoir, the differential changes in entropy may be written in similar forms. Details of the

93

derivation maybe found in a paper previously published by Elliott, Elmoazzen and McGann in 2000 [6]. By making some other assumptions such as conservation of mass and volume as illustrated by Elliott, Elmoazzen and McGann, [6], the rate of entropy production may be written as follows:

(Eq. 4- 25)

$$dS_{sys} = \frac{\left(\mu_w^o - \mu_w^i\right)}{T} dN_w^i + \frac{\left(\mu_s^o - \mu_s^i\right)}{T} dN_s^i$$

The rate of entropy production can be written in terms of the rate of change of the number of water and solute molecules inside the cell, $\dot{N}_w^i$ and $\dot{N}_s^i$, respectively. Thus, (Eq. 4- 25) may be re-written as:

(Eq. 4- 26)

$$\frac{dS_{sys}}{dt} = \frac{\left(\mu_w^o - \mu_w^i\right)}{T} \dot{N}_w^i + \frac{\left(\mu_s^o - \mu_s^i\right)}{T} \dot{N}_s^i$$

Kedem and Katchalsky [21] obtained the rate of entropy production given in (Eq. 4- 26).

The chemical potential is a measure of the ability of a system to do chemical work. The chemical potential is, in general, a function of temperature, pressure and the concentration of all species [44].

For a thermodynamically dilute solution the difference in the chemical potential of water across the membrane may be written as [3]:

(Eq. 4- 27)

$$\mu_w^o - \mu_w^i = v_w\left(P^o - P^i\right) - RT\left(x_s^o - x_s^i\right)$$

94

where v_w is the partial molar volume of water and x_s is the mole fraction of solute which may approximately be written as:

(Eq. 4- 28)

$$x_s \approx \frac{c_s}{c_w^*}$$

where c_s is the concentration of solute and c_w^* is the concentration of pure water. The difference in the chemical potential of the ideal, dilute solute across the membrane may be written as:

(Eq. 4- 29)

$$\mu_s^o - \mu_s^i = v_s \left(P^o - P^i \right) + RT \left[\ln(x_s^o) - \ln(x_s^i) \right]$$

where v_s, is the partial molar volume of the solute. We may re-write the term in the square brackets in (Eq. 4- 29) as:

(Eq. 4- 30)

$$\ln(x_s^o) - \ln(x_s^i) = \frac{c_s^o - c_s^i}{\tilde{c}_s}$$

where

(Eq. 4- 31)

$$\tilde{c}_s \equiv \frac{c_s^o - c_s^i}{\ln\left(\frac{x_s^o}{x_s^i}\right)} = \frac{c_s^o - c_s^i}{\ln\left(\frac{c_s^o}{c_s^i}\right)} = \frac{c_s^o - c_s^i}{\ln\left(\frac{c_s^i + \left(c_s^o - c_s^i\right)}{c_s^i}\right)} = \frac{c_s^o - c_s^i}{\ln\left(1 + \frac{c_s^o - c_s^i}{c_s^i}\right)}$$

If $c_s^o - c_s^i \ll c_s^i$, then (Eq. 4- 31) can be expanded and reduces to:

(Eq. 4- 32)

$$\tilde{c}_s \approx \frac{c_s^o - c_s^i}{2}$$

95

Since the condition given in (Eq. 4- 32) is more stringent than the dilute solution assumption, (Eq. 4- 31) will be taken as a definition and $\tilde{c}_s$ will be left in the equations. Kedem and Katchalsky made the assumption in (Eq. 4- 32) for the solute equations in their 1958 paper [21]. By using (Eq. 4- 32), Kedem and Katchalsky made a near equilibrium assumption. A near equilibrium assumption means that the difference in concentration between the inside and the outside of the cell is quite small.

Substituting (Eq. 4- 27) through (Eq. 4- 30) into (Eq. 4- 26) yields the following expression:

(Eq. 4- 33)

$$\frac{dS_{sys}}{dt} = \left[v_s \dot{N}_s^i + v_w \dot{N}_w^i \right] \left(P^o - P^i \right) + \left[\frac{\dot{N}_s^i}{\tilde{c}_s} - \frac{\dot{N}_w^i}{c_w^*} \right] RT \left(c_s^o - c_s^i \right)$$

(Eq. 4- 34)

$$\frac{dS_{sys}}{dt} = J_V \left(P^o - P^i \right) + J_D RT \left(c_s^o - c_s^i \right)$$

In (Eq. 4- 33), the term in the first set of square brackets is the total volume flux, J_V, across the cell membrane; the driving force for which is a pressure gradient. The term in the second set of square brackets is the differential volume flux, J_D, between solute and water molecules. The driving force for this term is $RT \left(c_s^o - c_s^i \right)$, which is related to the concentration gradient. By using the linearity assumptions of the Onsager approach and by identifying the terms in the square

96

brackets as fluxes and the factors multiplying them as thermodynamic forces, the following relations are obtained:

(Eq. 4- 35)

$$\left[\overline{v}_s \dot{N}_s^i + \overline{v}_w \dot{N}_w^i\right] = L_{11}\left(P^o - P^i\right) + L_{12}RT\left(c_s^o - c_s^i\right)$$

(Eq. 4- 36)

$$\left[\frac{\dot{N}_s^i}{\widetilde{c}_s} - \frac{\dot{N}_w^i}{c_w^*}\right] = L_{21}\left(P^o - P^i\right) + L_{22}RT\left(c_s^o - c_s^i\right)$$

where the L's are phenomenological coefficients and where the cross coefficients, L_{12} and L_{21} are equal. In order to have notation similar to that used by Kedem and Katchalsky, L_{11} may be replaced with L_p, the hydraulic conductivity. Similarly, L_{12} and L_{21} may be replaced with L_{Dp} and L_{pD} respectively and L_{22} may be replaced with L_D. (Eq. 4- 35) and (Eq. 4- 36) may then be written as follows to utilize the same notation as Kedem and Katchalsky:

(Eq. 4- 37)

$$J_V = L_P\Delta P + L_{pD}RT\Delta c_s$$

(Eq. 4- 38)

$$J_D = L_{Dp}\Delta P + L_D RT\Delta c_s$$

In their 1958 paper [21], Kedem and Katchalsky outlined equations for various transport situations such as zero concentration difference, zero pressure difference, constant volume flow, as well as others. In developing their

97

equations, Kedem and Katchalsky made use of a reflection coefficient which was defined as:

(Eq. 4- 39)

$$L_{pD} = -\sigma L_p$$

As well, they introduced a definition for the mobility of the solute, ω, which was written in terms of the phenomenological coefficients L_p, L_D, L_{pD} as well as σ. Recall that the solute mobility is related to the solute permeability, P_s, ($P_s = \widetilde{\omega}RT$).

(Eq. 4- 40)

$$\widetilde{\omega} = \frac{L_p L_D - (L_{pD})^2}{L_p} \widetilde{c}_s = (L_D - L_p \sigma^2)\widetilde{c}_s$$

In deriving their equations, Kedem and Katchalsky made dilute solution assumptions; as well they assumed that the volume fraction of all solutes was small. Kedem and Katchalsky transcribed their permeability equations in terms of L_p, σ, and ω. After doing this, they utilized (Eq. 4- 37) - (Eq. 4- 40) to develop an equation to describe the change in water and solute volume with time in the absence of a pressure gradient that is given as follows [21]:

(Eq. 4- 41)

$$\frac{dV_{w+s}}{dt} = -L_p ART\{(C_n^e - C_n^i) + \sigma(C_s^e - C_s^i)\}$$

where again L_p is the membrane hydraulic conductivity, A is the area of the cell, R is the universal gas constant, and T is absolute temperature. C is the molarity with the superscripts denoting the internal cell solution (i) and the

98

solution external to the cell (e) and the subscripts denoting the non-permeating solutes (n) and the permeating solutes (s). Kedem and Katchalsky built on the work of Staverman and used the reflection coefficient in their equations. The K-K reflection coefficient, σ , has a different physical meaning than the reflection coefficient, $\tilde{\sigma}$ used by Staverman.

The equation to describe the change in intracellular, permeating solute is given as follows:

(Eq. 4- 42)

$$\frac{dN_s}{dt} = (1-\sigma)\left(\frac{1}{2}\right)\left(C_s^e + C_s^i\right)\frac{dV_{w+s}}{dt} + P_s A\left(C_s^e - C_s^i\right)$$

where N_s is the number of moles of solute in the cell and again P_s is the membrane solute permeability.

In the K-K equations, σ is constrained by the following condition:

(Eq. 4- 43)

$$0 \leq \sigma \leq 1 - \frac{P_s v_s}{RTL_p}$$

In developing their equations, Kedem and Katchalsky assumed that the solute and solvent transport are physically coupled [21] and that the degree of interaction was characterized by the reflection coefficient. They assumed that solvent and solute interacted with each other. The extent of the interaction in the passage through the membrane depended on the nature of the system. Systems in which the solvent and solute followed different paths through the membrane

99

had the lowest degree of interaction, such as aqueous solutions of liquid soluble substances passing through a mosaic membrane. The highest degree of interaction of solvent and solute occurs in free diffusion. This occurs in coarse capillary membranes [21].

In general, there is often some confusion with the transport equations which are often written in a finite difference form. Delcastillo [4] points out that final-difference forms are the result of the integration of the fundamental differential equations across a cell membrane and as a result, average values are often obtained. However, the average concentration appropriate for one transport equation, like the volume flow, may not be appropriate for another transport equation such as the solute flux.

4.4e Kleinhans

In 1998, Kleinhans wrote a review paper comparing the 2-P formalism with the K-K formalism [23]. In his paper Kleinhans argues that although the K-K formalism is the most general and the most commonly used formalism in cryobiology, it is not without drawbacks. Particularly he argues that the introduction of sigma adds to the complexity and says that "unfortunately, as a result of this complexity, sigma is often misunderstood, misinterpreted, and improperly calculated by cryobiologists" [23]. In his paper, Kleinhans discusses how recent discoveries in molecular biology have shown that co-transport in biological membranes is often unlikely. Some cells are known to exhibit rapid trans-membrane water transport

100

through specialized water channels [26,39,46]. The water transport proteins are known as "aquaporins" and they account for the water flux. Most water channels are highly selective and do not act as a common water channel for both water and solute and as a result, cryoprotectants are often excluded [39,46]. As a result of this, Kleinhans proposed that the K-K formalism and sigma were often unnecessary and demonstrated that the 2-P formalism worked just as well as the K-K formalism and essentially gave the same results for a number of different transport situations in which a common channel for solute and solvent was not present. Using simulations, he demonstrated this to be true for a number of circumstances including (i) bilayer transport in which the solute and water diffuse across the bilayer, (ii) transport in which water only moves through a selective channel and the solute diffuses across the bilayer and (iii) transport in which the water and solute use separate channels. Kleinhans noted that at the 2-P model and the K-K model deviated from each other at high concentrations, but that there were no practical differences between the two models up to solute concentrations of several molar [23].

4.5   The Reflection Coefficients σ and $\tilde{\sigma}$

When Staverman first introduced the reflection coefficient, it was proposed to describe membranes that were permeable to solutes and ranged from $0 \leq \tilde{\sigma} \leq 1$. $\tilde{\sigma} = 0$ applied to a non-selective membrane and $\tilde{\sigma} = 1$ applied to an ideally selective membrane permeable to the solvent only [43]. When Kedem and Katchalsky used the reflection coefficient, for their equations, it had a different

range, from $0 \leq \sigma \leq 1 - \dfrac{P_s v_s}{RTL_p}$. It has been recognized by many in the literature

that there are often many interpretational problems of the reflection coefficient

when using the K-K equations [5,18,19,23,33] and the validity and necessity of

sigma has been questioned [5,45]. The K-K equations were designed to deal

with co-transport across cell membranes. In deriving the limits for sigma, Kedem

and Katchalsky used the solute driving force which was based on the chemical

potential of the solute. In deriving the solute driving force equations, both a near

equilibrium and a dilute solution assumption were made. The limits of sigma for

the K-K equations are based on a hydrodynamic interaction. When water and

solute move across the membrane using independent pathways, this is the non-

interacting case and $\sigma = 1 - \dfrac{P_s v_s}{RTL_p}$. In this case, σ is completely dependent of

the values of L_p and P_s and is not an independent parameter. For situations

were solute and solvent move through a common channel, there is a greater

possibility of a hydrodynamic interaction in the membrane. For this interacting

case, $\sigma < 1 - \dfrac{P_s v_s}{RTL_p}$ and in this situation, sigma is an independent parameter

which depends on the strength of the flux interaction [21]. In the literature it is

often thought that the limits of σ for the K-K equation are the same as those of $\tilde{\sigma}$

in Staverman's original equations. As pointed out by Kleinhans as well [23],

people often mistakenly believe that a $\sigma < 1$ means that there is a solute-solvent

interaction [49], which is not true.

102

In Kleinhans' paper, he discusses the issue and misconceptions that are often present when people assume a value for $\sigma = 1$. Let us first recall that a $\sigma = 1$ means that there is 100% reflection of the solute back from the membrane (no solute permeability, i.e. - $P_s = 0$). If we substitute $\sigma = 1$ into the K-K equations, then (Eq. 4- 41) takes the following form:

(Eq. 4- 44)

$$\frac{dV_{w+s}}{dt} = -L_p ART \left(C^e - C^i \right)$$

Kleinhans points out that it is often thought that when substituting $\sigma = 1$ into the K-K equation, (Eq. 4- 44), it leads to an equation that looks like the 2-P formalism (Eq. 4- 9). Recall, the 2-P equation in terms of molarity had the following form:

(Eq. 4- 9)

$$\frac{dV_w}{dt} = -L_p ART \left(C^e - C^i \right)$$

Kleinhans argues that when comparing (Eq. 4- 9) with (Eq. 4- 44) we can see that the 2-P equation accounts for only the water volume flux while (Eq. 4- 44) is total volume flux of both the solute and the solvent, so the two equations are not the same.

As Kleinhans discusses, if $\sigma = 1$ is substituted into the K-K solute flux equation, (Eq. 4- 42) is reduced to the following:

(Eq. 4- 45)

$$\frac{dN_s}{dt} = P_s A \left(C_s^e - C_s^i \right)$$

103

which is identical to the 2-P solute flux equation, (Eq. 4- 10):

(Eq. 4- 10)

$$\frac{dN_s}{dt} = P_s A\left(C_s^e - C_s^i\right)$$

He argues that when σ = 1, there should be no solute flux present and this is part of the confusion when using sigma and the K-K equations. This, compounded with the fact that people often use the incorrect limits for sigma when using the K-K equations, leads to much confusion. However, it is important to note that by Staverman's definition, a σ = 1 means that there is 100% reflection of the solute back from the membrane and no solute permeability ($P_s = 0$). So if $P_s = 0$, it means that $\frac{dV_s}{dt} = 0$. As a result, there is no problem when comparing (Eq. 4- 9) and (Eq. 4- 44). So even though Kleinhans argues that the two equations look different, they are in fact the same since by definition σ = 1 means that $\frac{dV_s}{dt} = 0$.

Kleinhans argued that when σ = 1, there should be no solute flux present, but says when substituting σ = 1 into the K-K solute flux equation we get (Eq. 4- 45). However, again there is no problem with this because when σ = 1, $P_s = 0$, $\frac{dN_s}{dt} = 0$, and (Eq. 4- 45) is correct. In the literature when using the K-K equations and solving for L_p, P_s and σ, people often end up with a value of $\sigma = 1$ [1] even when $P_s \neq 0$. However, in doing this they are violating the conditions of the K-K equations because σ cannot equal 1 if $P_s \neq 0$.

104

In the literature the 2-P model is often preferred over the K-K model because of the fewer parameters required to describe the osmotic response of cells. People have noted that despite the fact that the K-K model accurately describes cell volume data, the model lacks the capability to detect changes in σ and that it is often phenomenalogically inconsistent with application for high permeability solutes [47]. As well, it has been pointed out that the interpretational value of σ to identify the transport pathway can be problematic [9].

4.6   Comparing the 2-P and the K-K Equations

To look at the total solute and solvent volume flux using the 2-P equations, we add together the water volume flux given in (Eq. 4- 9) in terms of molarity, with the solute volume flux given in (Eq. 4- 11) and use the definition of the extracellular solution molarity $\left(C^e = C_n^e + C_s^e\right)$ and the intracellular solution molarity $\left(C^i = C_n^i + C_s^i\right)$ to get the following:

(Eq. 4- 46)

$$\frac{dV_{w+s}}{dt} = \frac{dV_w}{dt} + \frac{dV_s}{dt} = -L_p ART \left\{ \left(C_n^e - C_n^i\right) + \left(1 - \frac{P_s v_s}{L_p RT}\right)\left(C_s^e - C_s^i\right)\right\}$$

We can compare the total volume flux obtained from the 2-P equations with the total volume flux of the K-K equations as given in (Eq. 4- 41).

(Eq. 4- 41)

$$\frac{dV_{w+s}}{dt} = -L_p ART \left\{\left(C_n^e - C_n^i\right) + \sigma\left(C_s^e - C_s^i\right)\right\}$$

105

It is interesting to note that the two equations look identical except there is a σ in (Eq. 4- 41) and in the 2-P equation, (Eq. 4- 46), there is the following expression instead: $\left(1-\frac{P_s v_s}{L_p RT}\right)$, which is the upper limit of sigma in the K-K equations. As mentioned earlier, the upper limit of sigma (the non-interacting case) occurs in the situation when water and solute move across the membrane using independent pathways. So for situations when there is no interaction between the water and solute, the 2-P and the K-K equations are essentially the same. Kleinhans demonstrated, using simulations, that when co-transporting channels are absent, the 2-P and the K-K equations essentially give the same result. However, this could have been realized intuitively by looking at the two equations because for the non-interacting case, they are essentially the same equations. In the literature people have even stated that the 2-P model is more consistent than the K-K model for the assumption of independent pathways, which assumes that water and solute use different pathways to permeate the cell membrane [20]. However, they are the same equations for the non-interacting case. Also, people are often utilizing the K-K equations with the non-interacting case without realizing that they are actually using the 2-P equations [11,49]. Du et al., in 1994 [5] did a study looking at permeability of human spermatozoa to glycerol using the 2-P model and the non-interacting case of the K-K model. They found that the two models gave essentially identical volume swell curves. We can understand now that this is because the two sets of equations are the same. A paper by Xu et al., in 2003, [50], reported measurements of chondrocyte

106

membrane permeability to a number of cryoprotectants and compared them using the 2-P model and the K-K model. Examination of their graphs of normalized volume change during dimethyl sulfoxide addition in that study indicates that the 2-P model and the K-K model gave identical results. A back calculation of the non-interacting value of σ (i.e.- $\left(1 - \dfrac{P_s v_s}{L_p RT}\right)$), for that system, resulted in a value of σ = 0.918. The value of sigma reported in their paper when fitting the K-K equation was 0.91 ±0.09, again demonstrating that the 2-P and K-K model give identical results for σ in the non-interacting case.

Kleinhans noted that the 2-P model and the K-K model deviated from each other at high concentrations, but there were no practical differences between the two models up to solute concentrations of several molar [23]. Despite the fact that we demonstrated that for the non-interacting case (the situation when water and solute move across the membrane using independent pathways), the 2-P and the K-K equations are essentially the same, when fitting for the permeability parameters, the 2-P model uses only 2 parameters while the K-K model uses 3 parameters. It is possible then that the fitting of σ is simply adjusting for non-dilute behavior, since in both equations a dilute solution assumption is being made. In the literature it has been reported that there is no pattern that emerges which defines how the solute concentration effects membrane permeability characteristics [11,29] and at times researchers found solute inhibition of L_p [11]. At times the hydraulic conductivity seems to decrease in the presence of

107

increased solute concentrations [30] while in other instances it appears that exposing cells to a permeable solute increases the hydraulic conductivity [31]. It is possible that these reported variations of the hydraulic conductivity are a result of dilute solution expressions being used in the transport equations and may not be evident if non-dilute transport equations were utilized.

It has been shown in the literature that different values for the hydraulic conductivity and the solute permeability are obtained depending on the set of transport equations used [1,49]. This may be problematic when people try and compare transport results or to utilize the transport values obtained from different research groups to determine optimal cryopreservation protocols.

As discussed earlier, often in the literature, the concentration expressions in the volume flux equations for both the 2-P and the K-K equations are incorrectly referred to as osmolality, not osmolarity. In order to have the conventional units of L_p, the concentration must be in terms of osmolarity (or molarity). In order to convert between the two expressions of concentration, you need to use the value for the density of water. This may be why in the biology literature, osmolality and osmolarity are used interchangeably. For ideal dilute solutions, any convenient concentration unit can be used. However, it is important to note this is only true for a dilute solution and at 4°C where the density of water is equal to $1g/cm^3$. These conditions are not in general met in cryobiology and so care in converting between molarity and molality must be exercised. So despite what is often

108

thought in the literature, using either the 2-P or the K-K equations results in dilute solution assumptions being made, specifically in the solute transport equations wherein molarity cannot simply be replaced with osmolarity as is usually done. The confusion of using a reflection coefficient as well as the dilute solution assumptions currently made in the commonly used transport formalisms, suggests a strong need for new non-dilute transport equations to be developed and used.

4.7 References

[1]   Arnaud, F.G., Pegg, D.E., Permeation of Glycerol and Propane-1,2-Diol into Human Platelets, Cryobiology 27 (1990) 107-118.

[2]   Bannerman, R.C., Elliott, J.A.W., Porter, K. R., McGann, L. E., A multi-solute osmotic virial equation for solutions of interest in biology, Submitted to: Biophysical Journal (2005).

[3]   Callen, H.B., Thermodynamics and an Introduction to Thermostatistics (John Wiley & Sons, New York, 1985) 493 pp.

[4]   Delcastillo, L.F., Mason, E.A., Generalization of Membrane Reflection Coefficients for Nonideal, Nonisothermal, Multicomponent Systems with External Forces and Viscous-Flow, Journal of Membrane Science 28 (1986) 229-267.

[5]   Du, J.Y., Kleinhans, F.W., Mazur, P., Critser, J.K., Human Spermatozoa Glycerol Permeability and Activation-Energy Determined by Electron-Paramagnetic-Resonance, Biochimica Et Biophysica Acta-Biomembranes 1194 (1994) 1-11.

[6]   Elliott, J.A.W., Elmoazzen, H.Y., McGann, L.E., A method whereby Onsager coefficients may be evaluated, Journal of Chemical Physics 113 (2000) 6573-6578.

[7]   Elliott, J.A.W., Ward, C.A., Equilibria and Dynamics of Gas Adsorption on Heterogeneous Solid Surfaces, Studies in Surface Science and Catalysis, Vol. 104 (Elsevier, New York, 1997).

[8]   Elmoazzen, H.Y., Elliott, J.A.W., McGann, L.E., The effect of temperature on membrane hydraulic conductivity, Cryobiology 45 (2002) 68-79.

[9]   Finkelstein, A., Water Movement Through Lipid Bilayers, Pore, and Plasma Membranes: Theory and Reality (Wiley, New York, 1987).

[10]   Gao, D.Y., Liu, J., Liu, C., Mcgann, L.E., Watson, P.F., Kleinhans, F.W., Mazur, P., Critser, E.S., Critser, J.K., Prevention of Osmotic Injury to Human Spermatozoa During Addition and Removal of Glycerol, Human Reproduction 10 (1995) 1109-1122.

[11]   Gilmore, J.A., Mcgann, L.E., Liu, J., Gao, D.Y., Peter, A.T., Kleinhans, F.W., Critser, J.K., Effect of Cryoprotectant Solutes on Water Permeability of Human Spermatozoa, Biology of Reproduction 53 (1995) 985-995.

[12] Gutierrez, A.M., Gonzalez, E., Echevarria, M., Hernandez, C.S., Whittembury, G., The Proximal Straight Tubule (Pst) Basolateral Cell-Membrane Water Channel - Selectivity Characteristics, Journal of Membrane Biology 143 (1995) 189-197.

[13] Hanai, T., Haydon, D.A., Permeability to Water of Bimolicular Lipid Membranes, Journal of Theoretical Biology 11 (1966) 370-382.

[14] Hunt, C.J., Armitage, S.E., Pegg, D.E., Cryopreservation of umbilical cord blood: 1. Osmotically inactive volume, hydraulic conductivity and permeability of CD34(+) cells to dimethyl, sulphoxide, Cryobiology 46 (2003) 61-75.

[15] Jacobs, M.H., The simultaneous measurement of cell permeability to water and to dissolved substances, Journal of Cellular and Comparative Physiology 2 (1933) 427-444.

[16] Jacobs, M.H., Glassman, H.N., Parpart, A.K., Osmotic properties of the erythrocyte VII. The temperature coefficients of certain hemolytic processes, Journal of Cellular and Comparative Physiology 7 (1935) 197-225.

[17] Jacobs, M.H., Stewart, D.R., A simple method for the quantitative measurement of cell permeability, Journal of Cellular and Comparative Physiology 1 (1932) 71-82.

[18] Kargol, M., Kargol, A., Mechanistic equations for membrane substance transport and their identity with Kedem-Katchalsky equations, Biophysical Chemistry 103 (2003) 117-127.

[19] Kargol, M., Kargol, A., Mechanistic formalism for membrane transport generated by osmotic and mechanical pressure, General Physiology and Biophysics 22 (2003) 51-68.

[20] Katkov, I.I., A two-parameter model of cell membrane permeability for multisolute systems, Cryobiology 40 (2000) 64-83.

[21] Kedem, O., Katchalsky, A., Thermodynamic Analysis of the Permeability of Biological Membranes to Non-Electrolytes, Biochimica Et Biophysica Acta 27 (1958) 229-246.

[22] Kett, T.K., Anderson, D.K., Ternary Isothermal Diffusion and Validity of Onsager Reciprocal Relations in Nonassociating Systems, Journal of Physical Chemistry 73 (1969) 1268.

[23] Kleinhans, F.W., Membrane permeability modeling: Kedem-Katchalsky vs a two-parameter formalism, Cryobiology 37 (1998) 271-289.

[24] Koter, S., Transport of Electrolytes across Cation-Exchange Membranes - Test of Onsager Reciprocity in Zero-Current Processes, Journal of Membrane Science 78 (1993) 155-162.

[25] Lucke, B., McCutcheon, M., The Living Cell as an Osmotic System and its Permeability to Water, Physiological Reviews 12 (1932) 68-139.

[26] Macey, R.I., Transport of Water and Urea in Red-Blood-Cells, American Journal of Physiology 246 (1984) C195-C203.

[27] Madden, P.W., Pegg, D.E., Calculation of Corneal Endothelial-Cell Volume During the Addition and Removal of Cryoprotective Compounds, Cryo-Letters 13 (1992) 43-50.

[28] Mazur, P., Kinetics of water loss from cells at subzero temperatures and the likelihood of intracellular freezing, The Journal of General Physiology 47 (1963) 347-369.

[29] McGrath, J.J., Quantitative measurement of cell membrane transport: Technology and applications, Cryobiology 34 (1997) 315-334.

[30] McGrath, J.J., Diller, K.R. (Eds.), Low Temperature Biotechnology: Emerging Applications and Engineering Contributions, ASME Press, New York, 1988, 273-330.

[31] McGrath, J.J., Hunter, J. E., Bernard, A. G., Fuller, B. J., and Shaw, R. W., On the use of microdiffusion chamber methods to determine the coupled transport of water and cryoprotective agents across biological membranes, in: K.R. Diller, A. Shitzer (Eds.), Macroscopic and Microscopic Heat and Mass Transfer in Biomedical Engineering (International Centre for Heat and Mass Transfer Publications, 1992) 301-326.

[32] Mcmillan, W.G., Mayer, J.E., The Statistical Thermodynamics of Multicomponent Systems, Journal of Chemical Physics 13 (1945) 276-305.

[33] Mikuleck.Dc, Dilute-Solution Approximation and Generalization of Reflection Coefficient Method of Describing Volume and Solute Flows, Biophysical Journal 13 (1973) 994-999.

[34] Miller, D.G., Ternary Isothermal Diffusion and the Validity of the Onsager Reciprocity Relations, Journal of Physical Chemistry 63 (1959) 570-578.

[35] Moura, T.F., Macey, R.I., Chien, D.Y., Karan, D., Santos, H., Thermodynamics of All-or-None Water Channel Closure in Red-Cells, Journal of Membrane Biology 81 (1984) 105-111.

[36]   Newton, H., Pegg, D.E., Barrass, R., Gosden, R.G., Osmotically inactive volume, hydraulic conductivity, and permeability to dimethyl sulphoxide of human mature oocytes, Journal of Reproduction and Fertility 117 (1999) 27-33.

[37]   Onsager, L., Reciprocal relations in irreversible processes. I., Physical Review 37 (1931) 405-426.

[38]   Onsager, L., Reciprocal relations in irreversible processes. II., Physical Review 38 (1931) 2265-2279.

[39]   Preston, G.M., Carroll, T.P., Guggino, W.B., Agre, P., Appearance of Water Channels in Xenopus Oocytes Expressing Red-Cell Chip28 Protein, Science 256 (1992) 385-387.

[40]   Price, H.D., Thompson, T.E., Properties of Liquid Bilayer Membranes Separating 2 Aqueous Phases - Temperature Dependence of Water Permeability, Journal of Molecular Biology 41 (1969) 443-457.

[41]   Spallek, M., Hertz, H.G., Kashammer, S., Weingartner, H., Ternary Diffusion and Onsager Reciprocity Relations in Aqueous Zncl2+Kcl and Cdcl2+Kcl Revisited, Berichte Der Bunsen-Gesellschaft-Physical Chemistry Chemical Physics 96 (1992) 764-769.

[42]   Staverman, A.J., Apparent Osmotic Pressure of Solutions of Heterodisperse Polymers, Recueil Des Travaux Chimiques Des Pays-Bas-Journal of the Royal Netherlands Chemical Society 71 (1952) 623-633.

[43]   Staverman, A.J., The Theory of Measurement of Osmotic Pressure, Recueil Des Travaux Chimiques Des Pays-Bas-Journal of the Royal Netherlands Chemical Society 70 (1951) 344-352.

[44]   Stein, W.D., Transport and Diffusion across Cell Membranes (Academic Press, Orlando, 1986).

[45]   Tanaka, J.Y., Walsh, J.R., Diller, K.R., Brand, J.J., Aggarwal, S.J., Algae permeability to Me2SO from-3 to 23 degrees C, Cryobiology 42 (2001) 286-300.

[46]   Verkman, A.S., VanHoek, A.N., Ma, T.H., Frigeri, A., Skach, W.R., Mitra, A., Tamarappoo, B.K., Farinas, J., Water transport across mammalian cell membranes, American Journal of Physiology-Cell Physiology 39 (1996) C12-C30.

[47]   Walsh, J.R., Diller, K.R., Jerry, B., Measurement and simulation of water and methanol transport in algal cells, Journal of Biomechanical Engineering-Transactions of the Asme 126 (2004) 167-179.

[48]   Ward, C.A., Rate of Gas Absorption at a Liquid Interface, Journal of Chemical Physics 67 (1977) 229-235.

[49]   Woods, E.J., Liu, J., Zieger, M.A.J., Lakey, J.R.T., Critser, J.K., Water and cryoprotectant permeability characteristics of isolated human and canine pancreatic islets, Cell Transplantation 8 (1999) 549-559.

[50]   Xu, X., Cui, Z.F., Urban, J.P.G., Measurement of the chondrocyte membrane permeability to Me2SO, glycerol and 1,2-propanediol, Medical Engineering & Physics 25 (2003) 573-579.

[51]   Zelman, A., Membrane-Permeability - Generalization of Reflection Coefficient Method of Describing Volume and Solute Flows, Biophysical Journal 12 (1972) 414-419.

[52]   Zhang, S.Z., Chen, G.M., Analytical solution for the extremums of cell water volume and cell volume using a two-parameter model, Cryobiology 44 (2002) 204-209.

Figure 4-1 Model of plasma membrane

Image from: www.cancerquest.org/images/New_Membrane.jpg
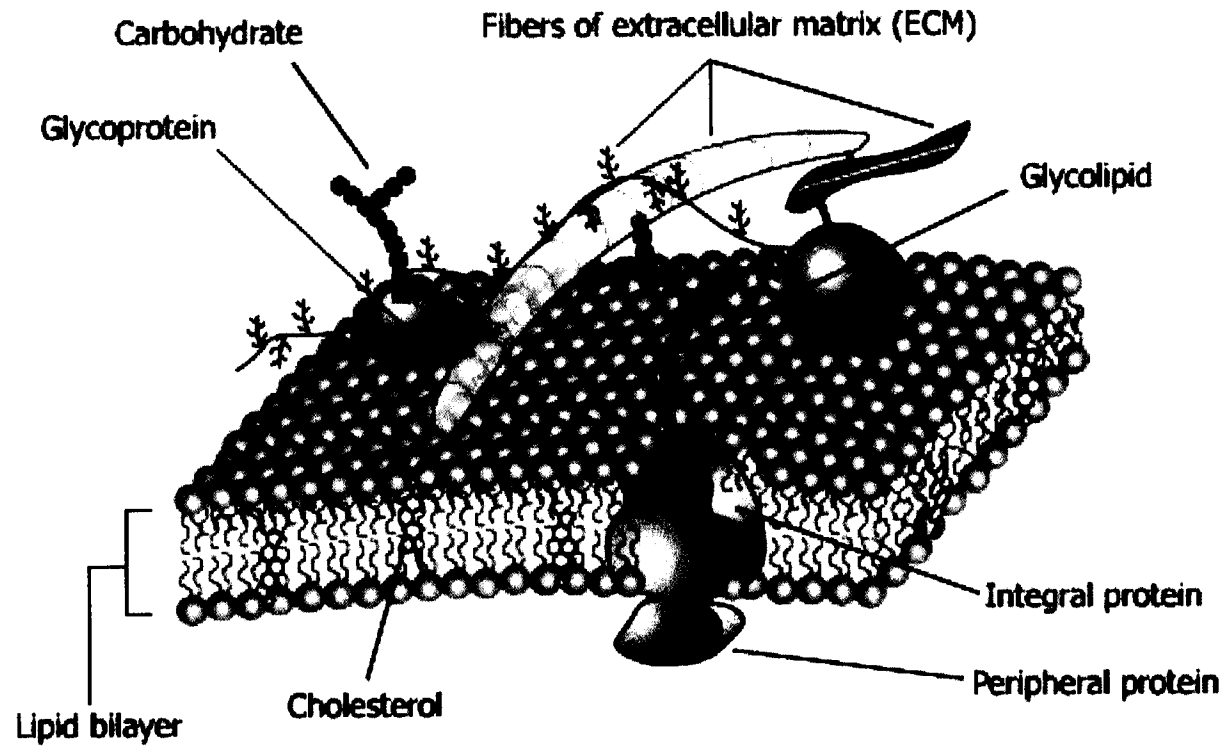
Figure 4-2   A two-component system of water and solute where both may permeate the cell membrane and where there is tension in the membrane

116
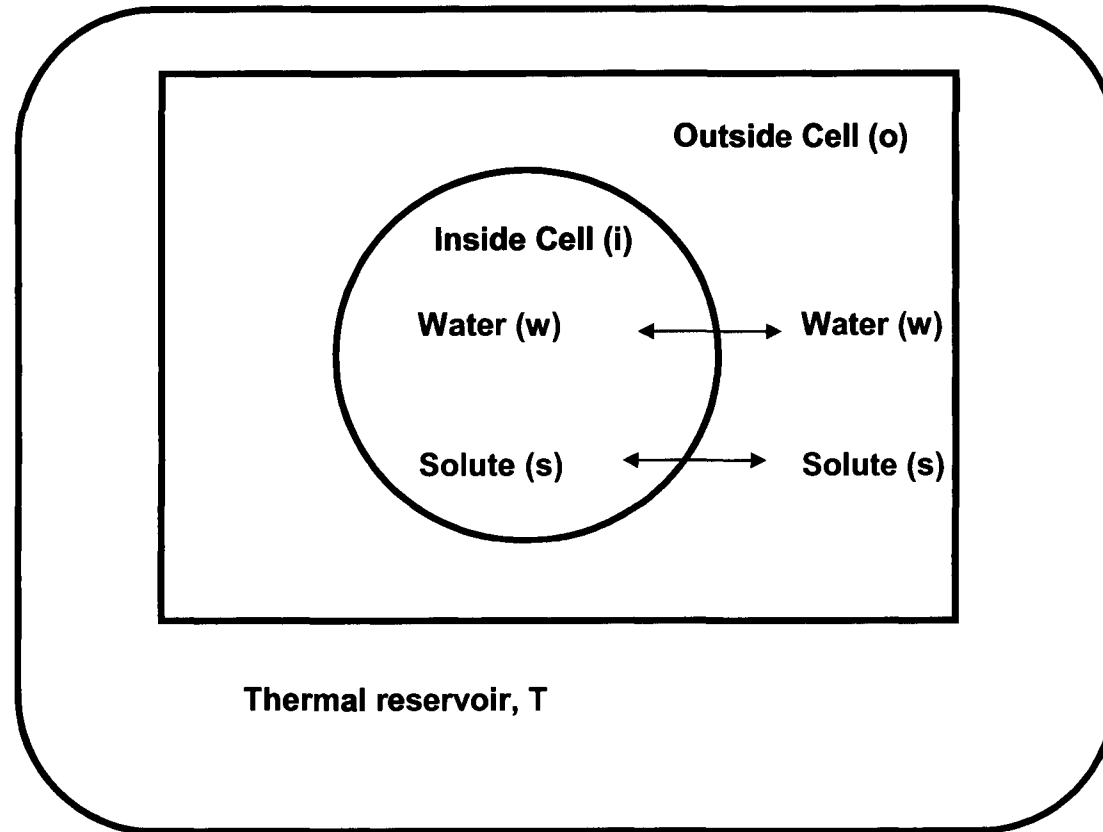
Chapter 5: Chemical Potential Equations

5.1 Introduction

Much of solution thermodynamics is concerned with the thermodynamic changes that occur when a molecule is moved from one environment to another. Various systems may contain different particles. If a mixture of two or more substances is thermodynamically favored, it is called a solution. In a solution, the predominant substance is referred to as the solvent and the other substances as solutes. There are chemical potentials μ_i for each component in a mixture. The chemical potential is a measure of how much the Gibbs free energy, G, of a system changes (by dG) if you add or remove a number, dN_i particles of the particle species i, keeping the number of other particles as well as the temperature (T) and pressure (P) constant. The units of chemical potential are that of energy per mole and it is the chemical potential that drives mass transport. Thus the chemical potential may be written as follows [3]:

(Eq. 5- 1)

$$dG = -SdT + VdP + \sum_i \mu_i dN_i$$

(Eq. 5- 2)

$$\mu_i = \left(\frac{\partial G}{\partial N_i} \right)_{T,P,N_{j \neq i}}$$

To derive the relevant chemical potential equations for the solvent and solutes, we will assume we have a system with two solutes inside and two solutes outside

117

a biological cell in the presence of a solvent as shown in Figure 5-1. N_1 = the number of moles of solvent (i.e. - water), N_2 = the number of moles of a permeating solute that may be present on the inside or outside of the cell membrane (i.e. DMSO), N_3 = the number of moles of a non-permeating solute on the inside of the cell (i.e. KCl) and N_4 = the number of moles of a non-permeating solute on the outside of the cell (i.e. NaCl).

5.2   Chemical Potential of the Solvent

The Gibbs free energy of a real solution may be separated into two parts as follows:

(Eq. 5- 3)

$$G = G_{ideal} + G_{excess}$$

where G_{ideal} is the Gibbs free energy of an ideal solution which may be written (for the three components 1, 2 and 3 inside the cell) as follows [2]:

(Eq. 5- 4)

$$G_{ideal}(T, P, N_1, N_2, N_3) = N_1 \mu_1^*(T, P) + N_2 \psi(T, P) + N_3 \varphi(T, P)$$

$$+ N_1 RT \ln\left(\frac{N_1}{N_1 + N_2 + N_3}\right) + N_2 RT \ln\left(\frac{N_2}{N_1 + N_2 + N_3}\right) + N_3 RT \ln\left(\frac{N_3}{N_1 + N_2 + N_3}\right)$$

where, μ_1^* is the chemical potential of the pure solvent. The standard state for the solvent, water, is usually taken to be pure water. ψ is an unspecified function of temperature and pressure related to the standard state of the permeating solute usually taken to be infinite dilution, and φ is another

118

unspecified function of temperature and pressure. R is the universal gas constant.

The simplest model for excess Gibbs energy (regular solution theory) is as follows [6]:

(Eq. 5- 5)

$$G_{excess} = \frac{\omega_2 N_1 N_2}{(N_1 + N_2 + N_3)} + \frac{\omega_3 N_1 N_3}{(N_1 + N_2 + N_3)}$$

ω_2 is the energy of interaction of solute N_2 with the solvent (water), ω_3 is the energy of interaction of solute N_3 with the solvent (water). This simple model includes the entropy of mixing of the solutes with the solvent but neglects mixing between different solutes. This will be a good assumption when $\omega_{23} N_2 N_3 \ll \omega_2 N_1 N_2$ or $\omega_3 N_1 N_3$, where ω_{23} is the energy of interaction of solute N_2 with solute N_3. If the interchange energies are about the same order of magnitude, this will be a good assumption if $N_2 N_3 \ll N_1 N_2$ or $N_1 N_3$. For example, for a 2 molal DMSO solution, the values for N_1, N_2 and N_3 are approximately 1×10^{-10}, 5×10^{-12}, and 4×10^{-13}, respectively, thus this assumption will hold true. As a result, we can write the total Gibbs energy as follows:

(Eq. 5- 6)

$$G(T, P, N_1, N_2, N_3) = N_1 \mu_1^*(T, P) + N_2 \psi(T, P) + N_3 \varphi(T, P)$$

$$+ N_1 RT \ln\left(\frac{N_1}{N_1 + N_2 + N_3}\right) + N_2 RT \ln\left(\frac{N_2}{N_1 + N_2 + N_3}\right) + N_3 RT \ln\left(\frac{N_3}{N_1 + N_2 + N_3}\right)$$

$$+ \frac{\omega_2 N_1 N_2}{(N_1 + N_2 + N_3)} + \frac{\omega_3 N_1 N_3}{(N_1 + N_2 + N_3)}$$

119

(Eq. 5- 6) maybe re-written as follows:

(Eq. 5- 7)

$$G(T,P,N_1,N_2,N_3) = N_1\mu_1^*(T,P) + N_2\mu_2^*(T,P) + N_3\mu_3^*(T,P) + N_1RT\ln(N_1)$$
$$- N_1RT\ln(N_1 + N_2 + N_3) + N_2RT\ln(N_2) - N_2RT\ln(N_1 + N_2 + N_3) + N_3RT\ln(N_3)$$
$$- N_3RT\ln(N_1 + N_2 + N_3) + (\omega_2 N_1 N_2)(N_1 + N_2 + N_3)^{-1} + (\omega_3 N_1 N_3)(N_1 + N_2 + N_3)^{-1}$$

The chemical potential of the solvent, μ_1, can then be found by differentiating (Eq. 5- 7) with respect to N_1:

(Eq. 5- 8)

$$\mu_1 = \frac{\partial G}{\partial N_1} = \mu_1^* + RT\ln(N_1) + \frac{N_1 RT}{N_1} - \left[RT\ln(N_1 + N_2 + N_3) + \frac{N_1 RT}{(N_1 + N_2 + N_3)} \right]$$
$$- \frac{N_2 RT}{(N_1 + N_2 + N_3)} - \frac{N_3 RT}{(N_1 + N_2 + N_3)} + \frac{\omega_2 N_2}{(N_1 + N_2 + N_3)} - (\omega_2 N_1 N_2)(N_1 + N_2 + N_3)^{-2}$$
$$+ \frac{\omega_3 N_3}{(N_1 + N_2 + N_3)} - (\omega_3 N_1 N_3)(N_1 + N_2 + N_3)^{-2}$$

By collecting the " RT " terms together, (Eq. 5- 8) may be re-written as:

(Eq. 5- 9)

$$\mu_1 = \mu_1^* + RT\left[\begin{array}{c} \ln(N_1) + 1 - \ln(N_1 + N_2 + N_3) - \dfrac{N_1}{(N_1 + N_2 + N_3)} - \dfrac{N_2}{(N_1 + N_2 + N_3)} \\ - \dfrac{N_3}{(N_1 + N_2 + N_3)} \end{array} \right]$$
$$+ \frac{\omega_2 N_2}{(N_1 + N_2 + N_3)} - (\omega_2 N_1 N_2)(N_1 + N_2 + N_3)^{-2} + \frac{\omega_3 N_3}{(N_1 + N_2 + N_3)} - (\omega_3 N_1 N_3)(N_1 + N_2 + N_3)^{-2}$$

120

The "1" in the square bracket may be re-written as: $\dfrac{(N_1 + N_2 + N_3)}{(N_1 + N_2 + N_3)}$. Therefore,

(Eq. 5- 9) maybe re-written as:

(Eq. 5- 10)

$$\mu_1 = \mu_1^* + RT\left[\ln(N_1) + \frac{(N_1 + N_2 + N_3)}{(N_1 + N_2 + N_3)} - \ln(N_1 + N_2 + N_3) - \frac{N_1}{(N_1 + N_2 + N_3)} - \frac{N_2}{(N_1 + N_2 + N_3)} - \frac{N_3}{(N_1 + N_2 + N_3)}\right]$$
$$+ \frac{\omega_2 N_2}{(N_1 + N_2 + N_3)} - (\omega_2 N_1 N_2)(N_1 + N_2 + N_3)^{-2} + \frac{\omega_3 N_3}{(N_1 + N_2 + N_3)} - (\omega_3 N_1 N_3)(N_1 + N_2 + N_3)^{-2}$$

Simplifying (Eq. 5- 10) results in the following:

(Eq. 5- 11)

$$\mu_1 = \mu_1^* + RT[\ln(N_1) - \ln(N_1 + N_2 + N_3)] + \frac{\omega_2 N_2}{(N_1 + N_2 + N_3)} - (\omega_2 N_1 N_2)(N_1 + N_2 + N_3)^{-2}$$
$$+ \frac{\omega_3 N_3}{(N_1 + N_2 + N_3)} - (\omega_3 N_1 N_3)(N_1 + N_2 + N_3)^{-2}$$

We may write (Eq. 5- 11) in terms of the mole fractions where x_1 is the mole fraction of the solvent, x_2 is the mole fraction of the permeating solute and x_3 is the mole fraction of the non-permeating solute.

(Eq. 5- 12)

$$x_1 = \frac{N_1}{(N_1 + N_2 + N_3)}$$

(Eq. 5- 13)

$$x_2 = \frac{N_2}{(N_1 + N_2 + N_3)}$$

121

(Eq. 5- 14)

$$x_3 = \frac{N_3}{(N_1 + N_2 + N_3)}$$

Also, we may make the following simplification:

(Eq. 5- 15)

$$\ln(N_1) - \ln(N_1 + N_2 + N_3) = \ln\left(\frac{N_1}{(N_1 + N_2 + N_3)}\right) = \ln(x_1)$$

By substituting (Eq. 5- 12) through (Eq. 5- 15) into (Eq. 5- 11), we get the following:

(Eq. 5- 16)

$$\mu_1 = \mu_1^* + RT[\ln(x_1)] + \omega_2 x_2 - (\omega_2 x_1 x_2) + \omega_3 x_3 - (\omega_3 x_1 x_3)$$

Note that:

(Eq. 5- 17)

$$x_1 + x_2 + x_3 = 1$$

(Eq. 5- 18)

$$x_1 = 1 - x_2 - x_3$$

We can substitute (Eq. 5- 18) into (Eq. 5- 16) to get the following expression:

(Eq. 5- 19)

$$\mu_1 = \mu_1^* + RT[\ln(1 - x_2 - x_3)] + \omega_2 x_2 - \omega_2 (1 - x_2 - x_3) x_2 + \omega_3 x_3 - \omega_3 (1 - x_2 - x_3) x_3$$

(Eq. 5- 19) may be re-arranged as follows:

(Eq. 5- 20)

$$\mu_1 = \mu_1^* + RT \ln(1 - x_2 - x_3) + \omega_2 x_2 (1 - (1 - x_2 - x_3)) + \omega_3 x_3 (1 - (1 - x_2 - x_3))$$

122

As a result, we may write the chemical potential of the solvent inside of the cell as follows:

(Eq. 5- 21)

$$\mu_1^i = \mu_1^* + RT \ln\left(1 - x_2^i - x_3^i\right) + \omega_2 x_2^i\left(x_2^i + x_3^i\right) + \omega_3 x_3^i\left(x_2^i + x_3^i\right)$$

To derive the chemical potential of the solvent outside of the cell, we again utilize (Eq. 5- 4) through (Eq. 5- 21) and replace the intracellular interchange energy, ω_3 (which is the energy of interaction of solute N_3 with the solvent) and the intracellular mole fraction, x_3 with the extracellular interchange energy, ω_4 (which is the energy of interaction of solute N_4 with the solvent) and the extracellular mole fraction, x_4. The chemical potential of the solvent on the outside of the cell may be written as:

(Eq. 5- 22)

$$\mu_1^o = \mu_1^* + RT \ln\left(1 - x_2^o - x_4^o\right) + \omega_2 x_2^o\left(x_2^o + x_4^o\right) + \omega_4 x_4^o\left(x_2^o + x_4^o\right)$$

We may combine the intracellular solute mole fractions as:

(Eq. 5- 23)

$$x_2^i + x_3^i = X^i$$

Similarly, we may combine the extracellular solute mole fractions as:

(Eq. 5- 24)

$$x_2^o + x_4^o = X^o$$

Using the definitions in (Eq. 5- 23) and (Eq. 5- 24), we may re-write the intracellular solvent chemical potential (Eq. 5- 22) and the extracellular solvent chemical potential (Eq. 5- 23) as follows:

123

(Eq. 5- 25)

$$\mu_1^i = \mu_1^* + RT\ln\!\left(1 - X^i\right) + \omega_2 x_2^i\!\left(X^i\right) + \omega_3 x_3^i\!\left(X^i\right)$$

(Eq. 5- 26)

$$\mu_1^o = \mu_1^* + RT\ln\!\left(1 - X^o\right) + \omega_2 x_2^o\!\left(X^o\right) + \omega_4 x_4^o\!\left(X^o\right)$$

The natural logarithms in (Eq. 5- 25) and (Eq. 5- 26) can be expanded, keeping terms up to second order in X as follows:

(Eq. 5- 27)

$$RT\ln\!\left(1 - X^i\right) = RT\left[\left(-X^i\right) - \left(\frac{\left(X^i\right)^2}{2}\right)\right]$$

(Eq. 5- 28)

$$RT\ln\!\left(1 - X^o\right) = RT\left[\left(-X^o\right) - \left(\frac{\left(X^o\right)^2}{2}\right)\right]$$

As a result, (Eq. 5- 25) and (Eq. 5- 26) may be expanded and re-written (to second order) as follows:

(Eq. 5- 29)

$$\mu_1^i = \mu_1^* - RTX^i - \frac{RT\left(X^i\right)^2}{2} + \omega_2 x_2^i\!\left(X^i\right) + \omega_3 x_3^i\!\left(X^i\right)$$

(Eq. 5- 30)

$$\mu_1^o = \mu_1^* - RTX^o - \frac{RT\left(X^o\right)^2}{2} + \omega_2 x_2^o\!\left(X^o\right) + \omega_4 x_4^o\!\left(X^o\right)$$

If we substitute (Eq. 5- 23) and (Eq. 5- 24) back into (Eq. 5- 29) and (Eq. 5- 30) we get the following:

124

(Eq. 5- 31)

$$\mu_1^i = \mu_1^* - RT\left(x_2^i + x_3^i\right) - \frac{RT}{2}\left(x_2^i + x_3^i\right)^2 + \omega_2 x_2^i\left(x_2^i + x_3^i\right) + \omega_3 x_3^i\left(x_2^i + x_3^i\right)$$

(Eq. 5- 32)

$$\mu_1^o = \mu_1^* - RT\left(x_2^o + x_4^o\right) - \frac{RT}{2}\left(x_2^o + x_4^o\right)^2 + \omega_2 x_2^o\left(x_2^o + x_4^o\right) + \omega_4 x_4^o\left(x_2^o + x_4^o\right)$$

Expanding (Eq. 5- 31) and (Eq. 5- 32) results in the following:

(Eq. 5- 33)

$$\mu_1^i = \mu_1^* - RTx_2^i - RTx_3^i - \frac{RT}{2}x_2^{i2} - RTx_2^i x_3^i - \frac{RT}{2}x_3^{i2} + \omega_2 x_2^{i2} + \omega_2 x_2^i x_3^i + \omega_3 x_3^{i2} + \omega_3 x_2^i x_3^i$$

(Eq. 5- 34)

$$\mu_1^o = \mu_1^* - RTx_2^o - RTx_4^o - \frac{RT}{2}x_2^{o2} - RTx_2^o x_4^o - \frac{RT}{2}x_4^{o2} + \omega_2 x_2^{o2} + \omega_2 x_2^o x_4^o + \omega_4 x_4^{o2} + \omega_4 x_2^o x_4^o$$

We can collect terms in (Eq. 5- 33) and (Eq. 5- 34) as follows:

(Eq. 5- 35)

$$\mu_1^i = \mu_1^* - RT\left(x_2^i + x_3^i\right) - RTx_2^{i2}\left(\frac{1}{2} - \frac{\omega_2}{RT}\right) - RTx_3^{i2}\left(\frac{1}{2} - \frac{\omega_3}{RT}\right) - RTx_2^i x_3^i\left(1 - \frac{\omega_2}{RT} - \frac{\omega_3}{RT}\right)$$

(Eq. 5- 36)

$$\mu_1^o = \mu_1^* - RT\left(x_2^o + x_4^o\right) - RTx_2^{o2}\left(\frac{1}{2} - \frac{\omega_2}{RT}\right) - RTx_4^{o2}\left(\frac{1}{2} - \frac{\omega_4}{RT}\right) - RTx_2^o x_4^o\left(1 - \frac{\omega_2}{RT} - \frac{\omega_4}{RT}\right)$$

We can redefine the expressions containing the interchange energies as follows:

125

(Eq. 5- 37)

$$B_2 = \frac{1}{2} - \frac{\omega_2}{RT}$$

(Eq. 5- 38)

$$B_3 = \frac{1}{2} - \frac{\omega_3}{RT}$$

(Eq. 5- 39)

$$B_4 = \frac{1}{2} - \frac{\omega_4}{RT}$$

Substituting (Eq. 5- 37), (Eq. 5- 38), and (Eq. 5- 39) into (Eq. 5- 35) and (Eq. 5- 36) results in the following:

(Eq. 5- 40)

$$\mu_1^i = \mu_1^* - RT\left(x_2^i + x_3^i\right) - B_2 RT x_2^{i2} - B_3 RT x_3^{i2} - \left(B_2 + B_3\right) RT x_2^i x_3^i$$

(Eq. 5- 41)

$$\mu_1^o = \mu_1^* - RT\left(x_2^o + x_4^o\right) - B_2 RT x_2^{o2} - B_4 RT x_4^{o2} - \left(B_2 + B_4\right) RT x_2^o x_4^o$$

The chemical potentials given in (Eq. 5- 40) and (Eq. 5- 41) are written in terms of the mole fraction.

The chemical potential may also be written in terms of molarity (C), instead of mole fraction. The mole fraction can be written in terms of the molarity as follows:

(Eq. 5- 42)

$$x = mol\,fraction = C\left(MW_{solution}\right) v_{solution}$$

126

where C is the molarity in units of $\left(\dfrac{mol_{solute}}{Volume_{solution}}\right)$, $MW_{solution}$ is the molecular

weight of the solution and $\upsilon_{solution}$ is the specific volume of the solution in units of

$\left(\dfrac{Volume_{solution}}{mass_{solution}}\right)$. As a result, we may rewrite the mole fractions of the intracellular

and extracellular components as follows:

(Eq. 5- 43)

$$x_2^i = C_2^i\left(MW_{solution}\right)\upsilon_{solution}$$

(Eq. 5- 44)

$$x_3^i = C_3^i\left(MW_{solution}\right)\upsilon_{solution}$$

(Eq. 5- 45)

$$x_2^o = C_2^o\left(MW_{solution}\right)\upsilon_{solution}$$

(Eq. 5- 46)

$$x_4^o = C_4^o\left(MW_{solution}\right)\upsilon_{solution}$$

(Eq. 5- 43) through (Eq. 5- 46) can be substituted into (Eq. 5- 40) and (Eq. 5- 41)

to get the chemical potential for the inside and the outside of the cell in terms of

molarity.

(Eq. 5- 47)

$$\mu_1^i = \mu_1^* - RTC_2^i\left(MW_{solution}\right)\upsilon_{solution} - RTC_3^i\left(MW_{solution}\right)\upsilon_{solution} - B_2RTC_2^{i2}\left(MW_{solution}\right)^2\upsilon_{solution}^2$$
$$- B_3RTC_3^{i2}\left(MW_{solution}\right)^2\upsilon_{solution}^2 - \left(B_2 + B_3\right)RTC_2^iC_3^i\left(MW_{solution}\right)^2\upsilon_{solution}^2$$

127

(Eq. 5- 48)

$$\mu_1^o = \mu_1^* - RTC_2^o \left(MW_{solution}\right)\!v_{solution} - RTC_4^o \left(MW_{solution}\right)\!v_{solution} - B_2 RTC_2^{o2}\left(MW_{solution}\right)^2 v_{solution}^2$$
$$- B_4 RTC_4^{o2}\left(MW_{solution}\right)^2 v_{solution}^2 - \left(B_2 + B_4\right)RTC_2^o C_4^o \left(MW_{solution}\right)^2 v_{solution}^2$$

We may re-write the B's from the chemical potentials written in terms of mole fraction in terms of new B's which we can label as B^*, to be used in chemical potential equations written in terms of molarity, where:

(Eq. 5- 49)

$$B_2^* = \left(\frac{1}{2} - \frac{\omega_2}{RT}\right)\!\left(MW_{solution}\right)\!v_{solution} = B_2\left(MW_{solution}\right)\!v_{solution}$$

(Eq. 5- 50)

$$B_3^* = \left(\frac{1}{2} - \frac{\omega_3}{RT}\right)\!\left(MW_{solution}\right)\!v_{solution} = B_3\left(MW_{solution}\right)\!v_{solution}$$

(Eq. 5- 51)

$$B_4^* = \left(\frac{1}{2} - \frac{\omega_4}{RT}\right)\!\left(MW_{solution}\right)\!v_{solution} = B_4\left(MW_{solution}\right)\!v_{solution}$$

Therefore, we can substitute (Eq. 5- 49) through (Eq. 5- 51) into (Eq. 5- 47) and (Eq. 5- 48) to obtain the following:

(Eq. 5- 52)

$$\mu_1^i = \mu_1^* - RTC_2^i \left(MW_{solution}\right)\!v_{solution} - RTC_3^i \left(MW_{solution}\right)\!v_{solution} - B_2^* RTC_2^{i2}\left(MW_{solution}\right)\!v_{solution}$$
$$- B_3^* RTC_3^{i2}\left(MW_{solution}\right)\!v_{solution} - \left(B_2^* + B_3^*\right)RTC_2^i C_3^i \left(MW_{solution}\right)\!v_{solution}$$

(Eq. 5- 53)

$$\mu_1^o = \mu_1^* - RTC_2^o \left(MW_{solution}\right)\!v_{solution} - RTC_4^o \left(MW_{solution}\right)\!v_{solution} - B_2^* RTC_2^{o2}\left(MW_{solution}\right)\!v_{solution}$$
$$- B_4^* RTC_4^{o2}\left(MW_{solution}\right)\!v_{solution} - \left(B_2^* + B_4^*\right)RTC_2^o C_4^o \left(MW_{solution}\right)\!v_{solution}$$

128

The chemical potentials in (Eq. 5- 52) and (Eq. 5- 53) are in terms of molarity C.

The chemical potential may also be written in terms of molality (m), instead of mole fraction or molarity. The mole fraction can be written in terms of the molality as follows:

(Eq. 5- 54)

$$x = mole\ fraction = m\ (MW_{solvent})x_{solvent}$$

where m is the molality in units of $\left(\dfrac{mol_{solute}}{kg_{solvent}}\right)$, $MW_{solvent}$ is the molecular weight of

the solvent and $x_{solvent}$ is the mole fraction of the solvent. As a result, we may

rewrite the mole fractions of the intracellular and extracellular components as

follows:

(Eq. 5- 55)

$$x_2^i = m_2^i(MW_{solvent})x_{solvent}$$

(Eq. 5- 56)

$$x_3^i = m_3^i(MW_{solvent})x_{solvent}$$

(Eq. 5- 57)

$$x_2^o = m_2^o(MW_{solvent})x_{solvent}$$

(Eq. 5- 58)

$$x_4^o = m_4^o(MW_{solvent})x_{solvent}$$

(Eq. 5- 55) through (Eq. 5- 58) can be substituted into (Eq. 5- 40) and (Eq. 5- 41)

to get the chemical potential for the inside and the outside of the cell in terms of

molality.

129

(Eq. 5- 59)

$$\mu_1^i = \mu_1^* - RTm_2^i \left(MW_{solvent}\right)x_{solvent} - RTm_3^i\left(MW_{solvent}\right)x_{solvent} - B_2 RTm_2^{i2}\left(MW_{solvent}\right)^2 x_{solvent}^2$$
$$- B_3 RTm_3^{i2}\left(MW_{solvent}\right)^2 x_{solvent}^2 - \left(B_2 + B_3\right)RTm_2^i m_3^i \left(MW_{solvent}\right)^2 x_{solvent}^2$$

(Eq. 5- 60)

$$\mu_1^o = \mu_1^* - RTm_2^o \left(MW_{solvent}\right)x_{solvent} - RTm_4^o\left(MW_{solvent}\right)x_{solvent} - B_2 RTm_2^{o2}\left(MW_{solvent}\right)^2 x_{solvent}^2$$
$$- B_4 RTm_4^{o2}\left(MW_{solvent}\right)^2 x_{solvent}^2 - \left(B_2 + B_4\right)RTm_2^o m_4^o \left(MW_{solvent}\right)^2 x_{solvent}^2$$

We may re-write the B's from the chemical potential equations written in terms of mole fraction in terms of new B's which we can label as B^+, for use in chemical potential equations written in terms of molality, where:

(Eq. 5- 61)

$$B_2^+ = \left(\frac{1}{2} - \frac{\omega_2}{RT}\right)MW_{solvent}x_{solvent} = B_2 MW_{solvent}x_{solvent}$$

(Eq. 5- 62)

$$B_3^+ = \left(\frac{1}{2} - \frac{\omega_3}{RT}\right)MW_{solvent}x_{solvent} = B_3 MW_{solvent}x_{solvent}$$

(Eq. 5- 63)

$$B_4^+ = \left(\frac{1}{2} - \frac{\omega_4}{RT}\right)MW_{solvent}x_{solvent} = B_4 MW_{solvent}x_{solvent}$$

Therefore, we can substitute (Eq. 5- 61) through (Eq. 5- 63) into (Eq. 5- 59) and (Eq. 5- 60) to obtain the following:

(Eq. 5- 64)

$$\mu_1^i = \mu_1^* - RTm_2^i \left(MW_{solvent}\right)x_{solvent} - RTm_3^i\left(MW_{solvent}\right)x_{solvent} - B_2^+ RTm_2^{i2}\left(MW_{solvent}\right)x_{solvent}$$
$$- B_3^+ RTm_3^{i2}\left(MW_{solvent}\right)x_{solvent} - \left(B_2^+ + B_3^+\right)RTm_2^i m_3^i \left(MW_{solvent}\right)x_{solvent}$$

130

(Eq. 5- 65)

$$\mu_1^o = \mu_1^* - RTm_2^o(MW_{solvent})x_{solvent} - RTm_4^o(MW_{solvent})x_{solvent} - B_2^+ RTm_2^{o2}(MW_{solvent})x_{solvnet}$$
$$- B_4^+ RTm_4^{o2}(MW_{solvent})x_{solvent} - (B_2^+ + B_4^+)RTm_2^o m_4^o(MW_{solvent})x_{solvent}$$

The chemical potentials in (Eq. 5- 64) and (Eq. 5- 65) are in terms of molality.

Note that while B_2, B_3 and B_4 are not in general dependent on the solution composition, B_2^* , B_3^* , B_4^* , B_2^+, B_3^+ and B_4^+ are dependent on solution composition though in practical circumstances this dependency may be negligible.

5.3 Chemical Potential of the Solute

Recall that for the inside of the cell the Gibbs free energy (G) maybe written as [2]:

(Eq. 5- 6)

$$G(T,P,N_1,N_2,N_3) = N_1\mu_1^*(T,P) + N_2\psi(T,P) + N_3\varphi(T,P)$$
$$+ N_1 RT\ln\left(\frac{N_1}{N_1+N_2+N_3}\right) + N_2 RT\ln\left(\frac{N_2}{N_1+N_2+N_3}\right) + N_3 RT\ln\left(\frac{N_3}{N_1+N_2+N_3}\right)$$
$$+ \frac{\omega_2 N_1 N_2}{(N_1+N_2+N_3)} + \frac{\omega_3 N_1 N_3}{(N_1+N_2+N_3)}$$

where, ω_2 is the energy of interaction of solute N_2 with the solvent (water) and ω_3 is the energy of interaction of solute N_3 with the solvent (water). We may re-write (Eq. 5- 6) as follows:

131

(Eq. 5- 7)

$$G(T,P,N_1,N_2,N_3) = N_1\mu_1^*(T,P) + N_2\psi(T,P) + N_3\varphi(T,P) + N_1RT\ln(N_1)$$
$$- N_1RT\ln(N_1 + N_2 + N_3) + N_2RT\ln(N_2) - N_2RT\ln(N_1 + N_2 + N_3) + N_3RT\ln(N_3)$$
$$- N_3RT\ln(N_1 + N_2 + N_3) + (\omega_2N_1N_2)(N_1 + N_2 + N_3)^{-1} + (\omega_3N_1N_3)(N_1 + N_2 + N_3)^{-1}$$

To get the chemical potential of the solute, N_2, we can differentiate (Eq. 5- 7) with respect to N_2:

(Eq. 5- 66)

$$\mu_2 = \frac{\partial G}{\partial N_2} = \psi - \frac{N_1RT}{(N_1 + N_2 + N_3)} + \frac{N_2RT}{N_2} + RT\ln(N_2)$$
$$- \left[RT\ln(N_1 + N_2 + N_3) + \frac{N_2RT}{(N_1 + N_2 + N_3)}\right] - \frac{N_3RT}{(N_1 + N_2 + N_3)} + \frac{\omega_2N_1}{(N_1 + N_2 + N_3)}$$
$$- (\omega_2N_1N_2)(N_1 + N_2 + N_3)^{-2} - (\omega_3N_1N_3)(N_1 + N_2 + N_3)^{-2}$$

By collecting the "RT" terms together, (Eq. 5- 66) maybe re-written as:

(Eq. 5- 67)

$$\mu_2 = \psi + RT\left[\begin{array}{c} \ln(N_2) + 1 - \ln(N_1 + N_2 + N_3) \\ -\frac{N_1}{(N_1 + N_2 + N_3)} - \frac{N_2}{(N_1 + N_2 + N_3)} - \frac{N_3}{(N_1 + N_2 + N_3)} \end{array}\right]$$
$$+ \frac{\omega_2N_1}{(N_1 + N_2 + N_3)} - (\omega_2N_1N_2)(N_1 + N_2 + N_3)^{-2} - (\omega_3N_1N_3)(N_1 + N_2 + N_3)^{-2}$$

The "1" in the square bracket may be re-written as: $\dfrac{(N_1 + N_2 + N_3)}{(N_1 + N_2 + N_3)}$ and as a

result, we may re-write (Eq. 5- 67) as follows:

132

(Eq. 5- 68)

$$\mu_2 = \psi + RT \left[\begin{array}{c} \ln(N_2) + \dfrac{(N_1 + N_2 + N_3)}{(N_1 + N_2 + N_3)} - \ln(N_1 + N_2 + N_3) \\[2mm] -\dfrac{N_1}{(N_1 + N_2 + N_3)} - \dfrac{N_2}{(N_1 + N_2 + N_3)} - \dfrac{N_3}{(N_1 + N_2 + N_3)} \end{array} \right]$$
$$+ \dfrac{\omega_2 N_1}{(N_1 + N_2 + N_3)} - (\omega_2 N_1 N_2)(N_1 + N_2 + N_3)^{-2} - (\omega_3 N_1 N_3)(N_1 + N_2 + N_3)^{-2}$$

Simplifying (Eq. 5- 68) results in the following:

(Eq. 5- 69)

$$\mu_2 = \psi + RT[\ln(N_2) - \ln(N_1 + N_2 + N_3)] + \dfrac{\omega_2 N_1}{(N_1 + N_2 + N_3)} - (\omega_2 N_1 N_2)(N_1 + N_2 + N_3)^{-2}$$
$$- (\omega_3 N_1 N_3)(N_1 + N_2 + N_3)^{-2}$$

We may write (Eq. 5- 69) in terms of the mole fractions where x_1 is the mole fraction of the solvent, x_2 is the mole fraction of the permeating solute and x_3 is the mole fraction of the non-permeating solute. Again we will use the following definitions of the mole fractions:

(Eq. 5- 12)

$$x_1 = \dfrac{N_1}{(N_1 + N_2 + N_3)}$$

(Eq. 5- 13)

$$x_2 = \dfrac{N_2}{(N_1 + N_2 + N_3)}$$

133

(Eq. 5- 14)

$$x_3 = \frac{N_3}{(N_1 + N_2 + N_3)}$$

Also, we may make the following simplification:

(Eq. 5- 70)

$$\ln(N_2) - \ln(N_1 + N_2 + N_3) = \ln\left(\frac{N_2}{(N_1 + N_2 + N_3)}\right) = \ln(x_2)$$

By substituting (Eq. 5- 12) through (Eq. 5- 14) and (Eq. 5- 70) into (Eq. 5- 69), we get the following:

(Eq. 5- 71)

$$\mu_2 = \psi + RT[\ln(x_2)] + \omega_2 x_1 - (\omega_2 x_1 x_2) - (\omega_3 x_1 x_3)$$

Again we will use:

(Eq. 5- 17)

$$x_1 + x_2 + x_3 = 1$$

(Eq. 5- 18)

$$x_1 = 1 - x_2 - x_3$$

We can substitute (Eq. 5- 18) into (Eq. 5- 71) to get the following expression:

(Eq. 5- 72)

$$\mu_2 = \psi + RT\ln(x_2) + \omega_2(1 - x_2 - x_3) - \omega_2(1 - x_2 - x_3)x_2 - \omega_3(1 - x_2 - x_3)x_3$$

(Eq. 5- 72) may be re-arranged as follows:

134

(Eq. 5- 73)

$$\mu_2 = \psi + RT\ln(x_2) + \omega_2(1 - x_2 - x_3)(1 - x_2) - \omega_3(1 - x_2 - x_3)x_3$$

As a result, the chemical potential of the solute inside the cell may be written as:

(Eq. 5- 74)

$$\mu_2^i = \psi + RT\ln(x_2^i) + \omega_2(1 - x_2^i - x_3^i)(1 - x_2^i) - \omega_3(1 - x_2^i - x_3^i)x_3^i$$

To derive the chemical potential of the solute outside the cell, we again follow the same approach taken to deriving the chemical potential of the solute inside the cell, however we replace the intracellular interchange energy, ω_3 (which is the energy of interaction of solute N_3 with the solvent) and the intracellular mole fraction, x_3 with the extracellular interchange energy, ω_4 (which is the energy of interaction of solute N_4 with the solvent) and the extracellular mole fraction, x_4. The chemical potential of the solute on the outside of the cell may be written as:

(Eq. 5- 75)

$$\mu_2^o = \psi + RT\ln(x_2^o) + \omega_2(1 - x_2^o - x_4^o)(1 - x_2^o) - \omega_4(1 - x_2^o - x_4^o)x_4^o$$

In the interest of having the same parameters appear in the equations for the solute and solvent chemical potentials, we will use the definitions for B_2, B_3, and B_4 that were derived from the solvent equations:

(Eq. 5- 37)

$$B_2 = \frac{1}{2} - \frac{\omega_2}{RT}$$

$$\omega_2 = RT\left(\frac{1}{2} - B_2\right)$$

135

(Eq. 5- 38)

$$B_3 = \frac{1}{2} - \frac{\omega_3}{RT}$$

$$\omega_3 = RT\left(\frac{1}{2} - B_3\right)$$

(Eq. 5- 39)

$$B_4 = \frac{1}{2} - \frac{\omega_4}{RT}$$

$$\omega_4 = RT\left(\frac{1}{2} - B_4\right)$$

Substituting (Eq. 5- 37), (Eq. 5- 38), and (Eq. 5- 39) into (Eq. 5- 74) and (Eq. 5- 75) results in the following:

(Eq. 5- 76)

$$\mu_2^i = \psi + RT\ln\left(x_2^i\right) + RT\left(\frac{1}{2} - B_2\right)\left(1 - x_2^i - x_3^i\right)\left(1 - x_2^i\right) - RT\left(\frac{1}{2} - B_3\right)\left(1 - x_2^i - x_3^i\right)x_3^i$$

(Eq. 5- 77)

$$\mu_2^o = \psi + RT\ln\left(x_2^o\right) + RT\left(\frac{1}{2} - B_2\right)\left(1 - x_2^o - x_4^o\right)\left(1 - x_2^o\right) - RT\left(\frac{1}{2} - B_4\right)\left(1 - x_2^o - x_4^o\right)x_4^o$$

The chemical potentials given in (Eq. 5- 76) and (Eq. 5- 77) are written in terms of the mole fraction. The chemical potential may also be written in terms of molarity (C) instead of mole fraction. Again, we may write the mole fraction in terms of molarity as follows:

(Eq. 5- 42)

$$x = mol\ fraction = C\left(MW_{solution}\right)v_{solution}$$

136

Again, we can use the definitions of mole fraction for the intracellular and extracellular components given in (Eq. 5- 43), (Eq. 5- 44), (Eq. 5- 45), and (Eq. 5-46).

(Eq. 5- 43)

$$x_2^i = C_2^i \left(MW_{solution} \right) \upsilon_{solution}$$

(Eq. 5- 44)

$$x_3^i = C_3^i \left(MW_{solution} \right) \upsilon_{solution}$$

(Eq. 5- 45)

$$x_2^o = C_2^o \left(MW_{solution} \right) \upsilon_{solution}$$

(Eq. 5- 46)

$$x_4^o = C_4^o \left(MW_{solution} \right) \upsilon_{solution}$$

These equations along with the definitions for B^* given from the solvent equations in (Eq. 5- 49), (Eq. 5- 50), and (Eq. 5- 51), which were in terms of molarity, can be substituted into (Eq. 5- 76) and (Eq. 5- 77) to get the chemical potential for the inside and the outside of the cell in terms of molarity:

(Eq. 5- 49)

$$B_2^* = \left(\frac{1}{2} - \frac{\omega_2}{RT} \right) \left(MW_{solution} \right) \upsilon_{solution} = B_2 \left(MW_{solution} \right) \upsilon_{solution}$$

(Eq. 5- 50)

$$B_3^* = \left(\frac{1}{2} - \frac{\omega_3}{RT} \right) \left(MW_{solution} \right) \upsilon_{solution} = B_3 \left(MW_{solution} \right) \upsilon_{solution}$$

137

(Eq. 5- 51)

$$B_4^* = \left(\frac{1}{2} - \frac{\omega_4}{RT}\right)\left(MW_{solution}\right)\!\upsilon_{solution} = B_4\left(MW_{solution}\right)\!\upsilon_{solution}$$

Therefore, the intracellular and extracellular chemical potentials of the solute in terms of molarity are given as follows:

(Eq. 5- 78)

$$\mu_2^i = \psi + RT\ln\!\left(C_2^i\left(MW_{solution}\right)\!\upsilon_{solution}\right)$$

$$+ RT\!\left(\frac{1}{2} - \frac{B_2^*}{\left(MW_{solution}\upsilon_{solution}\right)}\right)\!\left(1 - \left(C_2^i\left(MW_{solution}\right)\!\upsilon_{solution}\right) - \left(C_3^i\left(MW_{solution}\right)\!\upsilon_{solution}\right)\right)$$

$$\left(1 - \left(C_2^i\left(MW_{solution}\right)\!\upsilon_{solution}\right)\right) - RT\!\left(\frac{1}{2} - \frac{B_3^*}{\left(MW_{solution}\upsilon_{solution}\right)}\right)$$

$$\left(1 - \left(C_2^i\left(MW_{solution}\right)\!\upsilon_{solution}\right) - \left(C_3^i\left(MW_{solution}\right)\!\upsilon_{solution}\right)\right)\!C_3^i\left(MW_{solution}\right)\!\upsilon_{solution}$$

(Eq. 5- 79)

$$\mu_2^o = \psi + RT\ln\!\left(C_2^o\left(MW_{solution}\right)\!\upsilon_{solution}\right)$$

$$+ \left(RT\!\left(\frac{1}{2} - \frac{B_2^*}{\left(MW_{solution}\upsilon_{solution}\right)}\right)\right)\!\left(1 - \left(C_2^o\left(MW_{solution}\right)\!\upsilon_{solution}\right) - \left(C_4^o\left(MW_{solution}\right)\!\upsilon_{solution}\right)\right)$$

$$\left(1 - \left(C_2^o\left(MW_{solution}\right)\!\upsilon_{solution}\right)\right) - \left(RT\!\left(\frac{1}{2} - \frac{B_4^*}{\left(MW_{solution}\upsilon_{solution}\right)}\right)\right)$$

$$\left(1 - \left(C_2^o\left(MW_{solution}\right)\!\upsilon_{solution}\right) - \left(C_4^o\left(MW_{solution}\right)\!\upsilon_{solution}\right)\right)\!C_4^o\left(MW_{solution}\right)\!\upsilon_{solution}$$

The chemical potential of the solute may also be written in terms of molality (m), instead of mole fraction or molarity. Again, we may write the mole fraction in terms of molality as follows:

138

(Eq. 5- 54)

$$x = mole\ fraction = m\ (MW_{solvent})x_{solvent}$$

Again, we can use the definitions of mole fraction for the intracellular and extracellular components given in (Eq. 5- 55), (Eq. 5- 56), (Eq. 5- 57), and (Eq. 5-58)

(Eq. 5- 55)

$$x_2^i = m_2^i (MW_{solvent})x_{solvent}$$

(Eq. 5- 56)

$$x_3^i = m_3^i (MW_{solvent})x_{solvent}$$

(Eq. 5- 57)

$$x_2^o = m_2^o (MW_{solvent})x_{solvent}$$

(Eq. 5- 58)

$$x_4^o = m_4^o (MW_{solvent})x_{solvent}$$

These equations along with the definitions for B^+ given from the solvent equations in (Eq. 5- 61), (Eq. 5- 62), and (Eq. 5- 63), which were in terms of molality, can be substituted into (Eq. 5- 76) and (Eq. 5- 77) to get the chemical potential for the inside and outside of the cell in terms of molality:

(Eq. 5- 61)

$$B_2^+ = \left(\frac{1}{2} - \frac{\omega_2}{RT}\right)MW_{solvent}x_{solvent} = B_2 MW_{solvent}x_{solvent}$$

139

(Eq. 5- 62)

$$B_3^+ = \left(\frac{1}{2} - \frac{\omega_3}{RT}\right) MW_{solvent} x_{solvent} = B_3 MW_{solvent} x_{solvent}$$

(Eq. 5- 63)

$$B_4^+ = \left(\frac{1}{2} - \frac{\omega_4}{RT}\right) MW_{solvent} x_{solvent} = B_4 MW_{solvent} x_{solvent}$$

Therefore, the intracellular and extracellular chemical potentials of the solute in terms of molality are given as follows:

(Eq. 5- 80)

$$\mu_2^i = \psi + RT \ln\left(m_2^i (MW_{solvent}) x_{solvent}\right)$$

$$+ \left[RT\left(\frac{1}{2} - \frac{B_2^+}{(MW_{solvent} x_{solvent})}\right)\right]\left(1 - m_2^i (MW_{solvent}) x_{solvent} - m_3^i (MW_{solvent}) x_{solvent}\right)$$

$$\left(1 - m_2^i (MW_{solvent}) x_{solvent}\right) - \left[RT\left(\frac{1}{2} - \frac{B_3^+}{(MW_{solvent} x_{solvent})}\right)\right]$$

$$\left(1 - m_2^i (MW_{solvent}) x_{solvent} - m_3^i (MW_{solvent}) x_{solvent}\right) m_3^i (MW_{solvent}) x_{solvent}$$

(Eq. 5- 81)

$$\mu_2^o = \psi + RT \ln\left(m_2^o (MW_{solvent}) x_{solvent}\right)$$

$$+ \left[RT\left(\frac{1}{2} - \frac{B_2^+}{(MW_{solvent} x_{solvent})}\right)\right]\left(1 - m_2^o (MW_{solvent}) x_{solvent} - m_4^o (MW_{solvent}) x_{solvent}\right)$$

$$\left(1 - m_2^o (MW_{solvent}) x_{solvent}\right) - \left[RT\left(\frac{1}{2} - \frac{B_4^+}{(MW_{solvent} x_{solvent})}\right)\right]$$

$$\left(1 - m_2^o (MW_{solvent}) x_{solvent} - m_4^o (MW_{solvent}) x_{solvent}\right) m_4^o (MW_{solvent}) x_{solvent}$$

(Eq. 5- 80) and (Eq. 5- 81) are in terms of molarity.

5.4 Values for the Interaction Coefficients

In our laboratory, values for the interaction coefficients, B^+ and B for different solutes were calculated by fitting the osmolality of various solutions to a single solute osmotic viral equation truncated at the quadratic term as given in (Eq. 5-82) (in terms of molality) and in (Eq. 5- 83) (in terms of mole fraction).

(Eq. 5- 82)

$$\pi = m_i + B_i^+ m_i^2$$

(Eq. 5- 83)

$$\pi \cdot x_1 = \tilde{A}\left(x_i + B_i x_i^2\right)$$

$$\tilde{A} = \frac{1}{MW_{solvent}} = 55.49 \, \text{mole/kg}$$

$\tilde{A}$ is used to convert between units of molality and mole fraction. The osmolality as a function of concentration for different solutions was obtained from Richelle Bannerman who analyzed various freezing point depression data in the literature in terms of either mole fraction or molarity. The freezing point depression was converted to osmolality using the following equation:

(Eq. 5- 84)

$$FP = 1.86 * \pi \cdot x_1$$

where FP is the freezing point depression and 1.86 is the molal freezing point depression constant for water [7].

For solutes that dissociate, such as salts like KCl or NaCl, the concentration unit (molality) in (Eq. 5- 82) or (mole fraction) in (Eq. 5- 83), needs to be multiplied by a dissociation constant that is also fit for. The dissociation constant will be

141

different for the different units of concentration used. For solutes that do not dissociate, such as DSMO, glycerol or propylene glycol, the dissociation constant is simply equal to one. A list of the interaction coefficients for various solutes of interest are given in Table 5-1.

Table 5-1: Interaction parameters B and B^+ for various solutes in terms of mole fraction and molality

Solute	B value (in terms of mol fraction)	B^+ value (in terms of molality)
Dimethyl Sulfoxide (DMSO)	4.716	0.0843
Glycerol	2.950	0.0259
Propylene Glycol (PG)	3.415	0.0399
Potassium Chloride (KCl)	-0.057 (Dissociation constant = 1.79)	0.0000 (Dissociation constant = 1.74)
Sodium Chloride (NaCl)	2.759 (Dissociation constant = 1.68)	0.0299 (Dissociation constant = 1.70)

5.5 Discussion

5.5a Gibbs-Duhem equation

In deriving the chemical potential equations, the solvent and the solute equations must be consistent. The chemical potentials for both the solute and the solvent were derived from the same Gibbs free energy equation. Doing this guarantees that the chemical potential equations satisfy the Gibbs-Duhem equation. The Gibbs-Duhem equation is given as follows [3]:

142

(Eq. 5- 85)

$$0 = VdP - SdT + \sum_i N_i d\mu_i$$

where S is entropy, T is temperature, V is volume and P is pressure. At a

constant temperature and pressure, we get the following relationship:

(Eq. 5- 86)

$$\sum_i N_i d\mu_i = 0$$

In order to verify that the Gibbs-Duhem equation is satisfied, we can look at a

simple example of a two component system made up of a solvent, N_1 and one

solute, N_2 at a constant temperature and pressure. In making these

assumptions we get the following:

(Eq. 5- 87)

$$N_1 d\mu_1 + N_2 d\mu_2 = 0$$

Recall that N_1 and N_2 may be written in terms of mole fraction as follows:

(Eq. 5- 88)

$$x_1 = \frac{N_1}{(N_1 + N_2)}$$

(Eq. 5- 89)

$$x_2 = \frac{N_2}{(N_1 + N_2)}$$

Substituting (Eq. 5- 88) and (Eq. 5- 89) into (Eq. 5- 87), we get the following:

(Eq. 5- 90)

$$x_1 d\mu_1 + x_2 d\mu_2 = 0$$

Similarly, we may differentiate (Eq. 5- 90) with respect to x_2 as follows:

143

(Eq. 5- 91)

$$x_1 \frac{d\mu_1}{dx_2} + x_2 \frac{d\mu_2}{dx_2} = 0$$

We can test the Gibbs-Duhem relationship by using (Eq. 5- 16) and the relationship given in (Eq. 5- 18):

(Eq. 5- 16)

$$\mu_1 = \mu_1^* + RT[\ln(x_1)] + \omega_2 x_2 - (\omega_2 x_1 x_2) + \omega_3 x_3 - (\omega_3 x_1 x_3)$$

(Eq. 5- 18)

$$x_1 = 1 - x_2 - x_3$$

For a one solute system, (Eq. 5- 16) would take the following form:

(Eq. 5- 92)

$$\mu_1 = \mu_1^* + RT[\ln(1 - x_2)] + \omega_2 x_2 - (\omega_2 x_2)(1 - x_2)$$

We can take the derivative of (Eq. 5- 92) with respect to x_2 to get the following:

(Eq. 5- 93)

$$\frac{d\mu_1}{dx_2} = 2\omega_2 x_2 - \frac{RT}{(1 - x_2)}$$

Similarly we can use (Eq. 5- 71):

(Eq. 5- 71)

$$\mu_2 = \psi + RT[\ln(x_2)] + \omega_2 x_1 - (\omega_2 x_1 x_2) - (\omega_3 x_1 x_3)$$

Using (Eq. 5- 18), for a one solute system, (Eq. 5- 71) would take the following form:

144

(Eq. 5- 94)

$$\mu_2 = \psi + RT[\ln(x_2)] + \omega_2(1 - x_2) - (\omega_2 x_2)(1 - x_2)$$

We can take the derivative of (Eq. 5- 94) with respect to x_2 to get the following:

(Eq. 5- 95)

$$\frac{d\mu_2}{dx_2} = \frac{RT}{x_2} - 2\omega_2 + 2\omega_2 x_2$$

If we substitute (Eq. 5- 93) and (Eq. 5- 95) into (Eq. 5- 91) and utilize the relationship in (Eq. 5- 18), we see that the Gibbs-Duhem relationship is satisfied. Note that (Eq. 5- 33) and (Eq. 5- 71) do not exactly satisfy the Gibbs-Duhem relation since in (Eq. 5- 33) a natural logarithm has been expanded and only terms up to second order kept, while no such approximation was made in (Eq. 5- 71).

5.5b   Chemical potential definitions in the literature

When deriving the chemical potential equations, for all the various cases, for a dilute solution, we simply neglect the second order terms.   For example, the intracellular and extracellular solvent chemical potential in terms of mole fraction given in (Eq. 5- 40) and (Eq. 5- 41) for a dilute solution would be:

(Eq. 5- 96)

$$\mu_1^i = \mu_1^* - RT(x_2^i + x_3^i)$$

(Eq. 5- 97)

$$\mu_1^o = \mu_1^* - RT(x_2^o + x_4^o)$$

145

Similarly, the intracellular and extracellular solute chemical potentials in terms of mole fraction given in (Eq. 5- 76) and (Eq. 5- 77) for a dilute solution would be:

(Eq. 5- 98)

$$\mu_2^i = \mu_2^* + RT \ln\left(x_2^i\right)$$

(Eq. 5- 99)

$$\mu_2^o = \mu_2^* + RT \ln\left(x_2^o\right)$$

These are the common definitions of chemical potential that are often found in the literature [2]. Callen derives the dilute chemical potential equations from the Gibbs free energy and writes the chemical potentials in terms of mole fraction [2]. Landau and Lifshitz [4], derived the dilute chemical potential in terms of mole ratio instead of mole fraction and suggest that mole ratios be used for the non-dilute derivation as well. However, for a dilute solution, where the amount of solute is much less than the amount of solvent, using mole fraction or mole ratio essentially results in the same chemical potential equations.

5.5c   Thermodynamic basis for an osmotic virial equation mixing rule

As discussed in Chapter 4, there are a number of mathematical relationships in the literature to describe osmolarity or osmolality as a function of concentration. The osmotic virial equation treats osmolality (or osmolarity or osmotic pressure) as a polynomial expansion in concentration with the first term being linear in concentration. The osmotic virial equation for a binary mixture - a solution containing a solvent and a single solute, i, describes the osmolality, π, as a polynomial in molality of the solute, m_i.

146

(Eq. 4-1)

$$\pi = m_i + B_i^+ m_i^2 + C_i m_i^3 + ...$$

The B^+ and C^+ are known as osmotic virial coefficients. B_i^+ is called the second osmotic virial coefficient and C_i^+ the third osmotic virial coefficient, etc. In a ternary mixture (solvent plus two solutes), there are three pair-wise solute interactions in the solution: the interaction of the type 1 solute molecules with each other, the interaction of the type 2 solute molecules with each other and the interaction of the type 1 and type 2 molecules with each other [3].

Note that the chemical potential of the solvent may also be written in terms of the osmolality, π, the molecular weight of the solvent, $MW_{solvent}$ and the mole fraction of the solvent, $x_{solvent}$.

(Eq. 5- 100)

$$\mu_1 = \mu_1^* - RT\left(MW_{solvent}\right)x_{solvent}\pi$$

In the literature, when the osmotic virial equation is used for two solutes, one of two things is usually done: 1- it is assumed that the osmolalities are additive and the interactions between solutes are neglected [5], or 2- an empirical parameter multiplied by the $m_2 m_3$ term is estimated by fitting multi-solute data. Recall from Chapter 4, that a mixing rule was proposed by Bannerman et al., [1], using the arithmetic average of second osmotic virial coefficients of the pure species to

147

predict the cross coefficient from measurements of binary solutions alone. The coefficients were then used to make predictions for ternary solution osmolality without any additional fitting components. The osmotic virial equation they proposed to describe the osmolality for two solutes was expressed as follows [1]:

(Eq. 4- 4)

$$\pi = m_2 + m_3 + B_2^+ m_2^2 + B_3^+ m_3^2 + \left(B_2^+ + B_3^+\right) m_2 m_3$$

We can simplify (Eq. 5- 64) as follows:

(Eq. 5- 101)

$$\mu_1^i = \mu_1^* - RTMW_{solvent} x_{solvent} \left[m_2 + m_3 + B_2^+ m_2^2 + B_3^+ m_3^2 + \left(B_2^+ + B_3^+\right) m_2 m_3 \right]$$

If we compare the expressions for chemical potential given in (Eq. 5- 100) and (Eq. 5- 101), the expression for osmolality that comes out in the bracket in (Eq. 5- 101) is identical to the osmotic virial equation with the mixing term given in (Eq. 4-4). One of the key outcomes that resulted from the chemical potential derivations done in this chapter is that it provided a thermodynamic basis for the mixing rule proposed by Bannerman el al., [1]. As seen in (Eq. 5- 64), the interaction term that was derived from the Gibbs free energy equation was simply the arithmetic average of the pure species of the interaction parameters. The osmotic virial equation is therefore a simplification of regular solution theory and hence, if the osmotic virial equation is used, then the mixing rule will be valid.

Since the chemical potential equations were derived in mole fraction, molality

148

and molarity and the same form for the interaction parameter resulted in all three derivations, this tells us that the mixing rule is not unit dependent and will be valid regardless of if mole fraction, molality or molarity is used. This mixing rule will have use in other applications outside of cryobiology where one wishes to make a prediction of the osmolality of aqueous solutions with multiple solutes in the absence of ternary data. In cryobiology, it allows one to have more accurate predications of both the extracellular and intracellular solution osmolality and will improve the accuracy of protocol simulations.

149

5.6 References

[1] Bannerman, R.C., Elliott, J.A.W., Porter, K. R., McGann, L. E., A multi-solute osmotic virial equation for solutions of interest in biology, Submitted to: Biophysical Journal (2005).

[2] Callen, H.B., Thermodynamics and an Introduction to Thermostatistics (John Wiley & Sons, New York, 1985) 493 pp.

[3] Elliott, R.J., Lira, C. T., Introductory Chemical Engineering Thermodynamics (Prentice Hall PTR, Upper Saddle River, NJ, 1999).

[4] Landau, L.D., Lifhshitz, E. M., Statistical Physics (Pergamon Press Ltd, Oxford, 1980).

[5] Madden, P.W., Pegg, D.E., Calculation of Corneal Endothelial-Cell Volume During the Addition and Removal of Cryoprotective Compounds, Cryo-Letters 13 (1992) 43-50.

[6] Prausnitz, J.M., Molecular Thermodynamics of Fluid-Phase Equilibria (Prentice-Hall PTR, Upper Saddle River, N.J., 1999).

[7] Winzor, D.J., Reappraisal of disparities between osmolality estimates by freezing point depression and vapor pressure deficit methods, Biophysical Chemistry 107 (2004) 317-323.

Figure 5-1   A system of water, a permeating solute, an intracellular non-permeating solute and an extracellular non-permeating solute

Extracellular
Solution

Intracellular
Solution

Water N_1^i Water N_1^o

Permeating   Permeating
Solute N_2^i Solute N_2^o

Non-Permeating   Non-Permeating
Intracellular Solute N_3^i Intracellular Solute N_3^o
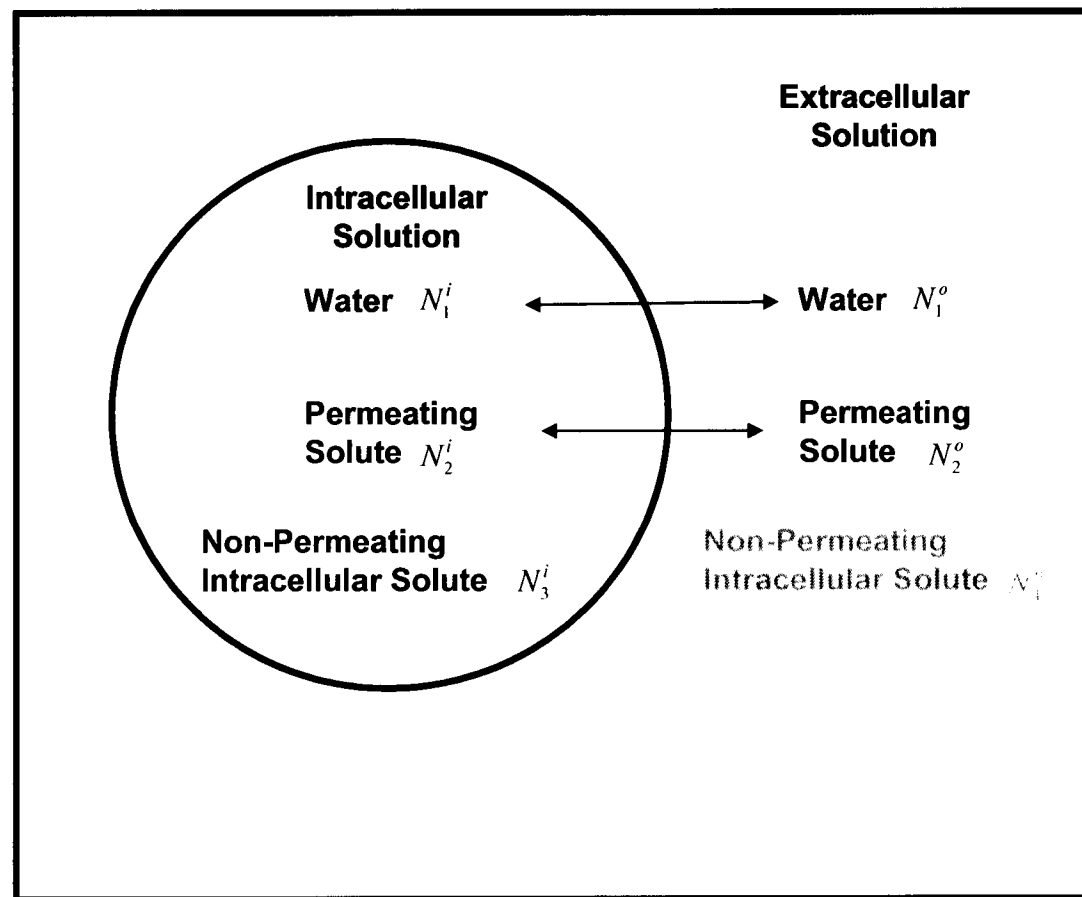
Chapter 6: New Transport Equations

6.1 Introduction

As discussed in Chapter 4, the transport equations used in cryobiology today, whether being the two parameter (2-P) formalism, developed from the work of Jacobs and Stewart [12,13] or the three parameter formalism, developed by Kedem and Katchalsky (K-K) [14] include dilute solution or near equilibrium assumptions. In their work, Jacobs and Stewart [12,13] suggested that in the transport equations, the expression for concentration should have units of osmolarity. However, it appears that they were actually using molar concentration rather than osmolar. In using molar concentration instead of osmolar, a dilute solution assumption is being made. In the literature it is often assumed that if the 2-P model is being used, there are no dilute solution restrictions on the transport equations [15], which is not true. Kedem and Katchalsky also made dilute solution assumptions in their transport equations. When using the chemical potentials of the solute to derive their transport equations, they also made a near-equilibrium assumption [14], in that the difference in concentration between the inside and the outside of the cell must be small. So despite what is often thought in the literature, using either the 2-P or the K-K equations results in dilute solution assumptions being made, specifically in the solute transport equations. It has been recognized that for various systems and scenarios, dilute solution approximations introduce appreciable errors in the transport formalisms [26], particularly in cryobiology where intracellular and extracellular solutions become clearly non-dilute.

As pointed out in the literature, the cell membrane transport properties are important parameters that often determine the fate of the cells [4]. In cryobiology, it has been shown that the membrane transport parameters must be measured accurately in order to analyze the cryopreservation of cells with any accuracy [4]. However, then equally as important to measuring the transport parameters, is using accurate equations to obtain the permeability parameters. As discussed in Chapter 4, the K-K model is the most commonly used model in the field of cryobiology [15,25]. The K-K model was specifically designed to describe the situation of co-transport of a solute and water across a cell membrane. Kleinhans suggested that recent discoveries of water channels in cell membranes, eliminated the possibility of co-transport of water and solute across the membrane and thus he questioned the validity of the K-K equations [15]. Kleinhans proposed that the K-K formalism and σ were often unnecessary and demonstrated that the 2-P formalism worked just as well as the K-K formalism and essentially gave the same results for a number of different transport situations in which a common channel for solute and solvent was not present. Using simulations, this was demonstrated to be true for a variety of circumstances. In Chapter 4, we demonstrated the reason for this is that for situations when there is no interaction between the water and solute (when water and solute move across the membrane using independent pathways), the 2-P and the K-K equations are essentially the same. Kleinhans noted that there were no practical differences up to solute concentrations of several molar, however, the 2-P model and the K-K model deviated from each other at high

153

concentrations [15]. It is possible then that σ is simply, empirically adjusting for non-dilute behavior, since in both equations a dilute solution assumption is being made. In the literature it has been reported that there is no pattern that emerges which defines how the solute concentration effects membrane permeability characteristics [17]. All of these insights were an indication to us that non-dilute solution equations need to be considered in the osmotic transport equations, particularly in cryobiology where dilute solution conditions are often not met, since concentrated solutions are present over large temperature ranges. As a result of this, non-dilute solution equations that make no near-equilibrium assumptions should be used in cryobiology.

6.2 Dilute Solution Solute Transport Equations

As discussed earlier, when deriving the equations for the osmotic transport of the solute, Kedem and Katchalsky made both a dilute solution and a near-equilibrium assumption [14]. In order to better understand osmotic transport, a closer look needs to be taken at the solute transport equations. The solute transport equations may be examined from a number of different perspectives including Fick's Law of Diffusion, the Onsager approach and Statistical Rate Theory.

6.2a Fick's law of diffusion

There are many different ways to analyze transport processes. The simplest model of diffusion fluxes is Fick's First Law of Diffusion:

(Eq. 6- 1)

$$J_s = -D_s \frac{\partial C_s}{\partial l}$$

where J_s is the diffusive flux of the solute, D_s is the diffusion coefficient, and C_s is the molar concentration which varies with distance l. It has been recognized in the literature that in some systems, such as electrolyte solutions, there are problems with (Eq. 6- 1) when determining the diffusion coefficients even in very dilute solutions [9] as well as problems in measuring non-equilibrium parameters related to the diffusion coefficient when using (Eq. 6- 1).

6.2b   Onsager approach

As discussed in Chapter 4, the thermodynamics of irreversible processes offers a description of transport. Based on the work of Onsager, it is assumed over some range that flux is directly proportional to a driving force. The Onsager phenomenological coefficient relates this flux to the force as follows:

(Eq. 6- 2)

$$J_s = LX$$

In the case of isothermal membrane transport, J_s is the flux of solute across a membrane, L is the Onsager phenomenological coefficient and X is the thermodynamic driving force. In the case of isothermal osmotic transport, this force may be written as follows:

(Eq. 6- 3)

$$X = -\left[\frac{\partial \mu_s}{\partial l} \right]$$

155

where μ_s is the chemical potential of a permeating solute. As discussed in Chapter 5, the dilute solution chemical potential of the solute in terms of mol fraction (where x_s is the solute mol fraction) may be written as follows:

(Eq. 6- 4)

$$\mu_s = \mu_s^* + RT \ln x_s$$

which may be also be written in terms of molar concentration:

(Eq. 6- 5)

$$\mu_s = \mu_s^* + RT \ln\left(C_s \left(MW_{solution}\right) v_{solution}\right)$$

where C_s is the molar concentration in units of moles of solute per volume of solution, $MW_{solution}$ is the molecular weight of the solution and $v_{solution}$ is the specific volume of the solution. (Eq. 6- 3) may be substituted into (Eq. 6- 2) to yield the following expression for the flux of solute on the outside of the cell membrane:

(Eq. 6- 6)

$$J_s = -L\left[\frac{\partial \mu_s}{\partial l}\right]\bigg|_{\text{Outside of membrane}}$$

(Eq. 6- 5) may be substituted in the new solute flux equation, (Eq. 6- 6), to yield the following expression:

(Eq. 6- 7)

$$J_s = -L\left[RT\frac{1}{C_s(l)\left(MW_{solution}\right)v_{solution}}\frac{\partial\left(C_s\left(MW_{solution}\right)v_{solution}\right)}{\partial l}\right] = -L\left[RT\frac{1}{C_s(l)}\frac{\partial C_s}{\partial l}\right]$$

Note, it is assumed that for a dilute solution, $MW_{solution}$ and $v_{solution}$ are constant.

156

C_s is a function of position, l. $C_s(l) = C_s^{ave}$, where C_s^{ave} is the average solute concentration across the membrane. This is an approximation that becomes exact as the thickness of the membrane (λ) becomes small (which it is). (Eq. 6-7) may be re-written as:

(Eq. 6- 8)

$$J_s = -L\left[\frac{RT}{C_s^{ave}}\left(\frac{\partial C_s}{\partial l}\right)\right]$$

Similarly, considering the membrane to be of infinitesimal thickness, (Eq. 6- 8) may be written as:

(Eq. 6- 9)

$$J_s = L\left[\frac{RT}{C_s^{ave}}\left(\frac{C_s^o - C_s^i}{\lambda}\right)\right]$$

As shown in Chapter 4, when deriving the transport equations, Kedem and Katchalsky arrived at a similar relationship for the transport of the solute, i.e., flux being proportional to a difference in concentration divided by the average concentration of the solute. However, Kedem and Katchalsky arrived at this relationship by making a near equilibrium assumption and assuming that the difference in concentration between the inside and the outside of the cell was quite small, while the relation in (Eq. 6- 9) was derived from calculus, assuming the membrane thickness was small.

157

6.2c Comparing Fick's law and Onsager

Irreversible thermodynamics gives no guidance as to the concentration dependence of the Onsager phenomenological coefficients [9]. The relationship between the diffusion coefficient and the Onsager phenomenological coefficient can be obtained in a straightforward exercise by comparing the solute flux equations obtained from Fick's Law of Diffusion (Eq. 6- 1) with the solute flux equation obtained from the Onsager approach (Eq. 6- 8). From this relationship, some insight into the concentration dependence of the Onsager coefficients may be obtained. Comparing (Eq. 6- 1) with (Eq. 6- 8), we see that:

(Eq. 6- 10)

$$L = \frac{D_s C_s^{ave}}{RT}$$

This relationship has been noted in the past, directly [1], and indirectly [9]. By comparing the two methods for obtaining solute flux, we can get a relationship between the phenomenological coefficient, L, and the diffusion coefficient, D_s. However, we do not know how L and D_s depend on the solute concentration.

As discussed in Chapter 4, the solute transport equation is often written as:

(Eq. 6- 11)

$$\frac{dN_s}{dt} = P_s A \left(C_s^o - C_s^i \right)$$

By comparing (Eq. 6- 9) with (Eq. 6- 11), we get the following relationship for the solute permeability coefficient, P_s:

(Eq. 6- 12)

$$P_s = \frac{LRT}{C_s^{ave}}$$

However, we still do not know the concentration dependence of the phenomenological coefficient, L.

The solute flux, (Eq. 6- 6), may also have been written in the following form:

(Eq. 6- 13)

$$J_s = -L\frac{\left(\mu_s^i - \mu_s^o\right)}{l} = L\frac{\left(\mu_s^o - \mu_s^i\right)}{l}$$

(Eq. 6- 5) may be used for the dilute solution chemical potential of the solute. As a result, (Eq. 6- 13) may be written as:

(Eq. 6- 14)

$$J_s = \frac{LRT}{l}\ln\left(\frac{C_s^o\left(MW_{solution}\right)\nu_{solution}}{C_s^i\left(MW_{solution}\right)\nu_{solution}}\right) = \frac{LRT}{l}\ln\left(\frac{C_s^o}{C_s^i}\right)$$

We may re-write $\frac{LRT}{l}$ to be equal to P_s^* as shown in (Eq. 6- 15):

(Eq. 6- 15)

$$P_s^* = \frac{LRT}{l}$$

As a result, (Eq. 6- 14) may be re-written as:

(Eq. 6- 16)

$$J_s = P_s^* \ln\left(\frac{C_s^o}{C_s^i}\right)$$

159

We can compare (Eq. 6- 12) with (Eq. 6- 15) to get a relationship between P_s

and P_s^*.

<div align="center">

(Eq. 6- 17)

$$P_s^* = \frac{P_s \cdot C_s^{ave}}{l}$$

</div>

6.2d Statistical rate theory

Statistical Rate Theory is a relatively new theory of non-equilibrium thermodynamics proposed by C. A. Ward [23,24]. The theory is derived from a mathematical model that uses entropy and is based on a quantum mechanical description of an isolated multi-particle system [8,22,24]. Statistical Rate Theory provides an expression for the instantaneous net molecular transport rate across the interface of two similar or different phases. No equilibrium assumptions are made in the development of Statistical Rate Theory and it can be used to derive rate equations that may be written entirely in terms of experimental and thermodynamic variables that may be tabulated, measured or controlled. Elliott, Elmoazzen and McGann [7] give the instantaneous net rate of solute molecule transport across a cell boundary as follows:

<div align="center">

(Eq. 6- 18)

$$\frac{dN_s}{dt} = K_s^e \left[\exp\left(\frac{\mu_s^o - \mu_s^i}{RT} \right) - \exp\left(\frac{\mu_s^i - \mu_s^o}{RT} \right) \right]$$

</div>

where K_s^e is the equilibrium exchange rate of the solute molecules crossing the membrane once the isolated system has reached thermodynamic equilibrium.

<div align="center">160</div>

(Eq. 6- 18) is a complete non-equilibrium thermodynamic equation that describes the osmotic transport of solute across a cell membrane without any near-equilibrium assumptions being made. In order to be able to compare with Onsager's linear, near-equilibrium equations, the exponentials can be linearized.[*] Thus for small chemical potential differences, (Eq. 6- 18) becomes:

(Eq. 6- 19)

$$\frac{dN_s}{dt} = \frac{2K_s^e}{RT}\left(\mu_s^o - \mu_s^i\right)$$

(Eq. 6- 5) may be used for the dilute solution chemical potential of the solute. As a result, (Eq. 6- 19) may be written as:

(Eq. 6- 20)

$$\frac{dN_s}{dt} = 2K_s^e \ln\left[\frac{C_s^o}{C_s^i}\right]$$

By comparing (Eq. 6- 16) with (Eq. 6- 20), we see that:

(Eq. 6- 21)

$$P_s^* = 2K_s^e$$

Recall that from (Eq. 6- 15), that we saw that:

(Eq. 6- 15)

$$P_s^* = \frac{LRT}{l}$$

By comparing (Eq. 6- 15) with (Eq. 6- 21), we can find a relationship between the equilibrium exchange rate, K_s^e and the phenomenological coefficient, L:

---

[*] For small values of y, exp (y) = 1 + y + ½ y^2 + ...

161

(Eq. 6- 22)

$$2K_s^e = \frac{LRT}{l}$$

Recall from (Eq. 6- 10), that there was a relationship between the phenomenological coefficient, L and the diffusion coefficient, D_s.

(Eq. 6- 10)

$$L = \frac{D_s C_s^{ave}}{RT}$$

We can compare (Eq. 6- 10) with (Eq. 6- 22) and find a relationship between the equilibrium exchange rate and the diffusion coefficient:

(Eq. 6- 23)

$$2K_s^e = \frac{D_s C_s^{ave}}{l}$$

While the Onsager phenomenological coefficients do not have a physical meaning accessible from within the theory, the equilibrium exchange rate does. It is defined as the number of molecules crossing the membrane per unit time at equilibrium. The equilibrium exchange rate depends on the specific system of interest and depends on the equilibrium concentration, C_{eq} of the solute:

(Eq. 6- 24)

$$K_s^e \propto C_{eq}$$

In this particular case of osmotic transport, we can identify our system as the isolated cell membrane. Statistical Rate Theory could have been used to describe the entire system, i.e. - a cell placed in an extracellular solution.

162

However, by choosing our system as the isolated cell membrane, Statistical Rate Theory flux equations can be compared with other flux equations such as those using the Onsager approach or Fick's Law of Diffusion. The equilibrium exchange rate depends on the equilibrium concentration, and for our system, the equilibrium concentration will be equal to the average concentration between the outside of the cell membrane and the inside of the cell membrane.

Since the value of K_s^e is by definition proportional to C_{eq}, we can get the concentration dependencies of the solute permeabilities P_s and P_s^*, the diffusion coefficient, D_s and for the phenomenological coefficient, L.

From (Eq. 6-21), we see that $P_s^* = 2K_s^e$. As a result, we can utilize (Eq. 6-21) and (Eq. 6-24) to get the following concentration dependence for P_s^*:

(Eq. 6-25)

$$P_s^* \alpha\ C_{eq}$$

By utilizing (Eq. 6-17), (Eq. 6-21), and (Eq. 6-24), we can see that P_s does not depend on concentration:

(Eq. 6-26)

$$P_s = \text{constant}$$

By using (Eq. 6-22) and (Eq. 6-24), we can see that the phenomenological coefficient, L, has a linear dependence on the equilibrium solute concentration:

163

(Eq. 6- 27)

$$L \alpha C_{eq}$$

By comparing (Eq. 6- 23) and (Eq. 6- 24), we see that the diffusion coefficient, D_s does not have a solute concentration dependence:

(Eq. 6- 28)

$$D_s = \text{constant}$$

Statistical Rate Theory allowed the determination of these dependencies, since the theory is written in terms of experimental and thermodynamic variables that may be tabulated, measured or controlled. Using Statistical Rate theory, we were able to obtain the concentration dependence of the solute permeabilities P_s and P_s^* as well as the phenomenological coefficient, L.

6.3 Non-Dilute Solvent Transport Equations

As discussed in Chapter 4, for a dilute solution with two solutes, 2 and 3, the osmolality, π, is expressed as a function of the molality, m:

(Eq. 4-5)

$$\pi = m_2 + m_3$$

For a non-dilute solution of two solutes, the osmolality is often incorrectly expressed without taking into account the interaction of the two solutes with one another (i.e. osmolalities assumed additive) as follows:

164

(Eq. 4-6)

$$\pi = m_2 + m_3 + B_2^+ m_2^2 + B_3^+ m_3^2$$

where the B^+ are known as the second osmotic virial coefficients and is unique for each type of solute. The osmolality of a non-dilute solution of two solutes may also be expressed to include a cross term, which takes into account the interactions of the two solutes with one another and may be expressed as follows [3]:

(Eq. 4-4)

$$\pi = m_2 + m_3 + B_2^+ m_2^2 + B_3^+ m_3^2 + \left(B_2^+ + B_3^+ \right) m_2 m_3$$

It is more correct and accurate to express the osmolality with the second order terms. The most correct way to express the osmolality would be to include the cross terms as shown in (Eq. 4-4). In Chapter 5, the chemical potential derivations provided an expression for the non-dilute solution osmolality as shown by comparing (Eq. 5-100) with (Eq. 5-101). As a result, a thermodynamic basis was provided for a new mixing rule.

For an ideal solute, the molality is the same as the osmolality as shown in (Eq. 4-5). In the literature, people have recognized that the non-ideal behavior of the solutes should be taken into account when working with the osmolalities in the osmotic transport equations [11]. To correct for the non-ideal behavior of intracellular solutes, an osmotic coefficient is sometimes used [2,11,16,20,21]. The osmotic coefficient relates the osmolality of a non-ideal solute to the molality and corrects for the increase in osmolality of non-ideal solutes and is defined as

$\dfrac{\pi}{m}$. Pegg et al. have used empirical adjustments of the Boyle van't Hoff plot to obtain the osmotic coefficients [20]. The non-ideality of cryoprotectant solutions has also been defined by calculating molar osmotic coefficients from freezing point depression data [2]. Quadratic equations were calculated to relate the osmotic coefficient to concentration [2,5]. This approach is similar to using the single solute form of (Eq. 4-6) up to cubic terms.

6.3a Model cell and simulations

In order to quantify the effects of using the various expressions for osmolality (i.e. (Eq. 4-4), (Eq. 4-5) or (Eq. 4-6)) on the typical two parameter formalism we consider a model (hypothetical) cell that contains a solution of water, a permeating solute such as DMSO and non-permeating solutes both on the inside and the outside of the cell as shown in Figure 6-1. The parameters of the model cell are chosen to be similar to those of human stromal fibroblast cells [6]. Details of the model cell are given in Table 6-1. We consider a cell which is moved from an isotonic buffer into differing concentrations (2, 4, 6, and 8 molal) of dimethyl sulfoxide. In such a simulation, the model cell will exhibit the typical shrink-swell response in which water initially rushes out of the cell and then re-swells as solute and water re-enter the cell.

166

Table 6-1 Model cell and hypothetical experiment

Parameter	Value	Symbol
Model Cell		
Isotonic cell volume	3580 μm^3	$iVto$
Osmotically inactive fraction	0.41	V_b
Hydraulic conductivity	0.24 $\mu m^3/\mu m^2$/min/atm	L_p
Solute permeability	0.48 μm/min	P_s
Model Experiment		
Temperature	4°C (277 K)	T
Universal gas constant	8.206 X 10^{13} μm^3·atm/mol·K	R
Initial intracellular salt molality (KCl)	0.172 molal (0.300 osmoles)	m_n^i
Extracellular salt molality (NaCl)	0.175 molal (0.300 osmoles)	m_n^e
Initial intracellular solute (DMSO) molality	0.0 molal	m_s^i
Extracellular solute (DMSO) molality	2, 4, 6 or 8 molal	m_s^e
Partial molar volume of solute (DMSO)	71.33 X 10^{12} μm^3/mol	v_s
Second osmotic virial coefficient for DMSO (in terms of molality)	0.0843	B_2^+
Second osmotic virial coefficient for KCl (in terms of molality)	0.0000 (Dissociation constant = 1.74)	B_3^+
Second osmotic virial coefficient for NaCl (in terms of molality)	0.0299 (Dissociation constant = 1.70)	B_4^+

6.3b Simulation procedure and software

The simulations in this chapter were performed using *Mathematica 5.1* (Wolfram Research, Champaign, IL, USA). The simulation program was used to determine the osmotic response of the model cell to varying concentrations of dimethyl sulfoxide with different expressions for osmolality (i.e. - (Eq. 4-4), (Eq. 4-5), or (Eq. 4-6)) in the modern day two parameter formalism (Eq. 4-9, 4-11, and 4-13) when solving using a fixed value for the hydraulic conductivity and solute permeability. The values for the second osmotic virial coefficients were obtained from Richelle Bannerman who analyzed freezing point depression data in the literature. For the complete Mathematica code used in the simulations, please see the appendix.

(Eq. 4-9)

$$\frac{dV_w}{dt} = -LART\left(\pi^e - \pi^i\right)$$

(Eq. 4-11)

$$\frac{dV_s}{dt} = v_s \frac{dN_s}{dt} = v_s P_s A\left(C_s^e - C_s^i\right)$$

(Eq. 4-13)

$$V_C = V_w + V_s + V_b$$

6.3c Results

Simulations of the response of a hypothetical cell with a known hydraulic conductivity and solute permeability with the different expressions for osmolality were performed. The normalized cell volume as a function of time for the

168

hypothetical cell exposed to 2 molal, 4 molal, 6 molal and 8 molal are given in Figures 6-2 to 6-5, respectively.

6.3d Discussion

A central idea to this section is that the osmotic response of a cell will differ depending on the expression for osmolality used in the modern day two parameter formalism as well as to highlight the effect of making dilute and non-dilute solution assumptions. When comparing simulations of the various osmotic responses of 2 molal dimethyl sulfoxide addition in Figure 6-2, there is a slight difference between the three expressions for osmolality (dilute, adding the quadratic terms without including the cross term, and non-dilute with the quadratic terms (i.e. our osmotic virial equation). As the concentration increased in the simulations (Figures 6-3, 6-4 and 6-5), the differences in the osmotic responses became magnified. There is a large difference between the osmotic responses when dilute or non-dilute solutions are assumed. The new cross term proposed in our lab for the osmotic virial equation (as discussed in Chapter 4 and derived in Chapter 5) contributes significantly to the non-dilute simulations. The differences become increasingly significant with increasing concentration. The simulations demonstrated that non-dilute transport equations gave different osmotic response of cells than dilute transport equations.   This difference motivates a closer look at the role of non-dilute solution thermodynamics in osmotic transport formalisms.

169

6.3e New solvent transport equations

To derive our set of solvent transport equations, consider an example situation of a cell that is immersed in a hypertonic or hypotonic solution and undergoes osmotic shrinkage or swelling, respectively. As shown in Figure 6-1, we assume that the intracellular solution contains molecules of water, denoted by N_1^i, a permeating solute such as a permeating cryoprotectant like DMSO, denoted as N_2^i, and a non-permeating intracellular solute such as KCl, denoted by N_3^i. We will assume that the extracellular environment will contain molecules of water, N_1^o, the permeating solute, N_2^o, and a non-permeating extracellular solute such as NaCl, denoted by N_4^o.

For the solvent transport equations, the change in the number of water molecules as a function of time will be proportional to some water permeability coefficient denoted by $\tilde{L}$, the cell surface area, A, and the difference in the chemical potential of the water outside and inside the cell as given by (Eq. 6- 29).

(Eq. 6- 29)

$$\frac{dN_w^i}{dt} = \tilde{L}A\left(\mu_w^o - \mu_w^i\right)$$

From Chapter 5, we saw that the chemical potential of the water outside in terms of the mol fraction, x, is:

(Eq. 6- 30)

$$\mu_w^o = \mu_w^* - RT\left(x_2^o - x_2^o\right) - B_2 RT\left(x_2^o\right)^2 - B_4 RT\left(x_4^o\right)^2 - \left(B_2 + B_4\right)RTx_2^o x_4^o$$

170

Similarly, the chemical potential of the water inside the cell in terms of the mol fraction, x, is:

(Eq. 6- 31)

$$\mu_w^i = \mu_w^* - RT\left(x_2^i - x_3^i\right) - B_2 RT\left(x_2^i\right)^2 - B_3 RT\left(x_3^i\right)^2 - \left(B_2 + B_3\right)RTx_2^i x_3^i$$

Substituting (Eq. 6- 30) and (Eq. 6- 31) into (Eq. 6- 29), yields the following expression:

(Eq. 6- 32)

$$\frac{dN_w^i}{dt} = -\widetilde{L}ART\begin{bmatrix}\left(x_2^o + x_4^o\right) + B_2\left(x_2^o\right)^2 + B_4\left(x_4^o\right)^2 + \left(B_2 + B_4\right)x_2^o x_4^o - \\ \left(x_2^i + x_3^i\right) - B_2\left(x_2^i\right)^2 - B_3\left(x_3^i\right)^2 - \left(B_2 + B_3\right)x_2^i x_3^i\end{bmatrix}$$

(Eq. 6- 32) represents the non-dilute solvent transport equation with no dilute solution or near equilibrium assumptions. If we wanted to write the dilute solution expression for (Eq. 6- 32), we would simply neglect the second order terms in the equation. Doing this yields the following expression:

(Eq. 6- 33)

$$\frac{dN_w^i}{dt} = -\widetilde{L}ART\left[\left(x_2^o + x_4^o\right) - \left(x_2^i + x_3^i\right)\right]$$

This equation is identical to the modern day two parameter formalism but is written in terms of mole fraction. It is important to note that (Eq. 6- 32) is equivalent to (Eq. 4-9) but with a specific expression for osmolality, π. So the literature is correct in using (Eq. 4-9).

171

6.4 Non-Dilute Solute Transport Equations

In the literature many of the non-dilute fixes to the transport equations, correct the solvent transport equations but not the solute transport equations. In the current solute transport equations utilized in the literature either a dilute solution assumption or near equilibrium assumption or both assumptions are made. Unlike the solvent transport equations, the solute transport equations cannot be extended to non-dilute situations by simply replacing molality with osmolality as is usually done.

6.4a New solute transport equations

To derive a new set of solute transport equations, we will again consider an example situation of a cell that is immersed in a hypertonic or hypotonic solution and undergoes osmotic shrinkage or swelling, respectively. As shown in Figure 6-1, we assume that the intracellular solution contains molecules of water, denoted as N_1^i, a permeating solute such as a permeating cryoprotectant like DMSO, denoted as N_2^i, and a non-permeating intracellular solute such as KCl, denoted by N_3^i. We will assume that the extracellular environment will contain molecules of water, N_1^o, the permeating solute, N_2^o, and a non-permeating extracellular solute such as NaCl, denoted by N_4^o.

For the solute transport equations, the change in the number of solute molecules as a function of time will be proportional to some solute permeability coefficient

172

denoted by $\widetilde{P}$, the cell surface area, A, and the difference in the chemical potential of the permeating solute outside and inside the cell as given by (Eq. 6-34).

(Eq. 6- 34)

$$\frac{dN_s^i}{dt} = \widetilde{P}A\left(\mu_s^o - \mu_s^i\right)$$

From Chapter 5, we saw that the chemical potential of the permeating solute outside the cell in terms of the mol fractions may be expressed as:

(Eq. 6- 35)

$$\mu_2^o = \mu_2^* + RT\ln\left(x_2^o\right) + RT\left(\frac{1}{2} - B_2\right)\left(1 - x_2^o - x_4^o\right)\left(1 - x_2^o\right) - RT\left(\frac{1}{2} - B_4\right)\left(1 - x_2^o - x_4^o\right)x_4^o$$

Similarly, the chemical potential of the permeating solute inside the cell in terms of the mol fractions is:

(Eq. 6- 36)

$$\mu_2^i = \mu_2^* + RT\ln\left(x_2^i\right) + RT\left(\frac{1}{2} - B_2\right)\left(1 - x_2^i - x_3^i\right)\left(1 - x_2^i\right) - RT\left(\frac{1}{2} - B_3\right)\left(1 - x_2^i - x_3^i\right)x_3^i$$

Substituting (Eq. 6- 35) and (Eq. 6- 36) into (Eq. 6- 34), yields the following expression:

(Eq. 6- 37)

$$\frac{dN_s^i}{dt} = \widetilde{P}ART\left[\begin{array}{l}\ln\left(x_2^o\right) + \left(\frac{1}{2} - B_2\right)\left(1 - x_2^o - x_4^o\right)\left(1 - x_2^o\right) - \left(\frac{1}{2} - B_4\right)\left(1 - x_2^o - x_4^o\right)x_4^o \\ - \ln\left(x_2^i\right) - \left(\frac{1}{2} - B_2\right)\left(1 - x_2^i - x_3^i\right)\left(1 - x_2^i\right) + \left(\frac{1}{2} - B_3\right)\left(1 - x_2^i - x_3^i\right)x_3^i\end{array}\right]$$

173

We will use (Eq. 6- 37) as a new non-dilute solute transport equation with no dilute solution or near equilibrium assumptions. To write the dilute solution expression for (Eq. 6- 37), the second order terms in the equation would simply be neglected. Doing this yields the following expression:

(Eq. 6- 38)

$$\frac{dN_s^i}{dt} = \widetilde{P}ART\left[\ln\frac{\left(x_2^o\right)}{\left(x_2^i\right)}\right]$$

(Eq. 6- 37) is very different from the one used in the modern day two parameter formalism, which is written as a simple difference in concentration. (Eq. 6- 38) is similar to the modern day two parameter formalism. In the derivation by Kedem and Katchalsky in their 1958 paper [14], for the chemical potential of the solute equations, they also arrived at this expression, but then made a near equilibrium assumption and wrote the concentration in terms of a difference across the cell membrane.

6.5 New Total Volume Change Transport Equations

To look at the total solute and solvent flux using our new transport equation, we add together the water flux given in (Eq. 6- 32) with the solute flux given in (Eq. 6- 37). To convert from a water flux to a water volume flux, we can multiply by the partial molar volume of the water, v_w, and similarly to convert from a solute flux to a solute volume flux, we can multiply by the partial molar volume of the solute, v_s. The total cell volume change as a function of time maybe written as follows:

(Eq. 6- 39)

$$\frac{dV_{w+s}}{dt} = v_w \frac{dN_w}{dt} + v_s \frac{dN_s}{dt}$$

(Eq. 6- 40)

$$\frac{dV_{w+s}}{dt} = -v_w \tilde{L}ART \begin{bmatrix} \left(x_2^o + x_4^o\right) + B_2\left(x_2^o\right)^2 + B_4\left(x_4^o\right)^2 + \left(B_2 + B_4\right)x_2^o x_4^o \\ -\left(x_2^i + x_3^i\right) - B_2\left(x_2^i\right)^2 - B_3\left(x_3^i\right)^2 - \left(B_2 + B_3\right)x_2^i x_3^i \end{bmatrix} +$$

$$v_s\tilde{P}ART \begin{bmatrix} \ln\left(x_2^o\right) + \left(\frac{1}{2} - B_2\right)\left(1 - x_2^o - x_4^o\right)\left(1 - x_2^o\right) - \left(\frac{1}{2} - B_4\right)\left(1 - x_2^o - x_4^o\right)x_4^o \\ -\ln\left(x_2^i\right) - \left(\frac{1}{2} - B_2\right)\left(1 - x_2^i - x_3^i\right)\left(1 - x_2^i\right) + \left(\frac{1}{2} - B_3\right)\left(1 - x_2^i - x_3^i\right)x_3^i \end{bmatrix}$$

The total cell volume, V_C, is given as:

(Eq. 6- 41)

$$V_C = V_w + V_S + V_b$$

where, V_w is the volume of water, V_S is the total solute volume (permeating and non-permeating solutes) and V_b is the osmotically inactive volume

(Eq. 6- 40) represents the complete non-dilute transport equation. In this equation there are no near-equilibrium or dilute solution assumptions made. If we were to write the dilute solution expression, we would again neglect any second order terms and (Eq. 6- 40) would take the following form:

(Eq. 6- 42)

$$\frac{dV_{w+s}}{dt} = -v_w\tilde{L}ART\left[\left(x_2^o + x_4^o\right) - \left(x_2^i + x_3^i\right)\right] + v_s\tilde{P}ART\left[\ln\frac{\left(x_2^o\right)}{\left(x_2^i\right)}\right]$$

6.5a Comparing to data and goodness of fit

In order to examine the effects of using our new transport equations, (Eq. 6- 40), compared to traditional transport formalisms, we re-analyzed data for human corneal epithelial cells exposed to various concentrations of DMSO (0.5M, 1M, and 2M) at 13°C. The solutions had measured osmolalities of 631, 1227 and 2589 mosm/kg, respectively. The data had been obtained and previously analyzed by Stacey Ebertz using a 3-parameter formalism and fitting for L_p, P_s and σ [6]. In Stacey Ebertz's work, an electrical particle counter was used to determine cryoprotectant permeabilities for cells in suspension. The raw Coulter data for the human corneal epithelial cells was re-analyzed using our new transport equation (Eq. 6- 40).

The data was fit using *Mathematica 5.1* (Wolfram Research, Champaign, IL, USA). The simulation program was used to fit our new transport equations to the raw Coulter data, and determine the osmotic parameters, $\tilde{L}$ and $\tilde{P}$, when exposed to the varying concentrations of DMSO. For the complete Mathematica code used, please see the appendix. The parameters used in the program are given in Table 6-2.

176

Table 6-2 Epithelial cell parameters

Parameter	Value	Symbol
Isotonic cell volume	3626 μm^3	iVto
Osmotically inactive fraction	0.41	V_b
Temperature	13°C (286 K)	T
Universal gas constant	8.206 X 10^{13} μm^3·atm/mol·K	R
Partial molar volume of water	18.02 X 10^{13} μm^3/mol	$\bar{V}_w$
Partial molar volume of DMSO	71.33 X 10^{12} μm^3/mol	$\bar{V}_s$
Second osmotic virial coefficient for DMSO (in terms of mole fraction)	4.716	B_2
Second osmotic virial coefficient for KCl (in terms of mole fraction)	-0.057 (Dissociation constant = 1.79)	B_3
Second osmotic virial coefficient for NaCl (in terms of mole fraction)	2.759 (Dissociation constant = 1.68)	B_4
Initial intracellular salt (KCl) mole fraction	0.003 (Mole fraction) = 0.172 molal = 0.300 osmoles	x_3^i initial
Initial Intracellular solute (DMSO) mole fraction	0.0 (Mole fraction)	x_2^i initial

For 0.5M DMSO

Parameter	Value	Symbol
Extracellular salt (NaCl) mole fraction	0.003 (Mol fraction) = 0.175 molal = 0.300 osmoles	x_4^o
Extracellular solute (DMSO) mole fraction	0.0112 (Mol fraction) = 0.5 molal = 0.631 osmoles	x_2^o

For 1M DMSO

Parameter	Value	Symbol
Extracellular salt (NaCl) mole fraction	0.003 (Mole fraction) = 0.175 molal = 0.300 osmoles	x_4^o
Extracellular solute (DMSO) mole fraction	0.0215 (Mol fraction) = 1 molal = 1.227 osmoles	x_2^o

For 2M DMSO

Parameter	Value	Symbol
Extracellular salt (NaCl) mole fraction	0.003 (Mole fraction) = 0.175 molal = (0.300 osmoles)	x_4^o
Extracellular solute (DMSO) mole fraction	0.0444 (Mol fraction) = 2 molal = 2.589 osmoles	x_2^o

6.5b Results

The result for one data set fit with the new transport equation for 2 molal DMSO is shown on two different volume scales in Figures 6-6 and 6-7. The new transport equations fit all the data sets quite well. Table 6-3a, 6-3b and 6-3c show a summary of the values obtained for the 3 parameter fit of the data as well as the values for the permeability coefficients of the new transport equations. For almost all the runs, the sum of the square error (SSE), was very similar for the two methods of fitting the data. In fact, for the highest concentration where we expect non-dilute equations to be of the most importance, the fit has the same SSE even though one less fitting parameter is used with the new transport equations. The units for $\widetilde{L}$ and $\widetilde{P}$ are in $mol^2/min \cdot atm \cdot \mu m^5$, while the units for L_p are in $\mu m^3/\mu m^2/min/atm$ and the units for P_s are in $\mu m/min$.

178

Table 6-3a Permeability parameters obtained from 0.5 molal DMSO data fit with the new transport equations and the 3-paramter equations

0.5 molal DMSO (day # - run#)	$\tilde{L}$ X 10^{-28} mol²/(min·atm·μm⁵)	$\tilde{P}$ X10^{-31} mol²/(min·atm·μm⁵)	SSE	L_p (μm³/μm²/min/atm)	P_s (μm/min)	σ	SSE
0.5 molal DMSO (1-1)	3.78	0.700	0.028	0.270	1.560	0.326	0.021
0.5 molal DMSO (1-2)	4.12	0.456	0.024	0.178	2.033	0.556	0.021
0.5 molal DMSO (1-3)	3.54	0.541	0.001	0.159	2.760	0.579	0.034
0.5 molal DMSO (2-1)	3.70	0.566	0.024	0.255	1.539	0.318	0.021
0.5 molal DMSO (2-2)	4.11	0.567	0.023	0.186	2.547	0.532	0.022
0.5 molal DMSO (2-3)	3.45	0.545	0.033	0.263	1.541	0.285	0.027
0.5 molal DMSO (3-1)	3.78	0.645	0.037	0.311	1.800	0.358	0.018
0.5 molal DMSO (3-2)	4.06	0.507	0.024	0.173	2.455	0.577	0.020
0.5 molal DMSO (3-3)	4.07	0.613	0.031	0.182	3.224	0.577	0.031
Average ± Standard Deviation	3.85 ± 0.26	0.571 ± 0.07	0.025 ± 0.01	0.220 ± 0.05	2.162 ± 0.61	0.456 ± 0.13	0.024 ± 0.01

179

Table 6-3b Permeability parameters obtained from 1.0 molal DMSO data fit with the new transport equations and the 3-paramter equations

1.0 molal DMSO (day # - run#)	$\widetilde{L}$ X 10^{-28} mol²/(min· atm·μm⁵)	$\widetilde{P}$ X10^{-31} mol²/(min· atm·μm⁵)	SSE	L_p (μm³/μm²/ min/atm)	P_s (μm/min)	σ	SSE
1.0 molal DMSO (1-1)	4.45	1.65	0.004	0.179	4.752	0.591	0.047
1.0 molal DMSO (1-2)	6.45	1.51	0.030	0.432	1.704	0.262	0.058
1.0 molal DMSO (1-3)	5.45	1.65	0.014	0.462	1.600	0.221	0.042
1.0 molal DMSO (2-1)	5.03	1.93	0.036	0.421	2.092	0.216	0.028
1.0 molal DMSO (2-2)	5.45	1.81	0.032	0.276	3.452	0.392	0.023
1.0 molal DMSO (2-3)	4.60	1.81	0.029	0.214	4.491	0.482	0.033
1.0 molal DMSO (3-1)	6.45	1.67	0.049	0.226	3.768	0.515	0.044
1.0 molal DMSO (3-2)	6.45	1.49	0.080	0.234	2.969	0.476	0.065
1.0 molal DMSO (3-3)	6.45	1.67	0.082	0.484	1.645	0.231	0.070
Average ± Standard Deviation	5.64 ± 0.83	1.69 ± 0.14	0.040 ± 0.03	0.325 ± 0.12	2.941 ± 1.24	0.376 ± 0.15	0.046 ± 0.02

180

Table 6-3c   Permeability parameters obtained from 2.0 molal DMSO data fit with the new transport equations and the 3-paramter equations

2.0 molal DMSO (day # - run#)	$\tilde{L}$ X 10^{-28} $mol^2/(min\cdot atm\cdot\mu m^5)$	$\tilde{P}$ X10^{-31} $mol^2/(min\cdot atm\cdot\mu m^5)$	SSE	L_p ($\mu m^3/\mu m^2/min/atm$)	P_s ($\mu m/min$)	σ	SSE
2.0 molal DMSO (1-1)	4.50	3.88	0.068	0.180	4.88	0.476	0.074
2.0 molal DMSO (1-2)	4.46	4.09	0.062	0.175	6.35	0.570	0.142
2.0 molal DMSO (1-3)	4.45	4.77	0.095	0.252	3.57	0.253	0.059
2.0 molal DMSO (2-1)	5.28	4.28	0.044	0.210	6.80	0.595	0.060
2.0 molal DMSO (2-2)	4.22	3.92	0.062	0.175	5.57	0.514	0.063
2.0 molal DMSO (2-3)	4.46	4.35	0.084	0.211	4.40	0.355	0.071
2.0 molal DMSO (3-1)	6.29	4.01	0.088	0.223	5.35	0.558	0.121
2.0 molal DMSO (3-2)	6.00	4.01	0.075	0.217	5.35	0.553	0.082
2.0 molal DMSO (3-3)	5.75	3.86	0.062	0.208	5.48	0.582	0.057
Average ± Standard Deviation	5.05 ± 0.82	4.13 ± 0.29	0.071 ± 0.02	0.206 ± 0.03	5.306 ± 0.96	0.495 ± 0.12	0.081 ± 0.03

181

6.6   Discussion and Conclusions

Despite the fact that for almost all the runs, the sum of square errors was very similar for the two methods of fitting the data, it is important to note that the new transport equations are fitting for only two parameters instead of three and can be extended to data at high concentrations.

When analyzing the data for fit with the new transport equations, there appears to be an obvious concentration dependence of $\tilde{P}$. As the concentration of exposure to DMSO increased, the value for $\tilde{P}$ also increased. By comparing (Eq. 6- 16) with (Eq. 6- 38), we can see that $\tilde{P}$ will have the same concentration dependency as P_s^*. Recall that we used (Eq. 6- 21) and (Eq. 6- 24) to get the concentration dependency of P_s^* in (Eq. 6- 25) and found that:

(Eq. 6- 25)

$$P_s^* \alpha \ C_{eq}$$
$$also \ \tilde{P} \ \alpha \ C_{eq}$$

This means that as the solute concentration increases, the value of P_s^* and hence $\tilde{P}$ will increase, which is what was observed. $\tilde{L}$ did not appear to have the same strong concentration dependence. Table 6-4 shows the various concentration relationships for $\tilde{P}$.

182

Table 6-4 Concentration relationships for $\tilde{P}$

Molal Concentration	Osmolal Concentration	$\tilde{P}$ $\times 10^{-31}$	$\left(\dfrac{\tilde{P}}{molal\ concentration}\right)$ $\times 10^{-31}$
0.5	0.631	0.571 ± 0.07	1.142 ± 0.07
1.0	1.227	1.69 ± 0.14	1.685 ± 0.14
2.0	2.589	4.13 ± 0.29	2.065 ± 0.29

In order to compare the concentration relationships for P_s and for $\tilde{P}$, we can compare the standard deviation of the average values as shown in Table 6-5.

Table 6-5 Concentration relationship comparisons for P_s and $\tilde{P}$

Molal Concentration	P_s	$\left(\dfrac{\tilde{P}}{molal\ concentration}\right)$ $\times 10^{-31}$
0.5	2.162 ± 0.61	1.142 ± 0.07
1.0	2.941 ± 1.24	$1.685\ 0.14$
2.0	5.306 ± 0.96	2.065 ± 0.29
Average value	3.470	1.632
Standard deviation of averages	1.647	0.464

Earlier on it was shown in (Eq. 6- 26) that theoretically, P_s should not depend on concentration. From Table 6-5, we see that there is a larger unexpected

183

deviation in concentration with the P_s values as compared to the $\tilde{P}$ values.

When the $\tilde{P}$ values are divided by concentration, there should not be any further concentration dependence. When the data for the human corneal epithelial cells was analyzed in the past [6], it was assumed that there was no cryoprotectant concentration dependence of the permeability parameters. However, the data for the epithelial cells exposed to various concentrations of DMSO (0.5M, 1M, and 2M) at 13°C showed that there was a statistical difference in the solute permeability coefficients at the higher 2 molal concentration. The reason cited for this was the possible linearity in the 3-parameter transport equations utilized. There was an assumption made that the molality was equal to the osmolality, which is significant at higher concentrations.

However, it is possible then that the fitting of σ in the three parameter formalism is simply adjusting for non-dilute behavior. In the literature it has been reported that there is no pattern that emerges which defines how the solute concentration effects membrane permeability characteristics and at times researchers found solute inhibition of L_p [10]. At times the hydraulic conductivity seems to decrease in the presence of increased solute concentrations [18], while in other instances it seems to increase the hydraulic conductivity [19]. It is possible that these reported variations of the hydraulic conductivity are a result of dilute solution expressions being used in the transport equations and may not be evident if non-dilute transport equations were utilized.

184

In this chapter we have been able to derive a new, complete set of transport equations that make no dilute solution or near –equilibrium assumptions, and can hence be applied to any concentration range. This is applicable to many fields including cryobiology where dilute solution conditions are not often met, since concentrated solutions are used over large temperature ranges. We were able to eliminate using σ and utilize our new transport equations that fit for 2 permeability coefficients. The fits with the new transport equations were as good with the two parameters as with the previous three parameter model. There is less unexpected concentration dependence with the new transport equations. In other words, some of the unexpected concentration dependence of permeability has been explained as being due to using inappropriate transport equations.

6.7 References

[1] Anderson, J., Paterson, R., Application of Irreversible Thermodynamics to Isotopic Diffusion .1. Isotope-Isotope Coupling Coefficients for Ions and Water in Concentrated Aqueous-Solutions of Alkali-Metal Chlorides at 298.16 K, Journal of the Chemical Society-Faraday Transactions I 71 (1975) 1335-1351.

[2] Arnaud, F.G., Pegg, D.E., Permeation of Glycerol and Propane-1,2-Diol into Human Platelets, Cryobiology 27 (1990) 107-118.

[3] Bannerman, R.C., Elliott, J.A.W., Porter, K. R., McGann, L. E., A multi-solute osmotic virial equation for solutions of interest in biology, Submitted to: Biophysical Journal (2005).

[4] Cui, Z.F., Dykhuizen, R.C., Nerem, R.M., Sembanis, A., Modeling of cryopreservation of engineered tissues with one-dimensional geometry, Biotechnology Progress 18 (2002) 354-361.

[5] Du, J.Y., Kleinhans, F.W., Mazur, P., Critser, J.K., Human Spermatozoa Glycerol Permeability and Activation-Energy Determined by Electron-Paramagnetic-Resonance, Biochimica Et Biophysica Acta-Biomembranes 1194 (1994) 1-11.

[6] Ebertz, S., Fundamental Cryobiology of Cells from a Bioengineered Human Corneal Equivalent, PhD, Medical Sciences - Laboratory Medicine and Pathology, University of Alberta, 2002.

[7] Elliott, J.A.W., Elmoazzen, H.Y., McGann, L.E., A method whereby Onsager coefficients may be evaluated, Journal of Chemical Physics 113 (2000) 6573-6578.

[8] Elliott, J.A.W., Ward, C.A., Equilibria and Dynamics of Gas Adsorption on Heterogeneous Solid Surfaces, Studies in Surface Science and Catalysis, Vol. 104 (Elsevier, New York, 1997).

[9] Felmy, A.R., Weare, J.H., Calculation of Multicomponent Ionic-Diffusion from Zero to High-Concentration .1. The System Na-K-Ca-Mg-Cl-So4-H2o at 25-Degrees-C, Geochimica Et Cosmochimica Acta 55 (1991) 113-131.

[10] Gilmore, J.A., Mcgann, L.E., Liu, J., Gao, D.Y., Peter, A.T., Kleinhans, F.W., Critser, J.K., Effect of Cryoprotectant Solutes on Water Permeability of Human Spermatozoa, Biology of Reproduction 53 (1995) 985-995.

[11] Hunt, C.J., Armitage, S.E., Pegg, D.E., Cryopreservation of umbilical cord blood: 1. Osmotically inactive volume, hydraulic conductivity and permeability of CD34(+) cells to dimethyl, sulphoxide, Cryobiology 46 (2003) 61-75.

[12] Jacobs, M.H., The simultaneous measurement of cell permeability to water and to dissolved substances, Journal of Cellular and Comparative Physiology 2 (1933) 427-444.

[13] Jacobs, M.H., Stewart, D.R., A simple method for the quantitative measurement of cell permeability, Journal of Cellular and Comparative Physiology 1 (1932) 71-82.

[14] Kedem, O., Katchalsky, A., Thermodynamic Analysis of the Permeability of Biological Membranes to Non-Electrolytes, Biochimica Et Biophysica Acta 27 (1958) 229-246.

[15] Kleinhans, F.W., Membrane permeability modeling: Kedem-Katchalsky vs a two-parameter formalism, Cryobiology 37 (1998) 271-289.

[16] Levin, R.L., Cravalho, E.G., Huggins, C.E., Effect of Solution Non-Ideality on Erythrocyte Volume Regulation, Biochimica Et Biophysica Acta 465 (1977) 179-190.

[17] McGrath, J.J., Quantitative measurement of cell membrane transport: Technology and applications, Cryobiology 34 (1997) 315-334.

[18] McGrath, J.J., Diller, K.R. (Eds.), Low Temperature Biotechnology: Emerging Applications and Engineering Contributions, ASME Press, New York, 1988, 273-330 pp.

[19] McGrath, J.J., Hunter, J. E., Bernard, A. G., Fuller, B. J., and Shaw, R. W., On the use of microdiffusion chamber methods to determine the coupled transport of water and cryoprotective agents across biological membranes, in: K.R. Diller, A. Shitzer (Eds.), Macroscopic and Microscopic Heat and Mass Transfer in Biomedical Engineering (International Centre for Heat and Mass Transfer Publications, 1992) 301-326.

[20] Pegg, D.E., Hunt, C.J., Fong, L.P., Osmotic Properties of the Rabbit Corneal Endothelium and Their Relevance to Cryopreservation, Cell Biophysics 10 (1987) 169-189.

[21] Wang, X.Q., Wexler, A.S., Marsh, D.J., The Effect of Solution Nonideality on Membrane-Transport in 3-Dimensional Models of the Renal Concentrating Mechanism, Bulletin of Mathematical Biology 56 (1994) 515-546.

[22] Ward, C.A., Effect of Concentration on the Rate of Chemical-Reactions, Journal of Chemical Physics 79 (1983) 5605-5615.

[23] Ward, C.A., Rate of Gas Absorption at a Liquid Interface, Journal of Chemical Physics 67 (1977) 229-235.

[24]   Ward, C.A., Findlay, R.D., Rizk, M., Statistical Rate Theory of Interfacial Transport .1. Theoretical Development, Journal of Chemical Physics 76 (1982) 5599-5605.

[25]   Xu, X., Cui, Z.F., Urban, J.P.G., Measurement of the chondrocyte membrane permeability to Me2SO, glycerol and 1,2-propanediol, Medical Engineering & Physics 25 (2003) 573-579.

[26]   Zelman, A., Membrane-Permeability - Generalization of Reflection Coefficient Method of Describing Volume and Solute Flows, Biophysical Journal 12 (1972) 414-419.

Figure 6-1   A system of water, a permeating solute, an intracellular non-permeating solute and an extracellular non-permeating solute
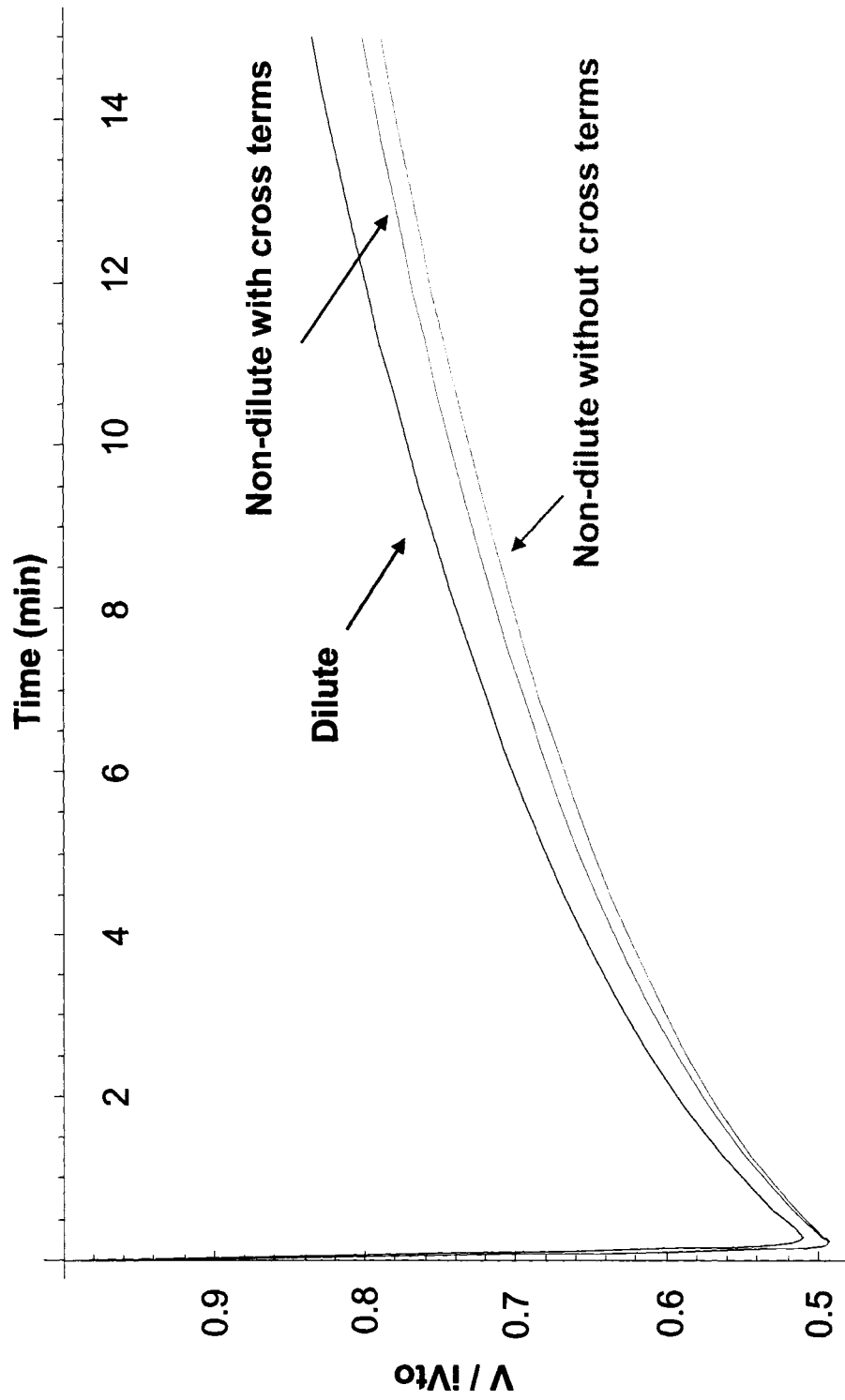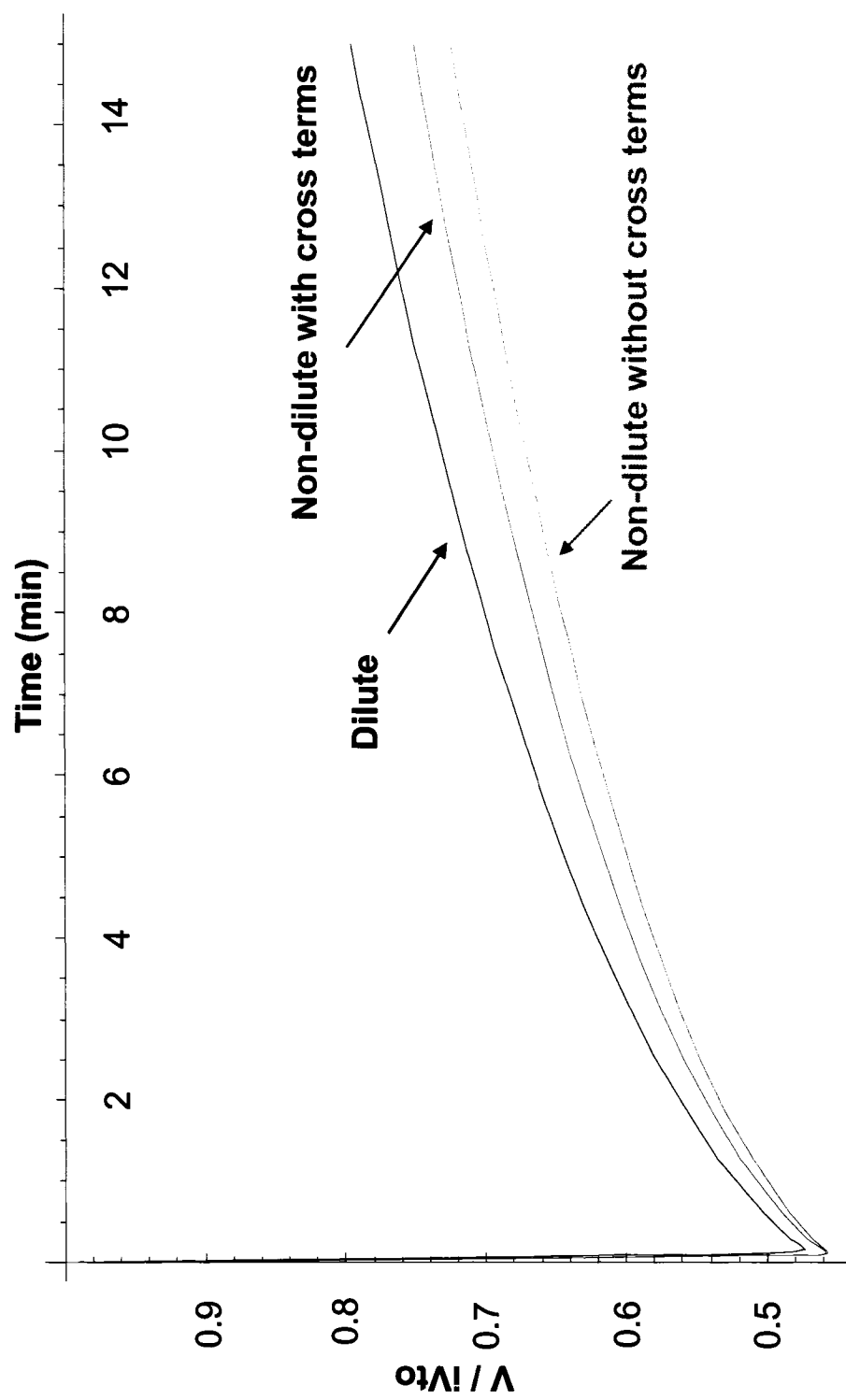
Extracellular Solution

Intracellular Solution

Water N_1^i ←————————→ Water N_1^o

Permeating Solute N_2^i ←————————→ Permeating Solute N_2^o

Non-Permeating Intracellular Solute N_3^i

Non-Permeating Intracellular Solute N_4^o
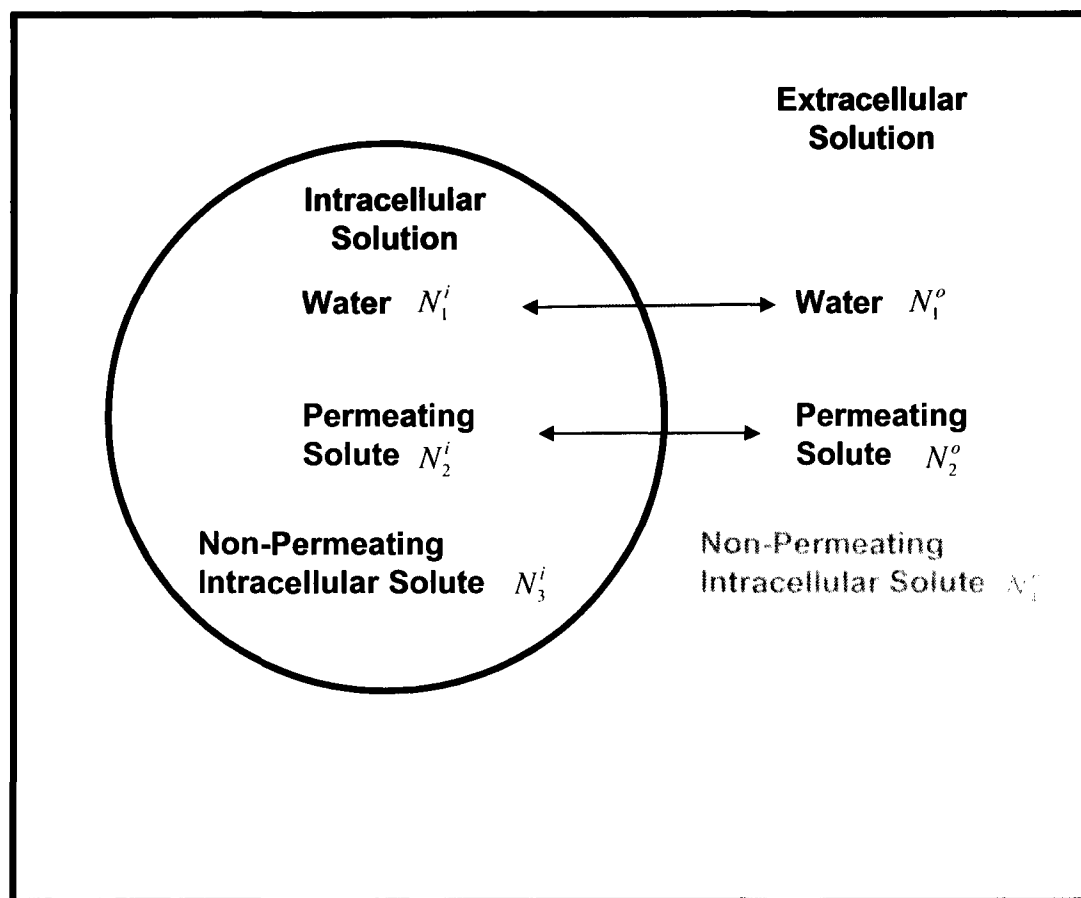
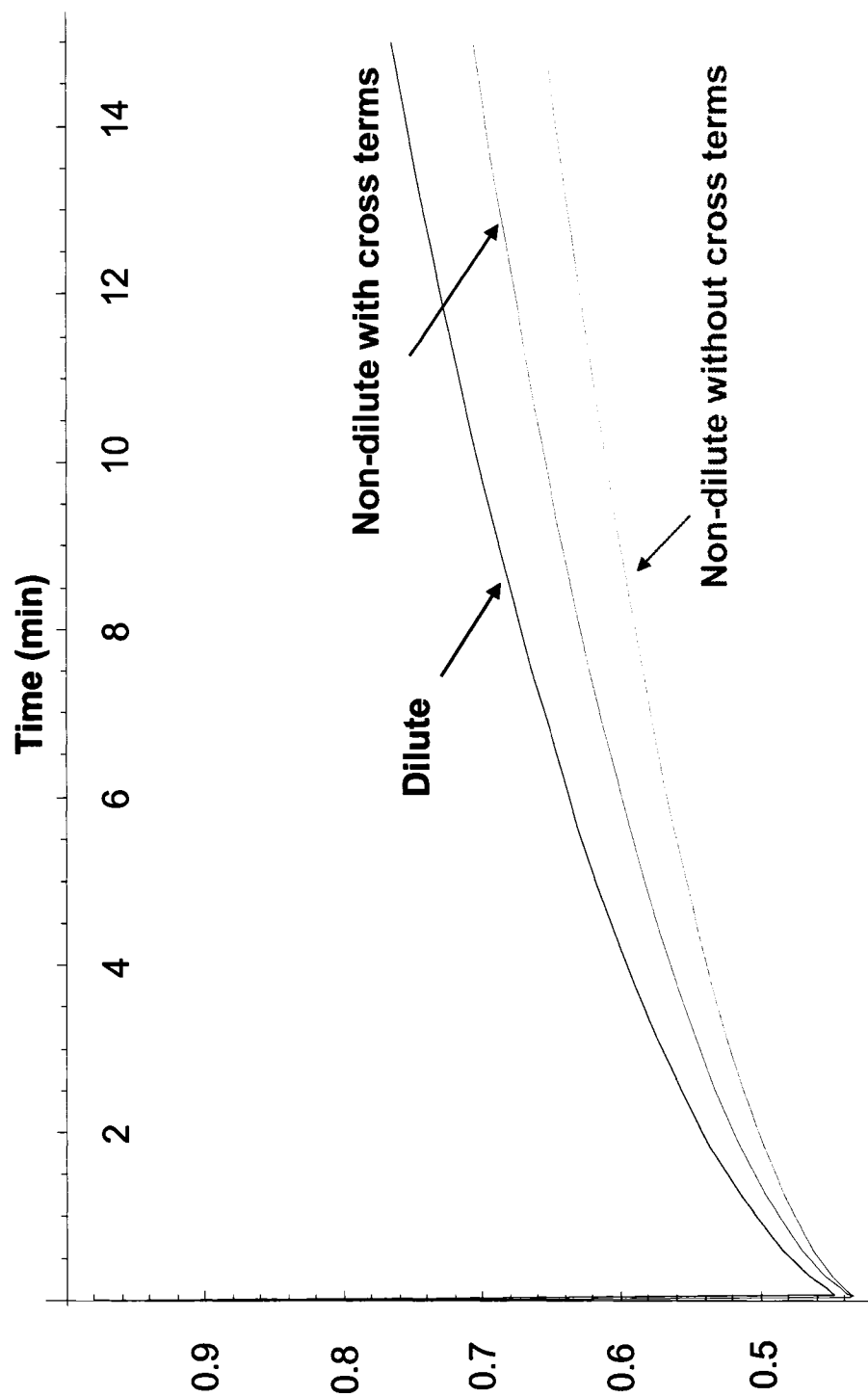Figure 6-2   Volume change on addition of 2 molal DMSO

190

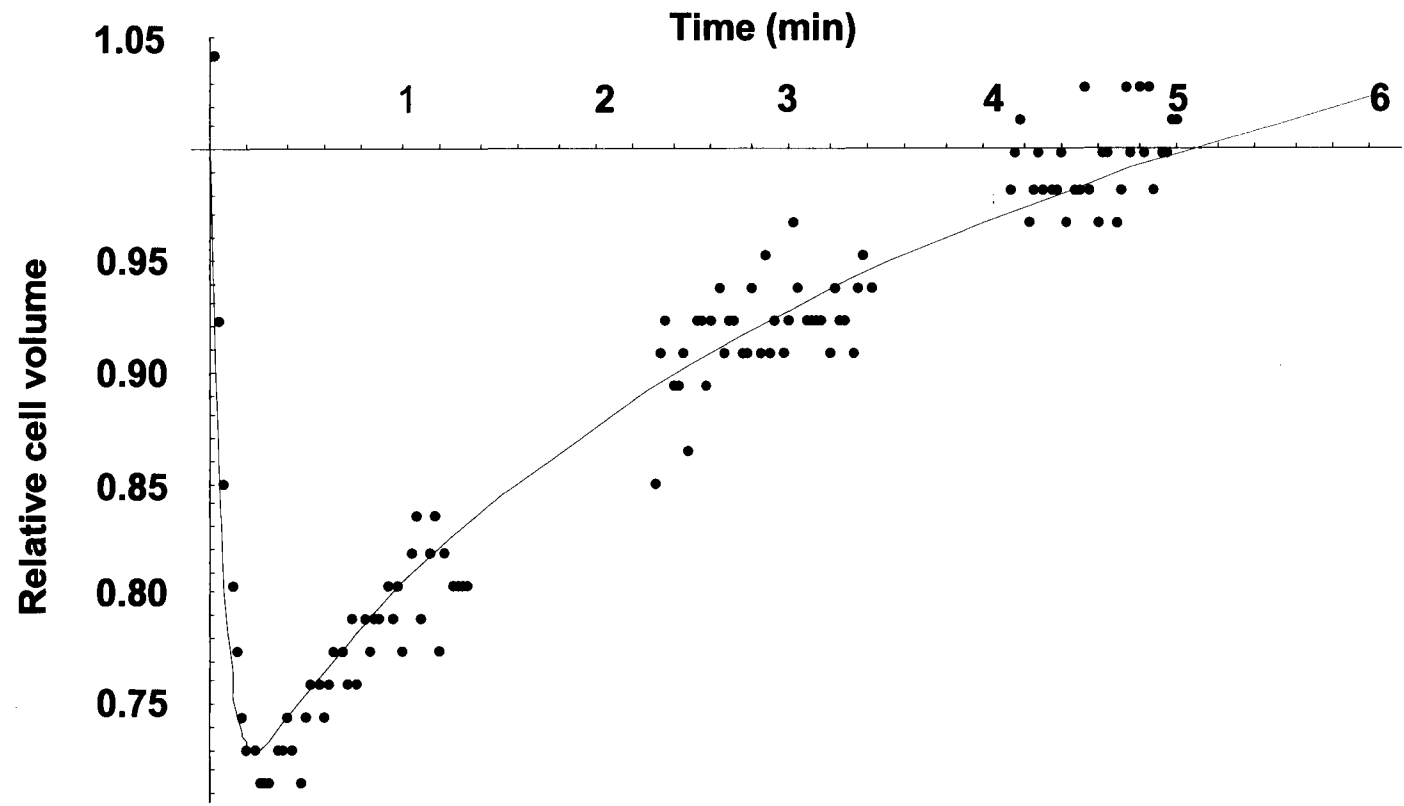Figure 6-3 Volume change on addition of 4 molal DMSO

191

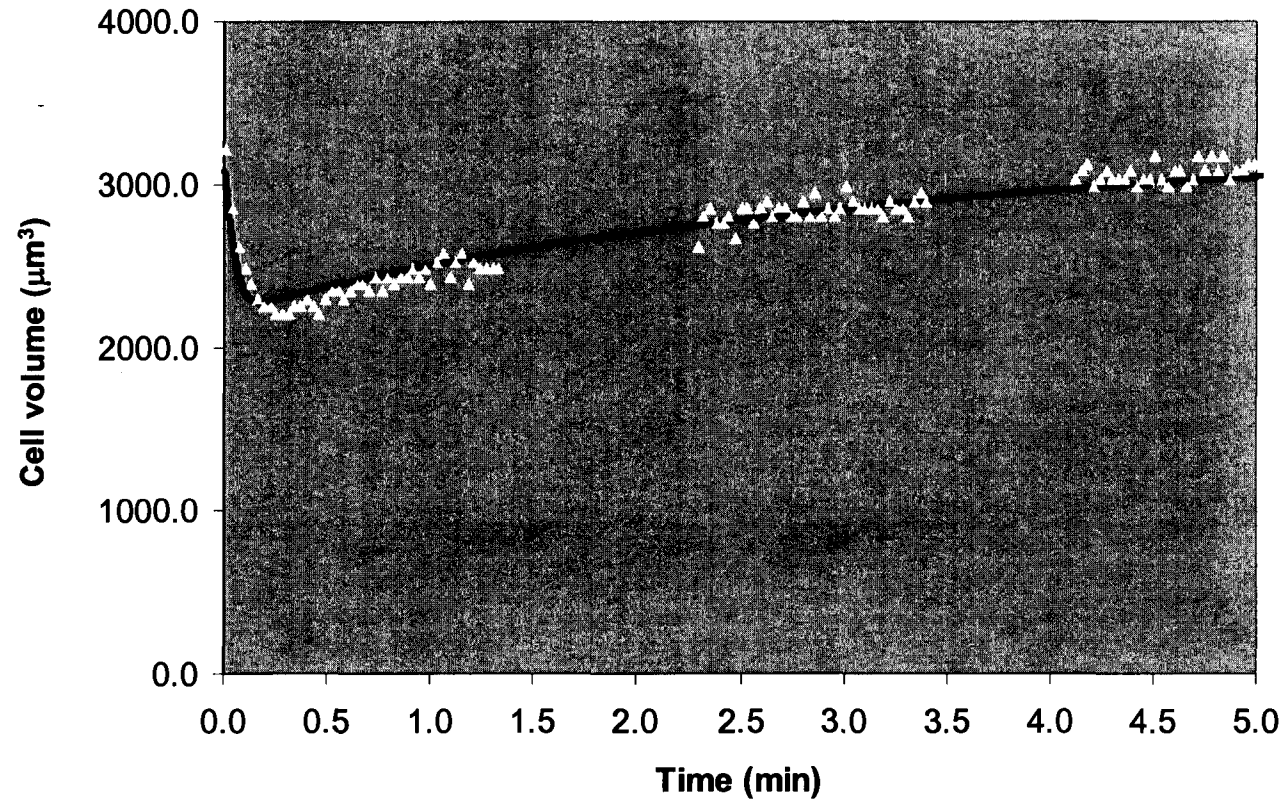**Figure 6-4   Volume change on addition of 6 molal DMSO**

192
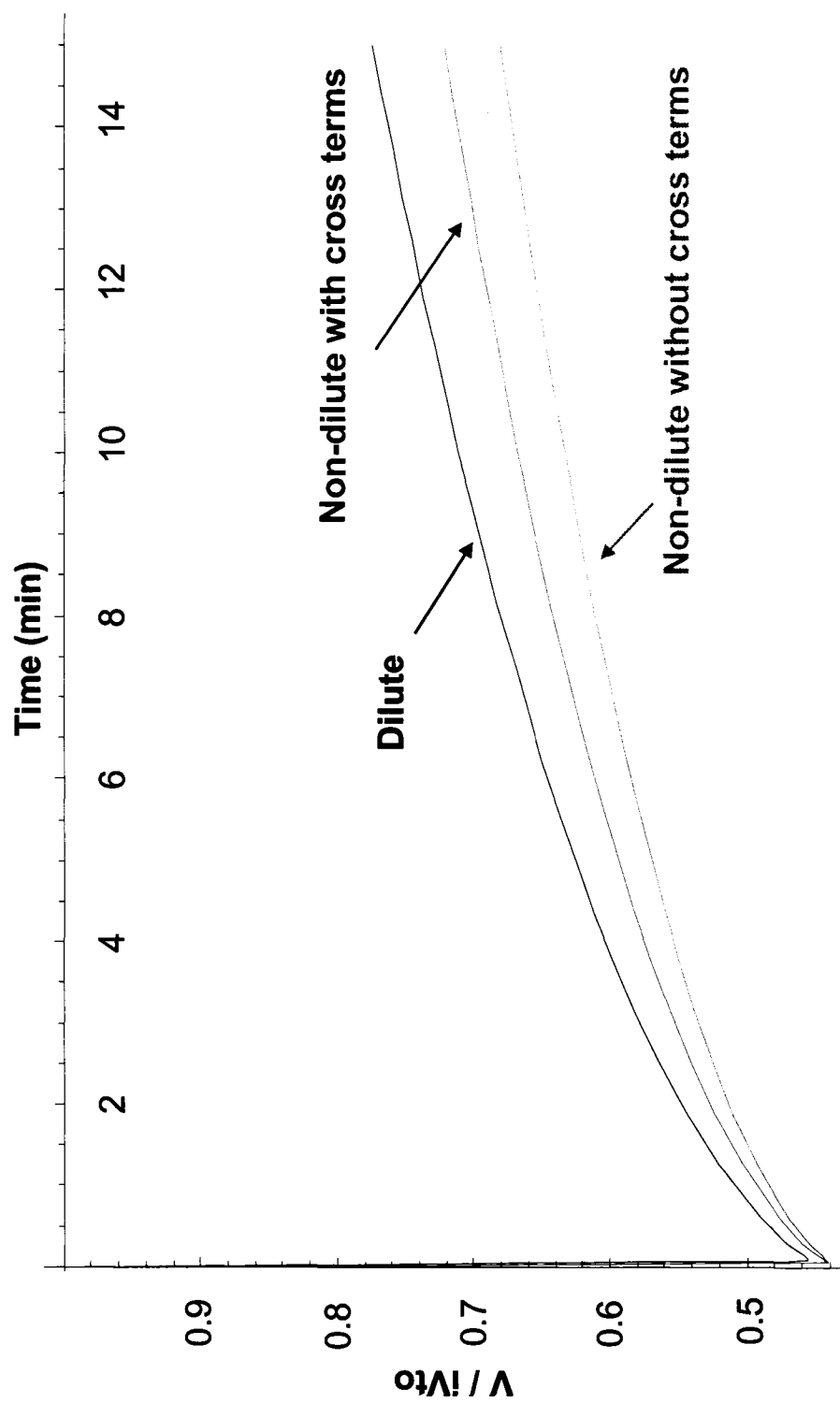
Figure 6-5   Volume change on addition of 8 molal DMSO

193

Figure 6-6 **Relative cell volume change of human corneal epithelial cells on addition of 2 molal DMSO**

Figure 6-7   Volume change of human corneal epithelial cells on
addition of 2 molal DMSO

Chapter 7: Conclusions

The main objective of this thesis was to provide a better understanding of osmotic transport in cryobiology. In depth knowledge of osmotic transport can help optimize the development of cryopreservation protocols and thus improve the viability of cells and tissues in many fields of interest, including transplant medicine. The purpose of this thesis was to understand the parameters that affect osmotic transport and to understand the limitations of the current transport formalism used in the literature, as well as to develop a new set of transport equations more applicable to cryobiology.

Cell size distribution was the first parameter for which the effect on permeability coefficients was examined. Analysis of the experimental data for both MDCK and V-79W cells, two cell types with different isotonic volumes and different cell size distributions, showed that the shapes of the cell size distributions did not stay constant over time when the cells were responding to a hypertonic environment. This implied that one must carefully choose the measure of central tendency to use when analyzing the osmotic response of cells with size distributions. A novel tool was developed to test which method of central tendency should be used when analyzing osmotic data. It was clearly shown that the mean or median cell volume rather than the mode should be used to analyze osmotic data.

196

The next major section of this thesis dealt with osmotic transport in tissue systems. The role of cryoprotectant equilibration in tissues was investigated. There have been reports of tissues having equilibrium cryoprotectant concentrations lower than that of the surrounding carrier solution. For various tissues, the equilibrium concentration of cryoprotectant inside the tissue is either equal to, or lower than the cryoprotectant concentration of the surrounding solution. Thermodynamics was applied to examine the role of pressure in tissue equilibration as a possible explanation as to why some tissue systems come to the same equilibrium concentration as the surrounding solutions and other systems do not. Thermodynamics predicted that the equilibrium concentration of cryoprotectant inside the tissue depended on the ability of the tissue system to maintain an equilibrium pressure difference. Tissues that were free to expand reached the same equilibrium cryoprotectant concentration as the surrounding solution. Tissues that were not free to expand and could maintain a pressure difference, did not reach the same equilibrium cryoprotectant concentration within the tissue as in the surrounding solution. This section proposed a possible explanation of the discrepancies often observed, but could not be used to predict the equilibrium concentration that would be reached by a tissue system. This section also re-iterated the importance of developing transport equations that could be used for non-dilute solutions.

In the next section of this thesis, a detailed look into the current status of osmotic transport in the literature was provided. The assumptions, limitations and

197

common misconceptions made when using the two-parameter formalism and the Kedem-Katchalsky formalism were examined. In the literature osmolarity and osmolality are used interchangeably; however, they are only equal for dilute solutions at 4°C. It was demonstrated that despite what is often stated in the literature, using either the 2-P or the K-K equations results in dilute solution assumptions being made, specifically in the solute transport equations wherein molarity cannot simply be replaced with osmolarity as is current practice. A detailed investigation and comparison into the 2-P and K-K formalism was provided and insight into the reflection coefficient was obtained. For situations where there was no interaction between water and solute, it was shown that the 2-P and the K-K equations are essentially the same, thus verifying the results obtained by Kleinhans which he demonstrated using simulations. Kleinhans noted that the 2-P formalism and the K-K formalism deviated from each other at high concentrations, but there were no practical differences between the two models up to solute concentrations of several molar. The 2-P model uses only two parameters while the K-K model uses three parameters. It is possible then that the fitting of σ is adjusting for non-dilute behavior, since in both equations a dilute solution assumption is being made. This section again highlighted the importance of developing non-dilute transport equations.

A detailed derivation of non-dilute chemical potential equations for the solvent and the solute were presented in the different units of concentration, including mole fraction, molality and molarity. The osmotic virial equation treats osmolality

198

(or osmolarity or osmotic pressure) as a polynomial expansion in concentration with the first term being linear in concentration and a thermodynamic basis for a new mixing rule for the osmotic virial equation was provided. Since the non-dilute chemical potential equations were derived in mole fraction, molality and molarity and the same form for the interaction parameter resulted in all three derivations, this demonstrated that the mixing rule was not unit dependent and will be valid for all units of concentration used.

The final section of this thesis provided an analysis of various equations for solute transport. Statistical Rate Theory was used to determine if the various solute permeability coefficients had a concentration-dependence. It was found that the solute permeability, P_s, and diffusion coefficient, D_s, did not depend on the solute concentration while the solute permeability, P_s^*, and the phenomenological coefficient, L, did depend on the concentration of the solute. Statistical Rate Theory allowed the determination of these dependencies, since the theory is written in terms of experimental and thermodynamic variables that may be tabulated, measured or controlled. As well, in the final section of this thesis, a new complete set of transport equations, that make no dilute solution or near–equilibrium assumptions and can be applied to any concentration range, were developed. These equations are much more applicable to many fields, including cryobiology where dilute solution conditions are not often met, since concentrated solutions are used over large temperature ranges. The use of σ was eliminated with the new transport equations that fit for two permeability

coefficients. The new transport equations were fit to experimental data for human corneal epithelial cells exposed to various concentrations of DMSO. It was shown that the new transport equations fit the data with two parameters as well as with the previous three-parameter fit. It was demonstrated that there is less unexpected concentration dependence with the new transport equations and hence some of the unexpected concentration dependence of the permeability coefficient has been explained as being due to the use of inappropriate transport equations.

In cryobiology, the addition and removal of cryoprotectants as well as the conversion of water to ice that takes place during freezing results in cells being exposed to highly concentrated, non-dilute solutions. There exists a definite need to obtain permeability parameters for water and solute movement across cell membranes under such conditions. As cryobiologists continue studying cells and tissues of increasing complexity, there is an even greater need for a better understanding of osmotic transport. More accurate osmotic parameters and equations will be necessary to design effective cryopreservation protocols where simulations are used to make protocol predictions that better match experimental outcome. Better simulations will cut down on experimental costs and allow for more complicated preservation protocols to be tested. This will be particularly important in cellular and tissue systems where vitrification is becoming a more utilized technique and high, non-dilute concentrations of cryoprotectants are used.

200

Overall this thesis has provided valuable insight into the role of non-dilute solution thermodynamics on passive osmotic transport in cryobiology for both cellular and tissue systems. The next stage of cryobiology research will move cryobiology from using simple "first order" assumptions to using more accurate descriptions of osmotic transport combined with similar advances in other areas of cryobiological modeling, such as heat and mass transfer and heterogeneity in tissues, ice nucleation and propagation, and more detailed understanding of biological mechanisms of cryoinjury, to make further advances in the field of cryobiology.

Appendix

A.1   Appendix for Section 6.3 b

(* Non-dilute expression for osmolality *)

(* Cellular Parameters *)

iVto := 3580   (* isotonic cell volume *)
iVdf := 0.41   (* osmotically inactive fraction *)
iVd := iVto * iVdf   (* osmotically inactive volume *)

(* Experimental Parameters *)

Tc := 4   (* temperature *)
PMV1 :=
 18.02 * 10^12   (* partial molar volume of water *)
PMV2 := 71.32 * 10^12   (* partial molar volume of DMSO *)
PMV3 := 37.51887 * 10^12   (* partial molar volume of KCl *)
x2out := 0.0979   (* DMSO mole fraction outside *)
x4out := 0.002856   (* NaCl mole fraction outside *)
B2 := 0.0843
(* interaction coefficient for DMSO *)
B3 := 0.0
(* interaction coefficient for KCl *)
B4 := 0.0299
(* interaction coefficient for NaCl *)
KNaCl := 1.70   (* dissociation constant of NaCl *)
KKCl := 1.74   (* dissociation constatnt of KCl *)
Lp := 0.24
(* hydraulic conductivity of water *)
Ps := 0.48   (* solute permeability coefficient *)

(* Fitting Paramters *)

Time0 := 0.0   (* time zero*)
tMax := 15   (* maximum time in minutes *)

(* Constants *)

GasConst := 8.2057 * 10^13   (* universal gas constant *)
Tk := Tc + 273.16   (* temperature in degrees Kelvin *)
RT := GasConst * Tk
   (* gas constant times temperature in degrees Kelvin *)

202

(* Initial Conditions at time=0 *)

x2ino := 0.0
(* initial solute mole fraction inside the cell *)
x3ino := 0.003089863
(* initial salt mole fraction inside the cell *)
x1ino := 1.0 - x3ino
   (* initial water mole fraction inside the cell *)

N2ino := 0.0
(* initial DSMO molecules inside the cell *)
N3ino := (iVto * (1 - iVdf)) / ((x1ino * PMV1 / x3ino) + PMV3)
(* initial salt molecules inside the cell *)
N1ino := x1ino * N3ino / x3ino
   (* initial water molecules inside the cell *)

(* Start non-dilute curve with cross terms *)

Vtotal[t_] :=
 N1in[t] * PMV1 + N2in[t] * PMV2 + N3ino * PMV3 + iVd   (* total cell volume *)

Area[t_] :=
 4 * N[Pi] * (3 * Vtotal[t] / 4 / N[Pi]) ^ (2 / 3)   (* cell surface area *)

x2in[t_] := N2in[t] / (N1in[t] + N2in[t] + N3ino)
 (* mole fraction of DMSO inside the cell as a function of time *)

x3in[t_] := N3ino / (N1in[t] + N2in[t] + N3ino)
 (* mole fraction of salt inside the cell as a function of time *)

x1in[t_] := 1 - x2in[t] - x3in[t]
(* mole fraction of water inside the cell as a function of time *)

convout := 1000 / (18.02 * (1 - x2out - x4out))
(* conversion factor between mole fraction and molality *)

convin[t_] := 1000 / (18.02 * x1in[t])
 (* conversion factor between mole fraction and molality *)

mout := x2out * convout + KNaCl * x4out * convout +
  B2 * (x2out * convout) ^ 2 + B4 * (KNaCl * x4out * convout) ^ 2 +
  (B2 + B4) * (x2out * convout * KNaCl * x4out * convout)
    (* extracellular osmolality *)

min[t_] :=
 x2in[t] * convin[t] + KKCl * x3in[t] * convin[t] + B2 * (x2in[t] * convin[t]) ^ 2 +
  B3 * (KKCl * x3in[t] * convin[t]) ^ 2 + (B2 + B3) * x2in[t] * convin[t] *
   KKCl * x3in[t] * convin[t]   (* intracellular osmolality *)

203

```
deltam[t_] := mout - min[t]
   (* difference between extracellular and intracellular osmolality *)

RHS1[t_] := -Lp * Area[t] * RT * deltam[t] / (PMV1 * 1 * 10^15)
   (* change in water volume as a function of time *)

m2out := x2out * convout
   (* extracellular solute molality *)

m2in[t_] := x2in[t] * convin[t]
   (* intracellular solute molality *)

deltam2[t_] := m2out - m2in[t]
   (* difference between extracellular and intracellular molality *)


RHS2[t_] := Ps * Area[t] * deltam2[t] / (1 * 10^15)
   (* change in solute molecules as a function of time *)

sol[N1in_, N2in_] :=
 NDSolve[{N1in'[t] == RHS1[t], N2in'[t] == RHS2[t], N1in[0] == N1ino,
    N2in[0] == N2ino }, {N1in[t], N2in[t]}, {t, 0, tMax},
   AccuracyGoal → 20, PrecisionGoal → 20, WorkingPrecision → 25]

additivenondiluteplot =
 Plot[Evaluate[(N1in[t] * PMV1 + N2in[t] * PMV2 + N3ino * PMV3 + iVd) / iVto /.
    sol[N1in, N2in]], {t, 0, tMax}, PlotStyle → {RGBColor[1, 0, 1]}]
```
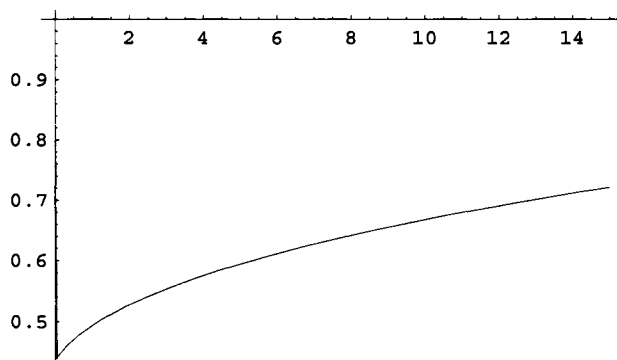
204

(* Plotting Vtotal Vs Time for non-dilute curve with cross term *)

- Graphics -

(* Start dilute curve *)

B2 := 0.0   (* Interaction coefficient for CPA *)
B3 := 0.0   (* Interaction coefficient for KCl *)
B4 := 0.0   (* Interaction coefficient for NaCl *)

Area[t_] := 4 * N[Pi] * (3 * Vtotal[t] / 4 / N[Pi]) ^ (2 / 3)

x2in[t_] := N2in[t] / (N1in[t] + N2in[t] + N3ino)

x3in[t_] := N3ino / (N1in[t] + N2in[t] + N3ino)

x1in[t_] := 1 - x2in[t] - x3in[t]

convout := 1000 / (18.02 * (1 - x2out - x4out))

convin[t_] := 1000 / (18.02 * x1in[t])

mout := x2out * convout + KNaCl * x4out * convout +
  B2 * (x2out * convout) ^ 2 + B4 * (KNaCl * x4out * convout) ^ 2 +
  (B2 + B4) * (x2out * convout * KNaCl * x4out * convout)

min[t_] := x2in[t] * convin[t] + KKCl * x3in[t] * convin[t] +
  B2 * (x2in[t] * convin[t]) ^ 2 + B3 * (KKCl * x3in[t] * convin[t]) ^ 2 +
  (B2 + B3) * x2in[t] * convin[t] * KKCl * x3in[t] * convin[t]

deltam[t_] := mout - min[t]

RHS1[t_] := -Lp * Area[t] * RT * deltam[t] / (PMV1 * 1 * 10 ^ 15)

m2out := x2out * convout

m2in[t_] := x2in[t] * convin[t]
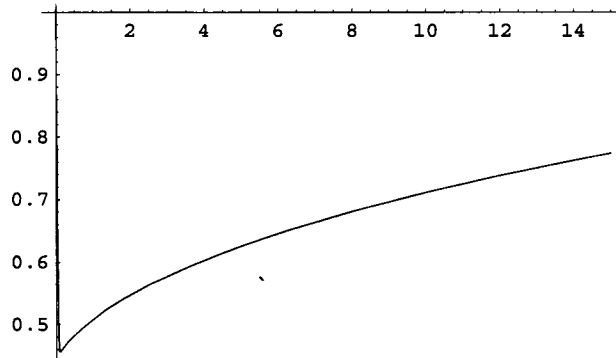

205

```
deltam2[t_] := m2out - m2in[t]

RHS2[t_] := Ps * Area[t] * deltam2[t] / (1 * 10^15)

sol[N1in_, N2in_] :=
 NDSolve[{N1in'[t] == RHS1[t], N2in'[t] == RHS2[t], N1in[0] == N1ino,
   N2in[0] == N2ino}, {N1in[t], N2in[t]}, {t, 0, tMax},
  AccuracyGoal → 20, PrecisionGoal → 20, WorkingPrecision → 25]



(* Plotting Vtotal Vs Time for dilute curve *)
```

206

```
diluteplot =
 Plot[Evaluate[(Nlin[t] * PMV1 + N2in[t] * PMV2 + N3ino * PMV3 + iVd) / iVto /.
    sol[Nlin, N2in]], {t, 0, tMax}]
```


- Graphics -


```
(* Cellular Parameters *)
iVto := 3580
iVdf := 0.41
iVd := iVto * iVdf        (* osmotically inactive volume*)


(* Experimental Parameters *)
Tc := 4
PMV1 := 18.02 * 10^12      (* Partial Molar Volume for Water *)
PMV2 := 71.32 * 10^12    (* Partial Molar Volume for CPA *)
PMV3 := 37.51887 * 10^12     (* Partial Molar Volume for KCl *)
x2out := 0.0979 (* CPA mole fraction out *)
x4out := 0.002856(* NaCl mole fraction out *)
B2 := 0.0843(* Interaction coefficient for CPA *)
B3 := 0.0        (* Interaction coefficient for KCl *)
B4 := 0.0299 (* Interaction coefficient for NaCl *)
KNaCl := 1.70 (* dissociation constant of NaCl*)
KKCl := 1.74 (* dissociation constatnt of KCl*)
Lp := 0.24   (* Hydraulic Conductivity of water *)
Ps := 0.48  (* Solute Permeability coefficient for CPA *)



(* Fitting Paramters *)
Time0 := 0.0
tMax := 15 (*time in minutes*)


(* Constants *)
GasConst := 8.2057 * 10^13
Tk := Tc + 273.16
RT := GasConst * Tk
```

207

```
(* Initial Conditions at t=0 *)
x2ino := 0.0
x3ino := 0.003089863
x1ino := 1.0 - x3ino

N2ino := 0.0

N3ino := (iVto * (1 - iVdf)) / ((x1ino * PMV1 / x3ino) + PMV3)

N1ino := x1ino * N3ino / x3ino



(* Start non-dilute curve without cross terms *)


Vtotal[t_] := N1in[t] * PMV1 + N2in[t] * PMV2 + N3ino * PMV3 + iVd

Area[t_] := 4 * N[Pi] * (3 * Vtotal[t] / 4 / N[Pi]) ^ (2 / 3)

x2in[t_] := N2in[t] / (N1in[t] + N2in[t] + N3ino)

x3in[t_] := N3ino / (N1in[t] + N2in[t] + N3ino)

x1in[t_] := 1 - x2in[t] - x3in[t]

convout := 1000 / (18.02 * (1 - x2out - x4out))

convin[t_] := 1000 / (18.02 * x1in[t])

mout := x2out * convout + KNaCl * x4out * convout +
    B2 * (x2out * convout) ^ 2 + B4 * ( KNaCl * x4out * convout) ^ 2

min[t_] := x2in[t] * convin[t] + KKCl * x3in[t] * convin[t] +
    B2 * (x2in[t] * convin[t]) ^ 2 + B3 * (KKCl * x3in[t] * convin[t]) ^ 2


deltam[t_] := mout - min[t]

RHS1[t_] := -Lp * Area[t] * RT * deltam[t] / (PMV1 * 1 * 10 ^ 15)

m2out := x2out * convout

m2in[t_] := x2in[t] * convin[t]

deltam2[t_] := m2out - m2in[t]
```

```
RHS2[t_] := Ps * Area[t] * deltam2[t] / (1 * 10^15)

sol[Nlin_, N2in_] :=
  NDSolve[{Nlin'[t] == RHS1[t], N2in'[t] == RHS2[t], Nlin[0] == Nlino,
    N2in[0] == N2ino}, {Nlin[t], N2in[t]}, {t, 0, tMax},
   AccuracyGoal -> 20, PrecisionGoal -> 20, WorkingPrecision -> 25]

(* Plotting Vtotal Vs Time for non-dilute curve without cross term *)

nondiluteplot =
  Plot[Evaluate[(Nlin[t] * PMV1 + N2in[t] * PMV2 + N3ino * PMV3 + iVd) / iVto /.
    sol[Nlin, N2in]], {t, 0, tMax}, PlotStyle -> {RGBColor[0, 1, 0]}]
```
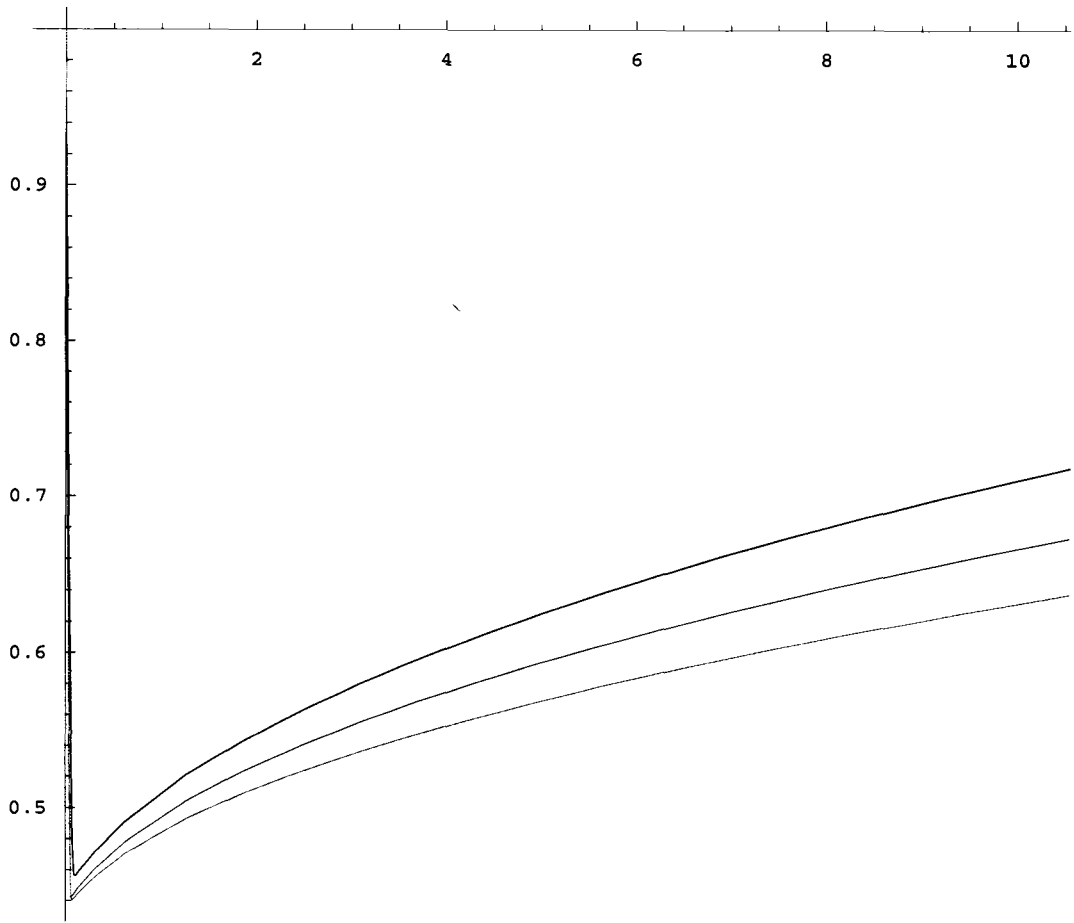

- Graphics -

209
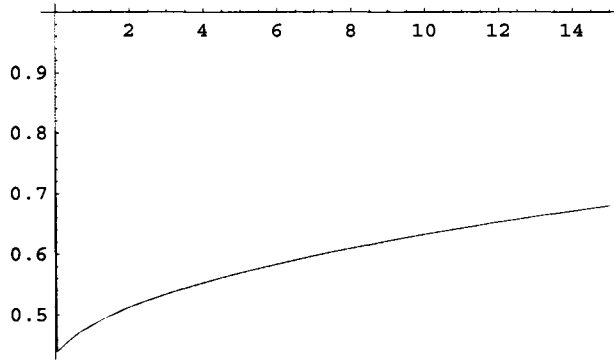
Show[additivenondiluteplot, diluteplot, nondiluteplot]

- Graphics -

210

A.2 Appendix for Section 6.5 a – Finding the Sum of the Squared Errors

```
(*CONSTANTS*)

(*Constants for loops*)
Lstart = 4.45*^-28 ;
IncrementL = 0.01*^-28;
StepsinL = 20;


P = 3.85*^-31 ;
IncrementP = 0.01*^-31 ;
StepsinP = 20;
```

(* Cellular Parameters *)
iVto = 3626;
iVdf = 0.41;
iVd = iVto*iVdf;

(* Experimental Parameters *)
Tc = 13;
PMV1 = 18.02*10^12;
PMV2 = 71.32*10^12;
PMV3 = 37.51887*10^12;
x2out = 0.044440322;
x4out = 0.00300388;
B2 = 4.716;
B3 = -0.057;
B4 = 2.759;
KNaCl = 1.68 ;
KKCl = 1.79 ;

CalF = 1;

(* Fitting Paramters *)
Time0 = 0.0;
tMax = 6 ;

(* Constants *)
GasConst = 8.2057*10^13;
Tk = Tc + 273.16;
RT = GasConst*Tk;

211

(*Initial conditions*)

x2ino = 1 * 10^-12;

x3ino = 0.003089863;

x1ino = 1.0 - x3ino - x2ino;

N3ino = (iVto * (1 - iVdf)) / ((x1ino * PMV1 / x3ino) + PMV3 + (x2ino * PMV2 / x3ino));

N2ino = x2ino * N3ino / x3ino;

N1ino = x1ino * N3ino / x3ino;

RawTimeData = {0.075, 0.105, 0.135, 0.165, 0.195, 0.225, 0.255, 0.285, 0.315, 0.345, 0.375, 0.405, 0.435, 0.465, 0.495,
    0.525, 0.555, 0.585, 0.615, 0.645, 0.675, 0.705, 0.735, 0.765, 0.795, 0.825, 0.855, 0.885, 0.915, 0.945, 0.975, 1.005,
    1.035, 1.065, 1.095, 1.125, 1.155, 1.185, 1.215, 1.245, 1.275, 1.305, 1.335, 1.365, 1.395, 1.425, 1.455, 1.485,
    1.515, 1.545, 2.385, 2.415, 2.445, 2.475, 2.505, 2.535, 2.565, 2.595, 2.625, 2.655, 2.685, 2.715, 2.745, 2.775,
    2.805, 2.835, 2.865, 2.895, 2.925, 2.955, 2.985, 3.015, 3.045, 3.075, 3.105, 3.135, 3.165, 3.195, 3.225, 3.255,
    3.285, 3.315, 3.345, 3.375, 3.405, 3.435, 3.465, 3.495, 3.525, 3.555, 3.585, 4.215, 4.245, 4.275, 4.305, 4.335,
    4.365, 4.395, 4.425, 4.455, 4.485, 4.515, 4.545, 4.575, 4.605, 4.635, 4.665, 4.695, 4.725, 4.755, 4.785, 4.815,
    4.845, 4.875, 4.905, 4.935, 4.965, 4.995, 5.025, 5.055, 5.085, 5.115, 5.145, 5.175, 5.205, 5.235, 5.265};

RawVolumeData = {3379, 3215.5, 2997.5, 2834, 2779.5, 2725, 2670.5, 2670.5, 2616, 2670.5, 2670.5, 2561.5, 2670.5,
    2670.5, 2670.5, 2725, 2670.5, 2725, 2670.5, 2670.5, 2725, 2725, 2834, 2834, 2725, 2725, 2779.5, 2725,
    2834, 2834, 2834, 2888.5, 2888.5, 2834, 2888.5, 2888.5, 2779.5, 2943, 2943, 2888.5, 2943, 2997.5,
    2888.5, 2888.5, 2888.5, 2943, 2888.5, 2997.5, 2943, 2943, 3161, 3215.5, 3052, 3215.5, 3106.5, 3215.5,
    3215.5, 3215.5, 3215.5, 3270, 3324.5, 3270, 3270, 3270, 3215.5, 3270, 3324.5, 3215.5, 3379, 3270,
    3324.5, 3270, 3324.5, 3324.5, 3215.5, 3379, 3324.5, 3270, 3324.5, 3379, 3379, 3324.5, 3270, 3324.5,
    3215.5, 3379, 3215.5, 3270, 3215.5, 3270, 3324.5, 3433.5, 3542.5, 3542.5, 3542.5, 3488, 3597, 3542.5,
    3542.5, 3542.5, 3542.5, 3542.5, 3597, 3488, 3433.5, 3488, 3542.5, 3651.5, 3597, 3542.5, 3597, 3542.5,
    3651.5, 3597, 3597, 3651.5, 3760.5, 3706, 3597, 3597, 3597, 3760.5, 3651.5, 3651.5, 3597, 3706, 3706};

NewSumSquareError = 1000;

loopcountB = 0;

(*CODE TO MINIMIZE SUMOFSQUARE
    ERRORS--*)

Label[Loop2];

loopcountA = 0;
L = Lstart;

Label[Loop1];

(*Solve*)
sol = NDSolve[{D[N1in[t], t] == -6^{2/3} * L * RT * N[Pi]

212

$$\left(\frac{iVd + N3ino * PMV3 + PMV1 * Nlin[t] + PMV2 * N2in[t]}{N[Pi]}\right)^{2/3}$$

$$\left(x2out + B2 * x2out^2 + KNaCl * x4out + (B2 + B4) * KNaCl * x2out * x4out +\right.$$

$$B4 * KNaCl^2 x4out^2 - \frac{B3 * KKCl^2 N3ino^2}{(N3ino + Nlin[t] + N2in[t])^2} -$$

$$\frac{(B2 + B3) * KKCl * N3ino * N2in[t]}{(N3ino + Nlin[t] + N2in[t])^2} - \frac{B2 * N2in[t]^2}{(N3ino + Nlin[t] + N2in[t])^2} -$$

$$\left.\frac{KKCl * N3ino}{N3ino + Nlin[t] + N2in[t]} - \frac{N2in[t]}{N3ino + Nlin[t] + N2in[t]}\right),$$

$$D[N2in[t], t] = 6^{2/3} * P * RT * N[Pi] *$$

$$\left(\frac{iVd + N3ino * PMV3 + PMV1 * Nlin[t] + PMV2 * N2in[t]}{N[Pi]}\right)^{2/3}$$

$$\left(\left(\frac{1}{2} - B2\right) * (1 - x2out) * (1 - x2out - KNaCl * x4out) -\right.$$

$$\left(\frac{1}{2} - B4\right) * KNaCl * x4out * (1 - x2out - KNaCl * x4out) +$$

$$Log[x2out] - Log\left[\frac{N2in[t]}{N3ino + Nlin[t] + N2in[t]}\right] +$$

$$\frac{(\frac{1}{2} - B3) * KKCl * N3ino * \left(1 - \frac{KKCl * N3ino}{N3ino + Nlin[t] + N2in[t]} - \frac{N2in[t]}{N3ino + Nlin[t] + N2in[t]}\right)}{N3ino + Nlin[t] + N2in[t]} -$$

$$\left(\frac{1}{2} - B2\right) * \left(1 - \frac{N2in[t]}{N3ino + Nlin[t] + N2in[t]}\right) *$$

$$\left.\left(1 - \frac{KKCl * N3ino}{N3ino + Nlin[t] + N2in[t]} - \frac{N2in[t]}{N3ino + Nlin[t] + N2in[t]}\right)\right),$$

Nlin[0] == Nlino, N2in[0] == N2ino }, {Nlin, N2in},
{t, 0, tMax}, AccuracyGoal → 20,
PrecisionGoal → 20] ;

tMinusTime0 = RawTimeData - Time0 / 60;
VoverViso = RawVolumeData * CalF / iVto;
modelNlin = Flatten[Nlin[RawTimeData] /. sol];
modelN2in = Flatten[N2in[RawTimeData] /. sol];

(*Sum Square Errors*)
ModelVoverViso =
(modelNlin * PMV1 + modelN2in * PMV2 + N3ino * PMV3 + iVd) / iVto;
SquareError = (ModelVoverViso - VoverViso) ^2;

For[{i = 1, SumSquareError = 0}, i < Length[RawVolumeData],
i++, SumSquareError = SquareError[[i]] + SumSquareError];

If[SumSquareError < NewSumSquareError,
NewSumSquareError = SumSquareError; Lfinal = L; Pfinal = P];

213

```
L = L + IncrementL;

Print["L=", N[L, 5], "          P=",
 N[P, 5], "          SSE=", N[SumSquareError, 5]];

If[loopcountA < StepsinL, loopcountA = loopcountA + 1; Goto[Loop1]];

)
|;
)




P = P + IncrementP;
 If[loopcountB < StepsinP, loopcountB = loopcountB + 1; Goto[Loop2]];
)
|;
)

Print["best values found: ", "     Lfinal=", N[Lfinal, 5],
 "          Pfinal=", N[Pfinal, 5], "          SSE=", NewSumSquareError];


Null

best values found:      Lfinal=4.5×10⁻²⁸
          Pfinal=3.88×10⁻³¹          SSE=0.0683274
```

$Lfinal=4.5 \times 10^{-28}$

$Pfinal=3.88 \times 10^{-31}$

A.3 Appendix for Section 6.5 a –
Plotting after Finding the Sum of the Squared Error

(*DATA*)

```
(* Cellular Parameters *)

iVto = 3087

3087

iVdf = 0.41

0.41

iVd = iVto*iVdf       (* osmotically inactive volume*)

1265.67


(* Experimental Parameters *)

Tc = 13

13

PMV1 = 18.02*10^12     (* Partial Molar Volume for Water *)

1.802×10^13

PMV2 = 71.32*10^12    (* Partial Molar Volume for CPA *)

7.132×10^13

PMV3 = 37.51887*10^12     (* Partial Molar Volume for KCl *)

3.75189×10^13

x2out = 0.044440322 (* CPA mole fraction out *)

0.0444403

x4out = 0.00300388 (* NaCl mole fraction out *)

0.00300388

B2 = 4.716 (* Interaction coefficient for CPA *)

4.716
```

215

B3 = -0.057 (* Interaction coefficient for KCl *)

-0.057

B4 = 2.759 (* Interaction coefficient for NaCl *)

2.759

KNaCl = 1.68 (* dissociation constant of NaCl*)

1.68

KKCl = 1.79 (* dissociation constatnt of KCl*)

1.79

L = 5.28 * 10^-28 (* Hydraulic Conductivity of water *)

5.28×10^{-28}

P = 4.28 * 10^-31 (* Solute Permeability coefficient for CPA *)

4.28×10^{-31}

CalF = 1

1

(* Fitting Paramters *)

Time0 = 0.0

0.

tMax = 6 (*time in minutes*)

6

(* Constants *)

GasConst = 8.2057 * 10^13

8.2057×10^{13}

Tk = Tc + 273.16

286.16

RT = GasConst * Tk

2.34814×10^{16}

216

```
(* Initial Conditions at t=0 *)

x2ino = 1 * 10^-12

      1
_____
1000000000000

x3ino = 0.003089863

0.00308986

x1ino = 1.0 - x3ino - x2ino

0.99691

N3ino =
 (iVto * (1 - iVdf)) / ((x1ino * PMV1 / x3ino) + PMV3 + (x2ino * PMV2 / x3ino))
```

3.1126×10^{-13}

```
N2ino = x2ino * N3ino / x3ino
```

1.00736×10^{-22}

```
N1ino = x1ino * N3ino / x3ino
```

1.00425×10^{-10}

```
RawTimeData = {0.011666667, 0.041666667, 0.071666667,
    0.101666667, 0.131666667, 0.161666667, 0.191666667, 0.221666667,
    0.251666667, 0.281666667, 0.311666667, 0.341666667, 0.371666667,
    0.401666667, 0.431666667, 0.461666667, 0.491666667, 0.521666667,
    0.551666667, 0.581666667, 0.611666667, 0.641666667, 0.671666667,
    0.701666667, 0.731666667, 0.761666667, 0.791666667, 0.821666667,
    0.851666667, 0.881666667, 0.911666667, 0.941666667, 0.971666667,
    1.001666667, 1.031666667, 1.061666667, 1.091666667, 1.121666667,
    1.151666667, 1.181666667, 1.211666667, 1.241666667, 1.271666667,
    1.301666667, 1.331666667, 2.291666667, 2.321666667, 2.351666667,
    2.381666667, 2.411666667, 2.441666667, 2.471666667, 2.501666667,
    2.531666667, 2.561666667, 2.591666667, 2.621666667, 2.651666667,
    2.681666667, 2.711666667, 2.741666667, 2.771666667, 2.801666667,
    2.831666667, 2.861666667, 2.891666667, 2.921666667, 2.951666667,
    2.981666667, 3.011666667, 3.041666667, 3.071666667, 3.101666667,
    3.131666667, 3.161666667, 3.191666667, 3.221666667, 3.251666667,
    3.281666667, 3.311666667, 3.341666667, 3.371666667, 3.401666667,
    4.121666667, 4.151666667, 4.181666667, 4.211666667, 4.241666667,
    4.271666667, 4.301666667, 4.331666667, 4.361666667, 4.391666667,
    4.421666667, 4.451666667, 4.481666667, 4.511666667, 4.541666667,
    4.571666667, 4.601666667, 4.631666667, 4.661666667, 4.691666667,
    4.721666667, 4.751666667, 4.781666667, 4.811666667, 4.841666667,
    4.871666667, 4.901666667, 4.931666667, 4.961666667, 4.991666667};
```

```
RawVolumeData = {3220, 2852, 2622, 2484, 2392, 2300, 2254, 2254, 2208, 2208,
    2208, 2254, 2254, 2300, 2254, 2208, 2300, 2346, 2346, 2300, 2346, 2392,
    2392, 2346, 2438, 2346, 2438, 2392, 2438, 2438, 2484, 2438, 2484, 2392,
    2530, 2576, 2438, 2530, 2576, 2392, 2530, 2484, 2484, 2484, 2484, 2622,
    2806, 2852, 2760, 2760, 2806, 2668, 2852, 2852, 2760, 2852, 2898, 2806,
    2852, 2852, 2806, 2806, 2898, 2806, 2944, 2806, 2852, 2806, 2852,
    2990, 2898, 2852, 2852, 2852, 2852, 2806, 2898, 2852, 2852, 2806,
    2898, 2944, 2898, 3036, 3082, 3128, 2990, 3036, 3082, 3036, 3036,
    3036, 3082, 2990, 3036, 3036, 3174, 3036, 2990, 3082, 3082, 2990,
    3036, 3174, 3082, 3174, 3082, 3174, 3036, 3082, 3082, 3128, 3128};
```

218

(*Solve Equations*)

$$sol = NDSolve\left[\left\{D[N1in[t], t] = -6^{2/3} * L * RT * N[Pi]\right.\right.$$

$$\left(\frac{iVd + N3ino * PMV3 + PMV1 * N1in[t] + PMV2 * N2in[t]}{N[Pi]}\right)^{2/3}$$

$$\left(x2out + B2 * x2out^2 + KNaCl * x4out + (B2 + B4) * KNaCl * x2out * x4out +\right.$$

$$B4 * KNaCl^2 x4out^2 - \frac{B3 * KKCl^2 N3ino^2}{(N3ino + N1in[t] + N2in[t])^2} -$$

$$\frac{(B2 + B3) * KKCl * N3ino * N2in[t]}{(N3ino + N1in[t] + N2in[t])^2} - \frac{B2 * N2in[t]^2}{(N3ino + N1in[t] + N2in[t])^2} -$$

$$\left.\frac{KKCl * N3ino}{N3ino + N1in[t] + N2in[t]} - \frac{N2in[t]}{N3ino + N1in[t] + N2in[t]}\right),$$

$$D[N2in[t], t] = 6^{2/3} * P * RT * N[Pi] *$$

$$\left(\frac{iVd + N3ino * PMV3 + PMV1 * N1in[t] + PMV2 * N2in[t]}{N[Pi]}\right)^{2/3}$$

$$\left(\left(\frac{1}{2} - B2\right) * (1 - x2out) * (1 - x2out - KNaCl * x4out) -\right.$$

$$\left(\frac{1}{2} - B4\right) * KNaCl * x4out * (1 - x2out - KNaCl * x4out) +$$

$$Log[x2out] - Log\left[\frac{N2in[t]}{N3ino + N1in[t] + N2in[t]}\right] +$$

$$\frac{(\frac{1}{2} - B3) * KKCl * N3ino * \left(1 - \frac{KKCl * N3ino}{N3ino+N1in[t]+N2in[t]} - \frac{N2in[t]}{N3ino+N1in[t]+N2in[t]}\right)}{N3ino + N1in[t] + N2in[t]} -$$

$$\left(\frac{1}{2} - B2\right) * \left(1 - \frac{N2in[t]}{N3ino + N1in[t] + N2in[t]}\right) *$$

$$\left.\left(1 - \frac{KKCl * N3ino}{N3ino + N1in[t] + N2in[t]} - \frac{N2in[t]}{N3ino + N1in[t] + N2in[t]}\right)\right),$$

N1in[0] == N1ino, N2in[0] == N2ino }, {N1in, N2in},

{t, 0, tMax}, AccuracyGoal → 20,

PrecisionGoal → 20]

tMinusTime0 = RawTimeData - Time0 / 60;

VoverViso = RawVolumeData * CalF / iVto;

modelN1in = Flatten[N1in[RawTimeData] /. sol];

modelN2in = Flatten[N2in[RawTimeData] /. sol];

219

```
Length[modelN1in]

113

Length[modelN2in]

113

Length[VoverViso]

113
```

(*Sum of Square Errors*)

```
ModelVoverViso = (modelN1in * PMV1 + modelN2in * PMV2 + N3ino * PMV3 + iVd) / iVto;

Length[ModelVoverViso]

113

SquareError = (ModelVoverViso - VoverViso) ^ 2;

For[{i = 1, SumSquareError = 0}, i < Length[VoverViso],
   i ++, SumSquareError = SquareError[[i]] + SumSquareError];

SumSquareError

0.0442504
```
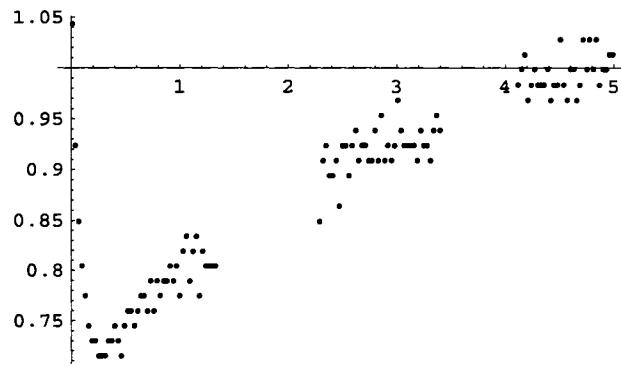
(*PLOT*)

```
coordinates =
   Table[{RawTimeData[[i]], VoverViso[[i]]}, {i, Length[RawTimeData]}];
```
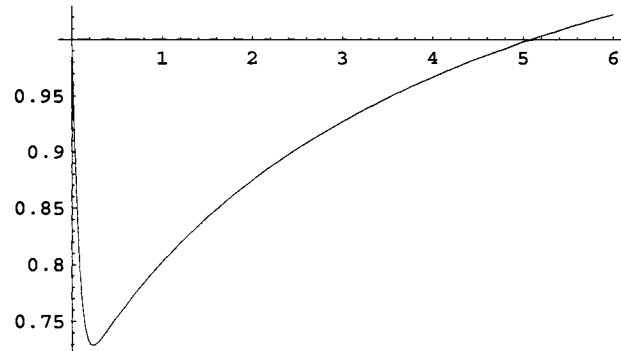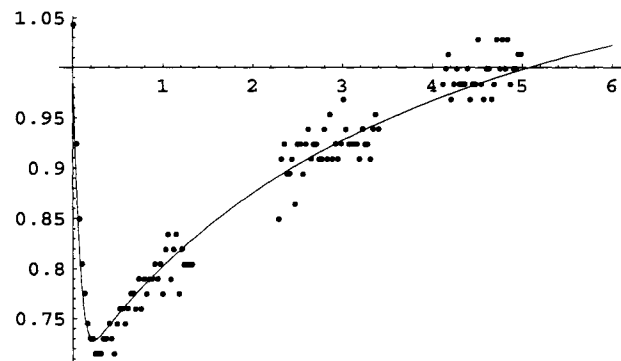
220

a = ListPlot[coordinates]

- Graphics -

b = Plot[
    Evaluate[(Nlin[t] * PMV1 + N2in[t] * PMV2 + N3ino * PMV3 + iVd) / iVto /. sol],
    {t, 0, tMax}, PlotStyle → {RGBColor[1, 0, 1]}]

- Graphics -

Show[a, b]

- Graphics -

221